

UNIVERSITY OF EDUCATION, WINNEBA
DEPARTMENT OF MECHANICAL/AUTOMOTIVE ENGINEERING
TECHNOLOGY

MODELLING AND SIMULATION OF A CONNECTING ROD OF AN
INTERNAL COMBUSTION ENGINE USING FINITE ELEMENT
METHOD



2021

UNIVERSITY OF EDUCATION, WINNEBA

DEPARTMENT OF MECHANICAL/AUTOMOTIVE ENGINEERING

TECHNOLOGY

MODELLING AND SIMULATION OF A CONNECTING ROD OF AN

INTERNAL COMBUSTION ENGINE USING FINITE ELEMENT

METHOD

The logo of the University of Education, Winneba, is a circular emblem. It features a central sunburst with a flame-like shape at its base. Below the sunburst are two interlocking circular symbols. The entire emblem is set against a red background with a white border. The text 'UNIVERSITY OF EDUCATION, WINNEBA' is written around the top inner edge of the circle, and 'EDUCATION FOR SERVICE' is written around the bottom inner edge.

JACOB KWAKU NKRUMAH

MASTER OF PHILOSOPHY (M. PHIL) IN AUTOMOTIVE ENGINEERING

TECHNOLOGY

2021



UNIVERSITY OF EDUCATION, WINNEBA

**MODELLING AND SIMULATION OF A CONNECTING ROD OF AN
INTERNAL COMBUSTION ENGINE USING FINITE ELEMENT
METHOD**

JACOB KWAKU NKRUMAH



**A Thesis in the Department of Mechanical and Automotive Engineering
Technology, Faculty of Technology Education, submitted to the School of
Graduate Studies in partial fulfilment of the requirements for the award of the
degree of Master of Philosophy (Automotive Engineering Technology) in the
University of Education, Winneba**

APRIL, 2021

DECLARATION

STUDIES' DECLARATION

I, Nkrumah Jacob Kwaku declare that this thesis, with the exception of quotations and references contained in published works which have all been identified and duly acknowledged, is entirely my own original work, and it has not been submitted, either in part or whole, for another degree elsewhere.

NAME: JACOB KWAKU NKRUMAH

SIGNATURE:

DATE:

SUPERVISOR'S DECLARATION

I hereby declare that the preparation and presentation of this work was supervised in accordance with the guidelines for supervision of thesis as laid down by the University of Education, Winneba

NAME: MR. CHIBUDO KENNETH NWORU

SIGNATURE:

DATE:

ACKNOWLEDGEMENTS

My deepest gratitude goes to my supervisor Mr Chibudo Kenneth Nworu for the direction he provided for this research, not forgetting his encouragement, inspiration and the time he spent on this work.

I would sincerely like to express my heartfelt gratitude to Dr Sherry Kwabla Amedorme, for his patience, many in-depth and constructive criticisms and valuable suggestions, which have immensely contributed to the success of this work. Am also grateful to my wife, Millicent Dentaah for giving me the moral support to successfully complete this work.



DEDICATION

This thesis is dedicated to my heavenly father Jehovah God and my spiritual father Prophet T.B Joshua of Synagogue Church of all Nation (SCOAN) Nigeria for strengthening and guiding me through my tribulations. The work is also dedicated to my dearest mother Ama Krah, my wife Dentaah Millicent and my children.



TABLE OF CONTENTS

	Pages
Declaration.....	iii
Acknowledgements.....	iv
Dedication.....	v
Table of Contents.....	vi
List of Tables.....	x
List of Figures.....	xii
Abstract.....	xvii
 CHAPTER ONE	
1.1 Background of the Study.....	1
1.2 Statement of the Design Problem.....	3
1.3 Objectives of the Study.....	5
1.4 Justification of the Study.....	6
1.5 Scope of the Study.....	7
1.6 Organisation of the Study.....	7
 CHAPTER TWO	
 LITERATURE REVIEW	
2.1 Weight and Cost Optimisation of the Connecting Rod.....	9

2.2 Connecting Rod Materials and Method of Manufacturing.....	15
2.2.1 The Aluminium Industry in Ghana.....	18
2.2.2 Aluminium Selection and Application.....	20
2.2.3 Alloy families for wrought compositions.....	21
2.2.4 Alloy families for casting compositions	22
2.3 Forces Acting on the Connecting Rod.....	28
2.4 The Automotive Industry in Ghana.....	30

CHAPTER THREE

METHODOLOGY

3.0 Introduction.....	34
3.1 Material Selection.....	34
3.2 Method of Manufacturing.....	36
3.3 Theoretical Design Calculations.....	37
3.3.1 Determination of buckling load of the connecting rod.....	38
3.3.2 Dimensioning of the I-Section of the connecting rod.....	39
3.3.3 Forces acting on a connecting rod.....	40
3.3.3.1 Force due to gas or steam pressure and inertia of reciprocating parts.....	40
3.3.3.2 Inertia bending forces.....	42
3.4 Engine Specification and Pressure Calculations.....	45
3.4.1 Pressure developed by the engine.....	46

3.5 Forces Acting on the Connecting Rod.....	47
3.5.1 Dimensions of the I-Section of the Connecting Rod.....	49
3.5.2 Dimensions of the Crankpin or the Big End Bearing	50
3.5.3 Dimensioning of the Piston Pin or Small End Bearing.....	51
3.5.4 Size of Bolts for Securing the Big End Cap.....	52
3.5.5 The Thickness of the Big End Cap.....	53
3.5.6 Determination of the outer diameters of Big end and small end.....	55
3.6 Modelling of Component in Autodesk Inventor 201.....	57
3.7 Procedure for the Numerical Methods.....	60
3.7.1 Meshing of Component.....	60
3.7.2 Grid Independence Test.....	61
3.7.3 The Boundary Conditions set for the Analysis.....	62
3.7 Fabrication of the Connecting Rod.....	63

CHAPTER FOUR

PRESENTATION OF DATA AND DISCUSSIONS

4.0 Introduction	65
4.3 Static Structural Analysis of the Connecting Rod.....	65
4.4 Discussion of Static Structural Analysis Results.....	91
4.5 Modal Analysis of the Connecting Rod.....	97
4.6 Discussion of the Modal Analysis Results.....	122
4.7 Test Results for Validation.....	124

4.8 Weight of the Connecting Rod Calculations..... 125

CHAPTER FIVE

SUMMARY OF FINDINGS, CONCLUSIONS AND RECOMMENDATIONS

5.0 Introduction..... 130

5.1 Summary of Findings..... 130

5.1.1 Findings from finite element analysis..... 130

5.1.2 Findings from test results..... 133

5.3 Conclusions..... 135

5.3 Recommendations..... 135

5.4 Future Studies..... 138

References..... 139



LIST OF TABLES

Table 2.1 Material Properties.....	15
Table 2.2 Strength Ranges of Various Wrought Aluminium Alloy.....	24
Table 2.3 Strength Ranges of Various Cast aluminium Alloys.....	25
Table 2.4 Selected Applications for Aluminium Casting (A. C.) Alloys.....	26
Table 2.5 Selected Applications for Aluminium Casting (A.C.) Alloys.....	27
Table 3.1 Properties of the Material (Al7075 T6)	35
Table 3.2 Properties of Cast Iron, Titanium Alloy and Structure Steel.....	36
Table 3.3 Specifications of the Connecting Rod.....	56
Table 3.4 Grid Independence Test Results.....	61
Table 4.1 Summary Results for Titanium Alloy material.....	70
Table 4.2 Results for Structural Steel material.....	77
Table 4.3 Results for Grey Cast Iron Material.....	84
Table 4.4 Results for Aluminium 7075 T6 Material.....	91
Table 4.5 Factor of Safety of the Connecting Rods of Four Different Materials...	95
Table 4.6 Deformations and natural frequencies of connecting rod of S. steel	103
Table 4.7 Deformations and natural frequencies of connecting rod of Titanium ...	109
Table 4.8 Deformations and natural frequencies of connecting rod of gray iron. ...	115
Table 4.9 Deformations and natural frequencies of connecting rod of Al7075 T6	121
Table 4. 10 Comparism of the Final Results.....	125

Table 4.11 Mass and weight of S. steel, G. C. Iron, Ti. Alloy and Al 7075 T6.... 128



LIST OF FIGURES

Figure 1.1 I-Section connecting rod with its parts.....	3
Figure 2.1 Processed Aluminium into Round Bars.....	19
Figure 2.2 Forces Acting on a connecting Rod.....	29
Figure 2.3 Bending Forces on the Connecting Rod.....	30
Figure 3.1 Cross -Section of an I-Section Connecting	39
Figure 3.2 Forces on a Connecting Rod.....	40
Figure 3.3 Inertia Bending Forces.....	43
Figure 3.4 Dimensioning of the Connecting Rod.....	57
Figure 3.5 Connecting Rod with the Big End Cap and Bottom End Joined.....	57
Figure 3.6 Connecting Rod with Big End Cap Splitted from the Bottom End....	58
Figure 3.7 Bolt of the Connecting Rod.....	58
Figure 3.8 Nut of the Connecting Rod.....	59
Figure 3.9 Assembly of the Connecting Rod after Al7075 was Applied.....	59
Figure 3.10 Component Meshed in Ansys.....	60
Figure 3.11 The boundary condition for the analysis.....	62
Figure 3.12 Sand Cast Rectangular Al7075 T6 Block.....	63
Figure 3.13 Crucible Finance.....	64
Figure 3.114 Fabrication of Al 7075 connecting rod.....	64
Figure 4.1 Total Deformation of Titanium Alloy Material.....	65

Figure 4.2 Directional Deformation of Titanium Alloy Material.....	66
Figure 4.3 Equivalent Elastic Strain of Titanium Alloy Material.....	67
Figure 4.4 Equivalent (Von Mises) Stress of Titanium Alloy Material.....	67
Figure 4.5 Maximum Principal Stress of Titanium Alloy Material.....	68
Figure 4.6 Minimum Principal Stress of Titanium Alloy Material.....	69
Figure 4.7 Factor of Safety of Titanium Alloy Material.....	70
Figure 4.8 Total Deformation of Structural Steel Material.....	71
Figure 4.9 Directional Deformation of Structural Steel Material.....	72
Figure 4.10 Equivalent Elast Strain of Structural Steel Material.....	73
Figure 4.11 Equivalent (Von Mises) Stress of Structural Steel Material.....	73
Figure 4.12 Maximum Principal Stress of Structural Steel Material.....	74
Figure 4.13 Minimum Principal of Structural Steel Material.....	75
Figure 4.14 Safety Factor of Structural Steel Material.....	76
Figure 4.15 Total deformation of gray cast iron material.....	77
Figure 4.16 Directional deformation of gray cast iron material.....	78
Figure 4.17 Equivalent Elastic Strain of gray cast iron material.....	79
Figure 4.18 Equivalent (Von Mises) Stress of gray cast iron material.....	80
Figure 4.19 Maximum Principal Stress of gray cast iron material.....	81
Figure 4.20 Minimum Principal Stress of gray cast iron material.....	82
Figure 4.21 Safety Factor of gray cast iron material.....	83

Figure 4.22 Total deformation of Aluminium 7075 T6 Alloy Material.....	84
Figure 4.23 Directional deformation of Aluminium 7075 T6 Alloy Material.....	85
Figure 4.24 Equivalent Elastic Strain of Aluminium 7075 T6 Alloy Material.....	86
Figure 4.25 Equivalent Stress of Aluminium 7075 T6 Alloy Material.....	87
Figure 4.26 Maximum Principal Stress of Aluminium 7075 T6 Alloy Material...	88
Figure 4.27 Minimum Principal Stress of Aluminium 7075 T6 Alloy Material....	89
Figure 4.28 Safety Factor of Aluminium 7075 T6 Alloy Material.....	90
Figure 4.29 Summarised Results for Total Deformation.....	91
Figure 4.30 Summarised Results for Directional Deformation.....	92
Figure 4.31 Summarised Results for Von Mises Stresses.....	93
Figure 4.32 Summarised Results for Equivalent Elastic Strains.....	96
Figure 4.33 Vibration Mode Shape with Natural Frequency 369.08 Hz.....	98
Figure 4.34 Vibration mode shape with natural frequency 702.93 Hz.....	98
Figure 4.35 Vibration mode shape with natural frequency 912.65 Hz.....	99
Figure 4.36 Vibration mode shape with natural frequency 2125.9 Hz.....	99
Figure 4.37 Vibration mode shape with natural frequency 2590.1 Hz.....	100
Figure 4.38 Vibration mode shape with natural frequency 4023.0 Hz.....	100
Figure 4.39 Vibration mode shape with natural frequency 4834.3 Hz.....	101
Figure 4.40 Vibration mode shape with natural frequency 5670.9 Hz.....	101
Figure 4.41 Vibration mode shape with natural frequency 6114.5.7 Hz.....	102

Figure 4.42 Vibration mode shape with natural frequency 7196.4 Hz.....	102
Figure 4.43 Vibration mode shape with natural frequency 408.3 Hz.....	104
Figure 4.44 Vibration mode shape with natural frequency 777.42 Hz.....	104
Figure 4.45 Vibration mode shape with natural frequency 1025.7 Hz.....	105
Figure 4.46 Vibration mode shape with natural frequency 2353.9 Hz.....	105
Figure 4.47 Vibration mode shape with natural frequency 2851.4 Hz.....	106
Figure 4.48 Vibration mode shape with natural frequency 4415.6 Hz.....	106
Figure 4.49 Vibration mode shape with natural frequency 5358.1 Hz.....	107
Figure 4.50 Vibration mode shape with natural frequency 6303.7 Hz.....	107
Figure 4.51 Vibration mode shape with natural frequency 6847.7 Hz.....	108
Figure 4.52 Vibration mode shape with natural frequency 7920.1 Hz.....	108
Figure 4.53 Vibration mode shape with natural frequency 316.10 Hz.....	110
Figure 4.54 Vibration mode shape with natural frequency 601.82 Hz.....	110
Figure 4.55 Vibration mode shape with natural frequency 798.46 Hz.....	111
Figure 4.56 Vibration mode shape with natural frequency 1823.0 Hz.....	111
Figure 4.57 Vibration mode shape with natural frequency 2204.70 Hz.....	112
Figure 4.58 Vibration mode shape with natural frequency 3410.70 Hz.....	112
Figure 4.59 Vibration mode shape with natural frequency 4151.80 Hz.....	113
Figure 4.60 Vibration mode shape with natural frequency 4888.80 Hz.....	113
Figure 4.61 Vibration mode shape with natural frequency 5324.00 Hz.....	114

Figure 4.62 Vibration mode shape with natural frequency 6123.0 Hz.....	114
Figure 4.63 Vibration mode shape with natural frequency 409.22 Hz.....	116
Figure 4.64 Vibration mode shape with natural frequency 779.26 Hz.....	116
Figure 4.65 Vibration mode shape with natural frequency 1019.80 Hz.....	117
Figure 4.66 Vibration mode shape with natural frequency 2358.00 Hz.....	117
Figure 4.67 Vibration mode shape with natural frequency 2864.2 Hz.....	118
Figure 4.68 Vibration mode shape with natural frequency 4442.10 Hz.....	118
Figure 4.69 Vibration mode shape with natural frequency 5364.3 Hz.....	119
Figure 4.70 Vibration mode shape with natural frequency 6302.10 Hz.....	119
Figure 4.71 Vibration mode shape with natural frequency 6820.50 Hz.....	120
Figure 4.72 Vibration mode shape with natural frequency 7957.00 Hz.....	120
Figure 4.73 Comparism of Deformations of Different Materials of Con. Rod.....	122
Figure 4.74 Comparism of Natural Frequencies of Connecting Rod Materials...	123

ABSTRACT

The connecting rod is one of the most important moving components in an internal combustion engine. It is the link between the piston and the crankshaft. Its primary function is to transmit the push and pull from the piston pin to the crankpin by so doing converting the reciprocating motion of the piston to rotary motion of the crankshaft. The main objective of this research was to design a connecting rod of an internal combustion engine for improvement in weight and cost reduction. The connecting rod was modelled using Autodesk Inventor 2017 software. The modelled connecting rod was then imported into Ansys for further analysis. Static structural and modal analysis were carried out on the connecting rod of the four different materials namely: structural steel, titanium alloy, grey cast iron and aluminium 7075 T6 alloy to determine the total deformation, directional deformation, equivalent elastic strain, equivalent Von Mises stress, maximum principal stress, minimum principal stress and the safety factor. It was found that Al 7075 T6 connecting rod has the highest deformation of 0.62979 mm representing 36 % which was more than all the other connecting rods. Structural steel connecting rod was found to have the lowest deformation of 0.22733 mm representing 13%. Titanium alloy and Al 7075 T6 connecting rods were found to have the lowest Von Mises stress of 372.51 MPa and 375.52 MPa respectively. It was also found that the induced stresses in all the connecting rods were lower than the yield strengths of the materials. Al 7075 T6, Titanium alloy and structural steel connecting rods were found to have their maximum factor of safety values of 15 which is good for the design. The weights of all the connecting rods for the four materials were compared and it was found that Al 7075 T6 connecting rod was lighter in weight than the remaining connecting rods.

CHAPTER ONE

INTRODUCTION

1.1 Background of the Study

The internal combustion engine consists of different components one of which is the connecting rod which connects the piston to the crankshaft. The core function of the connecting rod is to transmit force from the gudgeon pin to the crank pin by converting the reciprocating motion of the piston into rotary motion of the crankshaft. The connecting rod has two ends: the big end which connects it to the crank pin and the small end which is connected to the piston by means of the gudgeon pin. The connecting rod has a long shank which can be designed to take the form of rectangular, tubular, circular, I-section and H-section. Circular section is generally used on the slow speed engines while the I-section is used on high-speed engines. According to Mohankumar, and Rakesh (2017), I-section is both lightweight and strong but the type of material used limits its capacity to handle load. Whereas, H-section can handle much more stress without bending, so, they are used in high power engines.

This study considers the I-section of a connecting rod for high-speed internal combustion engines. In the view of Rhurmi and Gupta (2005), the connecting rod should be able to sustain or be strong enough to withstand buckling load at both x-axis and y-axis.

Nitturkar, Kalshetti and Nadaf (2020), opined that the connecting rod should be such that it can sustain the maximum load without any failure during high cycle fatigue. The connecting rod in the internal combustion engines is subjected to alternating direct compressive and tensile forces. Since the compressive forces are much higher than the

tensile forces, therefore the cross-section of the connecting rod is design as a strut and the Rankine's formula is used to determine the dimensions of the connecting rod.

Manufacturers of the Automobile are striving hard to reduce the weight of the vehicle to optimisespeed and reduce excessive energy loss. This research seeks to model a connecting rod using Aluminium Alloy with the following compositions: 90% Aluminium, 5.6% Zinc, 2.5% Magnesium, 0.23% Iron and 1.6% Copper. The choice of this metal for this research was based on the fact that, Aluminium Alloy is light in weight, strong and costs less as compared to other materials like Titanium, cast steel, cast iron and forged steel which are commonly used to manufacture connecting rod (Mohankumar & Rakesh, 2017). They went further to state that, one of the most common materials used to manufacture connecting rod is steel and its alloys. This study employed Autodesk Inventor 2017 software to model the connecting rod and imported to ANSYS software for the critical analysis. The ANSYS software was used to analyse the critical loads. In the stress analysis of the connecting rod the model connecting rod was mesh in ANSYS software. The Von Mises stress, total deformation, the principal stresses and the safety factor of the connecting rod made with Aluminium Alloy was compared to the same parameters of connecting rod made with structural steel, titanium alloy and gray cast iron. Figure 1 shows an I-section connecting rod with the parts.

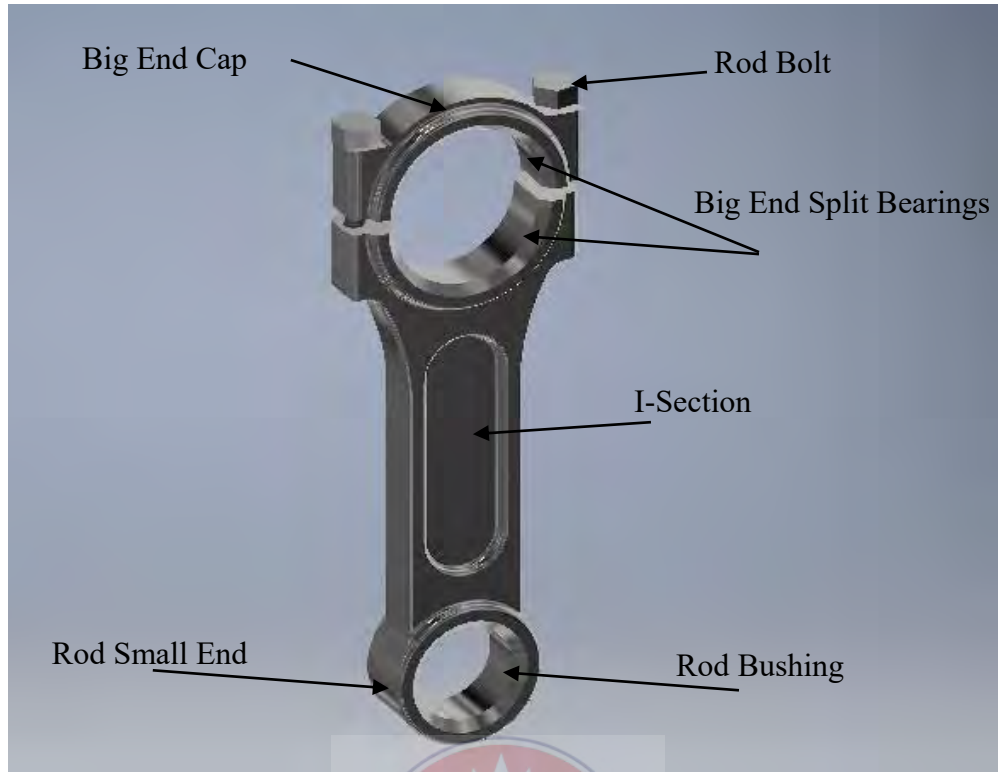


Figure 1.1 I-Section Connecting Rod with its Parts

1.2 Statement of the Problem

With the government of Ghana agenda to industrialise the country and also expand the Automotive industry through the One District One Factory (1D1F) policy, the industry is now experiencing tremendous growth with the influx of the automotive assembly plants such as VW, Kantanka and Toyota Ghana (Ministry of trade and industry, 2019). The country will therefore require Automotive Engineers at all levels to properly execute the policy. Furthermore, the Government of Ghana is currently advocating the “Ghana Beyond Aid” agenda, which supports the government’s desire to prudently manage the country’s natural resources in a manner that will allow the country’s development agenda to be financed without recourse to external assistance (Ghana Beyond Aid, 2019). The ultimate objective of these policies is to position

Ghana on the path of industrialisation. Ghana is endowed with abundant natural resources including bauxite. Alumina is obtained from a refined bauxite, hence, if the design and actualisation of a connecting rod of an internal combustion engine made with aluminium alloy becomes fit for purpose, then connecting rods made with aluminium alloy can be commercialised using localised materials for the production. This would go a long way to support the government of Ghana industrialisation drive. Ghana beyond aid meant that, Ghanaians should produce products using raw materials from Ghana, hence it is appropriate to ascertain the suitability of using local materials such as aluminium to design and manufacture a connecting rod to feed the local automotive industry.

Automobile designers worldwide are working very hard to reduce the weight of the vehicle in order to maximise the efficiency of the vehicle. A reduction in weight of the vehicle will enhance fuel efficiency and increase the speed of the vehicle. The aggregate or grand weight of the vehicle is the addition of all the weights of the individual components that constitute the vehicle. These components are made of materials and the weights of these component depends largely on the densities of these materials. The reduction in weight of each of these components will affect the total or grand weight of the vehicle. The challenge is to get a material to replace the known materials used to manufacture these components. The new material should have the same or better properties than the known materials for that component. The connecting rod is well known to be made of steel and its alloys. This research looked at the possibility of using Aluminium Alloy consisting of aluminium as the base material, Zinc, magnesium, Iron and copper. In the view of Nitturkar, Kalshetti and Nadaf (2020), “connecting rods are most usually made of steel for production engines, but can be made of aluminium for lightness, affordability and it has the ability to absorb high

impact”. Many researchers have written extensively on connecting design and manufacture but little has been said about materials for connecting rod for weight optimisation. Hence, the decision to assess the suitability of aluminium 7075 T6 alloy to manufacture connecting rod is very innovative and encouraging for the automotive industry.

1.3 Objectives of the Study

The research seeks to:

1. design a connecting rod using local Aluminium alloy in the proportion of 90% Aluminium, 5.6% Zinc, 2.5% Magnesium, 0.23% Iron and 1.6% Copper;
2. Test the performance of the material in terms of deformation, safety factor, stress using ANSYS;
3. design a connecting rod made with Aluminium Alloy for improvement in weight and cost reduction;
4. use the aluminium alloy to make a prototype of the connecting rod, and
5. contribute to the government of Ghana industrialisation drive and Ghana beyond aid agenda, by using our local materials to produce Automotive components to feed the local Automotive industry and the Automotive assembly plants in Ghana.

1.4 Justification of the Study

It is important to bring forth other materials that can be used to design and manufacture automotive components to reduce weight and cost. The automotive industry in Ghana over the years has grown sluggishly. This is because there was low skilled labour and

lack of interest by successive governments to develop the automotive sector in Ghana. Almost everything concerning the automotive industry in Ghana was imported. The government of Ghana of recent past has initiated the drive to industrialise the automotive sector in the country through government policies and programmes. This country has so far seen a tremendous growth in the automotive industry of late. There is now an influx of automotive assembling companies in Ghana. Companies such as Kantanka motors, Toyota and VW motors are now assembling vehicles in the country. For this industrialisation drive to be successful in the country there is the need for highly skilled automotive engineers to take the centre stage. Also, there is the need for component manufacturing. All the assembly plants currently do semi-knocked down. None of the components are manufactured in Ghana. This makes same vehicle more expensive in Ghana than in the country of origin.

Government through the ministry of trade and industry has brought forth the one district one factory policy to further enhance the industrialisation drive. The current President of Ghana is preaching Ghana beyond aid agenda. This agenda seeks to encourage local manufacturers to use the raw materials in the country to produce products and also encourage Ghanaians and companies within Ghana to patronise locally produced goods to spare the country's forex market from changing Cedis to Dollars for importation of goods.

This research seeks to contribute towards governments' effort to developing the automotive industry in Ghana. This work explores the possibility of using local materials such as aluminium to design and manufacture a connecting rod for an internal combustion engine for the local automotive industry in Ghana. Ghana is one of the countries in the world that can boast of large bauxite deposits and in recognition of that, the country has way back established Volta Aluminium Company to process the

country's bauxite to alumina and also, plans are far advance to setup integrated aluminium company in Ghana. The success of the government's effort to industrialise the automotive industry in Ghana is my greatest motivation behind this research.

1.5 Scope of the Study

The connecting rod is one of the most important components in an internal combustion engine. Its main function is to convert reciprocating motion to rotary motion of the crankshaft. There are different sizes of connecting rods for different engines. The engine size determines the size of the connecting rod. The vehicle whose connecting rod is under consideration or study, is a Nissan Pick Up NP300 diesel engine which has an engine capacity of 2.5 litre, displacement of 2488 cc, volume per cylinder of 622 cc, maximum power of 98 KW at 3600 r.p.m, maximum torque of 304 Nm at 2000 r.p.m and a compression ratio of 16.5:1. The vehicle under consideration is light duty vehicle with four (4) inline cylinders and develops a maximum pressure per cylinder of 6.32 N/mm². The vehicle has a manual gearbox of 5 speed and a cylinder bore and stroke of 100 mm×114 mm. The study intends to design a connecting rod made with local aluminium alloy to be able to withstand the maximum load and pressure of the aforementioned engine specification. The scope of this study is limited to design and simulation of a connecting rod of a 2.5 litre diesel engine of a compression ignition.

1.6 Organisation of the Study

Chapter 1 gives a brief description of the thesis. The chapter has the following sub-headings, introduction to the study, background of the study, the problem statement of the study, objectives of the study, justification and scope of the study. Chapter 2 covers

the literature review related to the study. Chapter 3 presents the method for computation of overall connecting rod manufacturing processes. Chapter 4 presents the modelling data, analysis and discussion of results. Chapter 5 covers the summary of findings from the design, conclusions, recommendations and suggestions for future work.



CHAPTER TWO

LITERATURE REVIEW

2.1 Materials for Connecting Rod for Weight Optimisation

Tanya Buddi et al (2021) share the opinion in their “Design and comparative Performance Analysis of Two-Wheeler Connecting Rod with Silicon Nitride and Aluminium 7068 by Finite element Analysis” that, A connecting rod is an intermediate link between the Piston and the Crankshaft. The primary function of the connecting rod is to transmit the motion from the piston pin to the crank pin, thus converting reciprocating motion of a piston into the rotary motion of crank. Connecting rod plays an important role while designing the Diesel or Petrol Engine. The changes in the material (Al7068 alloy and Si₃N₄) of the connecting rod to increase its strength to weight ratio while maintaining or reducing the maximum stress, maximum strain and the maximum deformation developed during loading. The performance of the component can be analysed by using the ANSYS software and the properties of the material can be found by performing different tests, after manufacturing the composite material by using an appropriate fabrication process, connecting rod has been modelled in CREO according to specific engine specifications of TVS Apache 150 model. Stress, Strain and the deformation analysis of the connecting rod is carried on the ANSYS WORKBENCH.

Pravardhan and Ali(2015) in their study into connecting rod optimisation for weight and cost reduction opined that, to reduce the weight and the manufacturing cost of a forged steel connecting rod subjected to by cyclic load comprising the peak compressive gas load and the peak dynamic tensile load, then there has to be material removal from less

stress regions or different material should be considered. The structural factors they considered for weight reduction during the optimization process included fatigue strength, static strength, buckling resistance, bending stiffness, and axial stiffness. Additional constraints imposed during the optimisation process included maintaining the forgeability as well as interchangeability of the optimised connecting rod with the existing one. In their findings, they found that, Cost was reduced by changing the material of the existing forged steel connecting rod to crackable forged steel (C-70). Their finding was an admission that, the cost and weight of the connecting rod depends largely on the type of material used.

Nachimuthu, Marlon and Vembaiyan (2014) conducted a study into analysis and optimising connecting rod for weight and cost reduction and concluded that, to reduce weight and manufacturing cost of steel connecting rod when it is subjected to by cyclic load composing of compressive gas load and the dynamic tensile load at different speed, corresponding with various crank angles. They indicated that cost was reduced by changing the material of the existing C45 steel connecting rod to C70 steel. They went further to state that, weight optimisation was performed under two cyclic loads composing of dynamic tensile and static compressive as the two extreme loads and also the cyclic loading conditions for life predictions analysis was also considered. They found that, in the optimisation process, fatigue strength was very significant factor. Their study resulted in an optimised connecting rod that was about 10% lighter and 25% less expensive, as compared to the existing connecting rod made with forged steel. They also collaborated with other authors that, different materials have weight and cost implications on the design.

The function of the connecting rod is to transmit the piston thrust to the crankshaft. Therefore, connecting rod should be capable to transmit different stresses caused by

thrust and pull on the piston, it must be very strong, rigid and as light as possible. In their study they found that, in many cases weight reduction of connecting rod was obtained by removing materials from certain regions of the connecting rod. The widely used materials in connecting rod manufacturing are carbon steel, cast iron, wrought steel or powder metal. So, there is a scope to try other materials like Titanium alloy, carbon fibre, aluminium alloy, glass fibre etc to produce light weight alternative. As these are light in weight, mass of the part will reduce. Therefore, the connecting rod can be optimised for weight reduction with the use of such materials (Nilam, Pundlik&Raghunath, 2017).

They also admitted that, to find a connecting rod which is both light in weight and cost effective, other materials such as aluminium alloy can be used.

OmPrakash, Natrayan and DineshKumar (2018) in their research into optimisation of connecting rod for weight reduction, they determined the loads acting on the connecting rod as a function of time. This was done to find out the minimum stress area and to remove the material in those areas. The relationship between the load and acceleration of the connecting rod for a given constant speed of the crankshaft were also determined. They opined that connecting rod can be designed and optimised under the loads ranging from tensile load, corresponding to 360-degree crank angle at the maximum engine speed as one extreme load and compressive load corresponding to the peak gas pressure as the other extreme load. They went further to replace the existing connecting rod material with a new composite material and they observed that the connecting rod was optimised by reducing the weight and cost.

In their design considerations for connecting rod, Srihersha and Sudhakar (2020) opined that connecting rod is one of the engine's key components which connect the piston to

the crankshaft and converts the piston's reciprocating motion into the crankshaft's rotation. In their assessment, connecting rod must be sufficiently strong to withstand the thrust from the piston during the combustion process. According to them, during connecting rod's lifespan, it faces a lot of tensile and compressive loads. Their study objective was to modify the connecting rod design and change the material of the connecting rod for weight reduction possibilities. They model the connecting rod designed with the help of INVENTOR and analysis was performed by using ANSYS. In their study, they obtained weight reduction of the connecting rod by removing material from big end of the connecting rod where stress values were low, weight reduction was also obtained by using Aluminium alloy and it was found that, the material has the lowest weight compared to other materials for the same loading conditions. They again used Titanium and the results shows that it has the highest factor of safety than other materials for the same loading conditions. So, they conclude that, Aluminium alloy or Titanium alloy are the best materials for the manufacturing of connecting rod with the ultimate aim of reducing weight and cost.

Akshaydatta and Swami (2017) reported in their study into optimisation of connecting rod used in heavy commercial vehicles with the aim of evaluating alternate material for connecting rod manufacturing with lesser stresses and lighter weight. They used ANSYS 18.1 software for determining stresses and deformation. The following were the findings from their study. The Aluminium alloy connecting rod shows nearly same number of stresses than existing carbon steel connecting rod. From the Dynamic analysis they saw that, the maximum stress generated when load was applied to piston end was almost same in all materials (In SAE = 423.17MPa, 42CrMo4 = 420.74MPa & Al 7075 = 445.06MPa) also when the same load was applied to crank end, the maximum stress generated in all materials was nearly same (In SAE 4340 = 523.38

MPa, 42CrMo4 =512.60 MPa & Al 7075= 553.73 MPa) but the weight of aluminium connecting rod was very less than that of the other two materials. The deflection of Aluminium alloy connecting rod is same compared to deflection of existing carbon steel (42CrMo4) connecting rod. It was also found that the Aluminium alloy connecting rod is light in weight (ie.35%) than existing carbon steel connecting rod approximately.

Venkatesh, et al (2014) conducted a research into design and analysis of connecting rod with modified materials and their objective was to reduce the weight of the connecting rod by replacing steel with aluminium fly ash composite material without losing any of its strength and hardness. They found that, by using aluminium fly ash composite material weight was greatly reduced up to 50% without losing any of its strength and hardness. They also analyse aluminium and steel connecting rods with the help of ANSYS and their results were compared with the experimental results. They found that, both results were given them the same values. They then concluded that both connecting rods were satisfactory

Sumit and Ankit (2019) opined that to decrease the weight and production expenses of a carbon steel connecting rod subjected to acyclic load including the peak compressive gas pressure at 2500 rpm, comparing to 360° crank angles. The basic components considered for weight ruination during the optimisation procedure included axial stiffness and static strength. They observed that, cost decreased by changing the material of the existing carbon steel connecting rod to Aluminium alloy. They found that, Stresses and natural frequency were essentially lower under states of assembly (with piston pin, crankshaft, and bearings) when contrasted with stresses obtained from unassembled connecting rod subjected to compressive gas loading. They opined that the shank portion of the connecting rod offered the best potential for weight lessening. The optimisation results were lighter than the current connecting rod for the equal stress,

disregarding endurance limit and lower yield strength of Aluminium compared with the current carbon steel. According to them, the existing carbon steel connecting rod was having a mass of 0.85 kg and after the material has been changed, the mass reduced to 0.31 kg which is about 63.53% weight reduction per unit of connecting rod. This amount of weight reduction became possible because of titanium alloyed with aluminium. They went further to state that, this is best known material for light weight construction. This weight reduction caused 0.54 kg of the material saving thus per unit raw material cost is reduced. The connecting rod analysed was for high-speed car or low commercial vehicles where weight and cost reduction are main concern. They found that the Aluminium alloy is much better than carbon steel material for accomplishing this purpose. But for heavy commercial vehicles where loading and power is major concern, carbon steel is best suited material than any other aluminium alloys.

Khurmi and Gupta (2005) dealt with the misunderstanding that is created, while using the various systems of units in the measurements of force and mass. This happens because of the lack of clear understanding of the difference between the mass and the weight. The following definitions of mass and weight should be clearly understood:

1. Mass. It is the amount of matter contained in a given body, and does not vary with the change in its position on the earth's surface. The mass of a body is measured by direct comparison with a standard mass by using a lever balance.
2. Weight. It is the amount of pull, which the earth exerts upon a given body. Since the pull varies with distance of the body from the centre of the earth, therefore the weight of the body will vary with its position on the earth's surface (say latitude and elevation). It is thus obvious, that the weight is a force. The earth's pull in metric units at sea level

and 45° latitude has been adopted as one force unit and named as one kilogram of force. Thus, it is a definite amount of force. But unfortunately, it has the same name as the unit of mass. The weight of a body is measured by the use of a spring balance which indicates the varying tension in the spring as the body is moved from place to place. Note: The confusion in the units of mass and weight is eliminated, to a great extent, in S.I. units. In this system, the mass is taken in Kilograms and force in Newtons.

The relation between the mass (m) and the weight (W) of a body is $W = mg$ or $m = W/g$ where W is in newtons, m is in kg and g is acceleration due to gravity.

2.2 Connecting Rod Materials and Methods of Manufacturing

In their analysis of connecting rod used in two-wheeler under static loading Raviraj and Abhay (2015) reported that there are different materials that can be used for connecting rod manufacturing, some of these materials are; cast iron, aluminium 360 and ASTM A216 GR WCB. They listed as shown in Table 2.1 all the required mechanical properties for analysis of all the materials used for connecting rod. The table indicates three different types of materials used for connecting rod manufacturing and their properties. The properties shown in the table are: Young's modulus of the materials, Poisson's ratios of the materials, the densities of the materials and the tensile strengths of the materials.

Table 2.1 Material Properties

Properties of material	Cast iron	ASTM A216 GR WCB	Aluminium 360
Young's Modulus (E)	170 GPa	210 GPa	71 GPa
Poisson's ratio	0.3	0.3	0.33

Density	7196 kg/m ³	7833 kg/m ³	2630 kg/m ³
Tensile Strength	200 MPa	485 MPa	300 MPa

Sources: Raviraj and Abhay (2015)

Mohankumar and Rakesh (2017) conveyed that their choice of metal for their project was Aluminium 7075 alloy. The reason for their choice was that aluminium 7075 alloy metal is light in weight and cost less. In their view, the choice of a metal for manufacturing connecting rod also depends on the type of requirement and preference. They went further to say that, metals such as Aluminium and Titanium are used for connecting rod manufacturing but the most common metal used for connecting rod manufacturing is Steel and its alloys.

Palamisamy, et al (2015) reported in their study into improvement of various parameters in different application of connecting rod that, there are different types of materials and production methods used in the creation of connecting rods. They also observed that, the most common types of Connecting rods are made of steel and aluminium. They opined that, the common methods use in connecting rod manufacturing are casting, forging and powdered metallurgy. They went further to state that, generally connecting rods are manufactured using carbon steel and in recent times aluminium alloys are finding its application in connecting rod manufacturing.

In the analysis of connecting rod, using analytical and finite element method Doshi and Ingole (2013) opined that, there are different types of materials and production methods used in the creation of connecting rods. They observed that most common types of Connecting rods are steel and aluminium and the most common types of manufacturing processes used in connecting rod manufacturing are casting, forging and powdered metallurgy.

Noor et al (2008), carbon steel, mild steel, brass and aluminium were considered in their study. They compare four different materials that had their endurance limit tested,

medium carbon steel has high endurance limit (29650 N) then follow by mild steel (low carbon steel), brass and aluminium. They concluded that medium carbon steel is suitable to make a connecting rod because it has high endurance limit besides high strength. From previous study, mild steel and aluminium were also used to make connecting rod of automotive vehicle. For mild steel, manufacturers design two-pieces to increase the strength but it also increases the weight. According to them, from experiment, aluminium that was used, was pure aluminium as a result it had the lowest endurance limit compare to other specimens that were tested. To improve the strength of aluminium, it was alloyed with other materials and as a result, the aluminium alloy connecting rod improved in static torque capability and fundamental natural frequency compare to mild steel. It also reduces the weight of the connecting rod by 25% compare to mild steel connecting rod.

In the design and analysis of connecting rod using aluminium alloy 7069 Mohamed, Prabhatkumar and Arvind (2014) opined that in modern automotive internal combustion engines, the connecting rods are most usually made of steel for production engines, but can be made of aluminium (for lightness and the ability to absorb high impact at the expense of durability) or titanium (for a combination of strength and lightness at the expense of affordability) for high performance engines, or of cast iron for applications such as motor scooters.

Leela Krishna and Gopal Vegi (2013) opined was consistent with Mohamed, Prabhatkumar and Arvind (2014), according to them in modern automotive internal combustion engines, the connecting rods are most usually made of steel for production engines, but can be made of aluminium (for lightness and the ability to absorb high impact at the expense of durability) or titanium (for a combination of strength and lightness at the expense of affordability) for high performance engines, or of cast iron

for applications such as motor scooters. In their findings, they found that, ANSYS Equivalent stress for both of the materials are same, the forged steel material factor of safety and stiffness was increase compared to existing carbon steel, the weight of the forged steel material was less than the existing carbon steel, the number of cycles for forged steel (8500×10^3) was more than the existing connecting rod (6255×10^3) and when compared to both of the materials, forged steel is cheaper than the existing connecting rod material.

Nitturkar, Kalshetti and Nadaf (2020) concluded in their study into design and analysis of connecting rod using different materials that connecting rods are most usually made of steel for production engines, but can be made of aluminium (for lightness and the ability to absorb high impact at the expense of durability) or titanium (for a combination of strength and lightness at the expense of affordability) for high performance engines or of cast iron for applications such as motor scooters. In their study, three materials Aluminium-360, Forged Steel, and Titanium Alloy were considered for analysis. They observed that the minimum stresses among all loading conditions, were found at crank end cap. So, they opined that material can be removed from those portions, thereby reducing material cost. They also observed from static analysis of their study that maximum stress was found at the small end of the connecting rod and Forged steel as a connecting rod material is less stiff and have more weight than Aluminium, magnesium and beryllium alloys connecting rods.

2.2.1 The aluminium industry in Ghana

The chairman of aluworks Ghana (2019) reported in his address to association of Ghana Manufacturers (AGM) that, Bauxite, the raw material of alumina was first

discovered in Ghana in 1914 in the Atewa Range near Kibi in the Eastern Region by Sir Albert Kitson, a renowned Geologist. In 1928, the British Aluminium Company was granted a concession to mine bauxite at Awaso in the Western Region. However, it was not until the 1940's that further exploration and mining really began. At present, the ore is still being mined only at Awaso even though major bauxite deposits occur at Kibi, Nyinahin and Ejuanema. The Government has also recently signed two Memoranda of Understanding (MOU) with ALCOA of USA and ALCAN of Canada over the Kibi and Nyinahin bauxite deposits. The main objective of the MOU is the development of an integrated aluminium industry in the country. According to the chairman, Aluminium has one of the most complex processing chains of all metals, with four major production steps leading from the raw material bauxite to raw aluminium sheets and profiles. The major steps in aluminium processing are; bauxite mining, refining of bauxite into alumina, smelting of alumina into raw aluminium ingots and processing or casting of aluminium ingots into sheets, coils, and profiles. The processed aluminium is the input for aluminium goods ranging from packaging material, automotive parts and construction elements to household goods. Figure 2.1 shows processed aluminium into round aluminium bars.



Figure. 2.1 Processed Aluminium into Round Bars

Ghana is home of almost all major production steps in aluminium processing, but not in an integrated form. While bauxite is exported to smelters in Scotland and Canada, alumina is imported from Jamaica and the US for the local smelter, Volta Aluminium Company Limited (VALCO). Aluworks is the only company that processes or casts aluminium ingots in Ghana and provides one of the vital links in the chain in aluminium processing in the country. The chairman reiterated that, until its intermittent shut downs, Valco employed over 1,500 people. This is a clear indication of the potential in the aluminium industry in Ghana to create jobs for the youth if the sector is managed well. The main competitors for Ghana's aluminium products are East Asian manufacturers. In general, the types of household goods manufactured in Ghana are not produced in developed countries. In the domestic market, closeness to the input material and low transportation costs results in a very cost-competitive position for the local industry. Exports to neighbouring countries however are in strong competition with goods from East Asia and other African countries. Hence, the prospects in the aluminium industry in Ghana is very bright if properly managed.

2.2.2 Aluminium selection and application

According to Aluminium Association, Inc. (1998), aluminium alloys can be categories under two main alloy designation systems namely; wrought alloys and cast alloys.

Davis (2019) in his Article titled Alloying: understanding the basics, reported that it is convenient to divide aluminium alloys into two major categories: wrought compositions and cast compositions. A further differentiation for each category is based on the primary mechanism of property development. Many alloys respond to thermal

treatment based on phase solubilities. These treatments include solution heat treatment, quenching, and precipitation, or age hardening. For either casting or wrought alloys, such alloys are described as heat treatable. A large number of other wrought compositions rely instead on work hardening through mechanical reduction, usually in combination with various annealing procedures for property development. These alloys are referred to as work hardening. Some casting alloys are essentially not heat treatable and are used only in as-cast or in thermally modified conditions unrelated to solution or precipitation effects. Cast and wrought alloy nomenclatures have been developed. The Aluminium Association system is most widely recognized in the United States. Their alloy identification system employs different nomenclatures for wrought and cast alloys, but divides alloys into families for simplification. For wrought alloys a four-digit system is used to produce a list of wrought composition families.



2.2.3 Alloy families for wrought compositions

The following are the international alloy designation for wrought alloys:

1xxx: Controlled unalloyed (pure) composition, used primarily in the electrical and chemical industries

2xxx: Alloys in which copper is the principal alloying element, although other elements, notably magnesium, may be specified. 2xxx series alloys are widely used in aircraft where their high strength (yield strengths as high as 455 MPa, or 66 ksi) is valued.

3xxx: Alloys in which manganese is the principal alloying element, used as general-purpose alloys for architectural applications and various products

4xxx:Alloys in which silicon is the principal alloying element,used in welding rods and brazing sheet

5xxx: Alloys in which magnesium is the principal alloying element, used in boat hulls, gangplanks, and other products exposed to marine environments

6xxx:Alloys in which magnesium and silicon are the principal alloying elements, commonly used for architectural extrusions and automotive components

7xxx:Alloys in which zinc is the principal alloying element (although other elements,such as copper,magnesium,chromium,and zirconium, may be specified), used in aircraft structural components and other high-strength applications. The 7xxxseries are the strongest aluminium alloys, with yield strengths ≥ 500 MPa (≥ 73 ksi) possible.

8xxx:Alloys characterizing miscellaneous compositions. The 8xxxseries alloys may contain appreciable amounts of tin,lithium,and/or iron.

9xxx: Reserved for future use.

Wrought alloys that constitute heat-treatable (precipitation-hardenability) aluminium alloys include the 2xxx, 6xxx, 7xxx, and some of the 8xxx alloys.

2.2.4 Alloy families for casting compositions

The Aluminium Association (AA) has adopted a nomenclature similar to that of wrought alloys British Standard and DIN have different designations. In the AA system, the second two digits reveal the minimum percentage of Aluminium, e.g. 150.x correspond to a minimum of 99.50% Aluminium. The digit after the decimal point takes a value of 0 or 1, denoting casting and ingot respectively. The main alloying elements in the AA system are as follows:

The series above can further be explained in detail as:

1xx.x: Controlled unalloyed (pure) compositions, especially for rotor manufacture

2xx.x:Alloys in which copper is the principal alloying element. Other alloying elements may be specified.

3xx.x: Alloys in which silicon is the principal alloying element. The other alloying elements such as copper and magnesium are specified. The 3xx.x series comprises nearly 90% of all shaped castings produced.

4xx.x:Alloys in which silicon is the principal alloying element.

5xx.x:Alloys in which magnesium is the principal alloying element.

6xx.x: Unused

7xx.x: Alloys in which zinc is the principal alloying element. Other alloying elements such as copper and magnesium may be specified.

8xx.x:Alloys in which tin is the principal alloying element.

9xx.x: Unused Heat-treatable casting alloys include the 2xx, 3xx, and 7xx series.

According to Davis (2019),more than 500 alloy designations/compositions have been registered by the Aluminium Association Incfor aluminium alloys. Composition limits for these alloys can be found in the Metals Handbook Desk Edition, 2nd ed., and in Registration Records on wrought alloys,castings,and ingots published by the Aluminium Association. He went further to state that, Aluminium alloys are economical in many applications. They are used in the automotive industry,aerospace industry,in construction of machines, appliances, and structures, as cooking utensils, as covers for housings for electronic equipment, as pressure vessels for cryogenic applications,and in innumerable other areas.

Table 2.2 Strength Ranges of Various Wrought Aluminium Alloys

Aluminium Association Series	Types of Alloy Composition	Strengthening Method	Tensile Strength Range	
			MPa	ksi
1xxx	Al	Cold work	70-175	10-25
2xxx	Al-Cu-Mg (1-2.5% Cu)	Heat treated	170-310	25-45
2xxx	Al-Cu-Mg-Si (3-6% Cu)	Heat treated	380-520	55-75
3xxx	Al-Mn-Mg	Cold work	140-280	20-40
4xxx	Al-Si	Cold work (some heat treated)	105-350	15-50
5xxx	Al-Mg (1-2.5% Mg)	Cold work	140-280	20-40
5xxx	Al-Mg-Mn (3-6% Mg)	Cold work	280-380	40-55
6xxx	Al-Mg-Si	Heat treated	150-380	22-55
7xxx	Al-Zn-Mg	Heat treated	380-520	55-75
7xxx	Al-Zn-Mg-Cu	Heat treated	520-620	75-90
8xxx	Al-Li-Cu-Mg	Heat treated	280-560	40-80

Source: Aluminium Association Inc.

Table 2.2 shows wrought aluminium alloys. The manufacturing processes that these materials can go through is by cold forging and hot forging. The components that required forging using aluminium alloy can employ any of the materials in Table 2.2 depending on the component properties required.

Table 2.3 Strength Ranges of Various Cast Aluminium Alloys

Alloy System (Aluminium Association Designation)	Tensile Strength Range	
	MPa	ksi
Heat treatable sand cast alloys (various tempers)		
Al-Cu (201–206)	353-467	51-68
Al-Cu-Ni-Mg (242)	186-221	27-35
Al-Cu-Si (295)	110-221	16-32
Al-Si-Cu (319)	186-248	27-36
Al-Si-Cu-Mg (355, 5% Si, 1.25% Cu, 0.5% Mg)	159-269	23-39
Al-Si-Mg (356, 357)	159-345	23-50
Al-Si-Cu-Mg (390, 17% Si, 4.5% Cu, 0.6% Mg)	179-276	26-40
Al-Zn (712, 713)	241	35
Non-heat treatable die cast alloys		
Al-Si (413, 443, F temper)	228-296	33-43
Al-Mg (513, 515, 518, F temper)	276-310	40-45
Non-heat treatable permanent mold cast alloys		
Al-Sn (850, 851, 852, T5 temper)	188-221	20-32

Source: Aluminium Association Inc.

The materials in Table 2.3 are the cast aluminium alloys with their tensile strength ranges that required using casting as a manufacturing process.

Table 2.4. Selected Applications for Aluminium Casting (A. C.) Alloys

A. C. Alloy	Representative applications
100.0	Electrical rotors larger than 152 mm (6 in.) in diameter
201.0	Structural members; cylinder heads and pistons; gear, pump, and aerospace housings
208.0	General-purpose castings; valve bodies, manifolds, and other pressure-tight parts
222.0	Bushings; meter parts; bearings; bearing caps; automotive pistons; cylinder heads
238.0	Sole plates for electric hand irons
242.0	Heavy-duty pistons; air-cooled cylinder heads; aircraft generator housings
A242.0	Diesel and aircraft pistons; air-cooled cylinder heads; aircraft generator housings
B295.0	Gear housings; aircraft fittings; compressor connecting rods; railway car seat frames
308.0	General-purpose permanent mould castings; ornamental grilles and reflectors
319.0	Engine crankcases; gasoline and oil tanks; oil pans; typewriter frames; engine parts
332.0	Automotive and heavy-duty pistons; pulleys, sheaves
333.0	Gas meter and regulator parts; gear blocks; pistons; general automotive castings
354.0	Premium-strength castings for the aerospace industry

Source: Aluminium Association Inc.

Table 2.5 Selected Applications for Aluminium Casting (A.C.) Alloys

A. C. Alloys	Representative applications
355.0	Sand: air compressor pistons; printing press bedplates; water jackets; crankcases. Permanent: impellers; aircraft fittings; timing gears; jet engine compressor cases
356.0	Sand: flywheel castings; automotive transmission cases; oil pans; pump bodies. Permanent: machine tool parts; aircraft wheels; airframe castings; bridge railings
A356.0	Structural parts requiring high strength; machine parts; truck chassis parts
357.0	Corrosion-resistant and pressure-tight applications
359.0	High-strength castings for the aerospace industry
A360.0	Cover plates; instrument cases; irrigation system parts; outboard motor parts; hinges
A380.0	Applications requiring strength at elevated temperature
384.0	Pistons and other severe service applications; automatic transmissions
390.0	Internal combustion engine pistons, blocks, manifolds, and cylinder heads
443.0	Cookware; pipe fittings; marine fittings; tire moulds; carburettor bodies
A514.0	Permanent mould casting of architectural fittings and ornamental
535.0	Instrument parts and other applications where dimensional stability is important
A712.0	General-purpose castings that require subsequent brazing
713.0	Automotive parts; pumps; trailer parts; mining equipment

850.0	Bushings and journal bearings for railroads
A850.0	Rolling mill bearings and similar applications

Source: Aluminium Association Inc.

2.3 Forces Acting on the Connecting Rod

Naga Malleshwara Rao (2013) conducted a research into design optimisation and analysis of a connecting rod and reported that the forces acting on the connecting rod includes; Forces on the piston due to gas pressure and inertia of the reciprocating parts, force due to inertia of the connecting rod or inertia bending forces, forces due to friction of the piston rings and of the piston, and Forces due to friction of the piston pin bearing and crank pin bearing. But in his study, he only considered the first two forces.

Khurmi and Gupta (2005) opined that connecting rod is subjected to the following forces.

1. Force due to gas or steam pressure and inertia of reciprocating parts, and
2. Inertia bending forces.

They went further to state that, the inertia force due to the acceleration of reciprocating parts, opposes the force on the piston. On the other hand, the inertia force due to retardation of the reciprocating parts, helps the force on the piston. Net force acting on the piston pin (or gudgeon or wrist pin) was given as:

$$F_p = \text{force due to pressure of gas or steam} \pm \text{inertia force} = F_L \pm F_I$$

The –ve sign is used when the piston is accelerated and +ve sign is used when the piston is retarded. Acceleration of reciprocating parts = $\omega^2 r (\cos\theta + \frac{\cos 2\theta}{n})$. It was also outlined in their book that, the force F_p gives rise to a force F_c in the connecting rod and

a thrust force F_N on the sides of the cylinder walls (or normal reaction on crosshead guides) from Figure 2.2, it can be seen that, the force in the connecting rod at any

$$\text{instant, } F_C = \frac{F_P}{\cos\theta} = \frac{F_P}{\sqrt{1 - \frac{\sin^2\theta}{n^2}}}$$

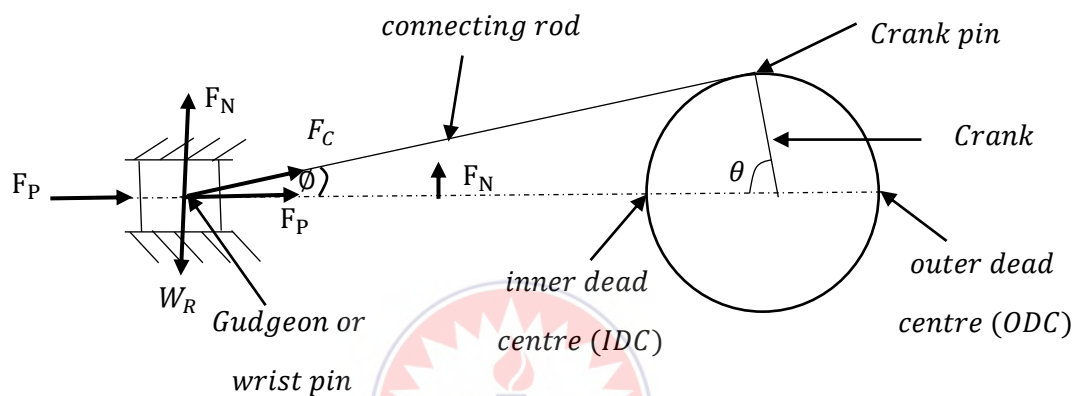


Figure 2. 2 Forces on a Connecting Rod

They stated that, the force in the connecting rod will be maximum when the crank and the connecting rod are perpendicular to each other (when $\theta = 90^\circ$). But at this position, the gas pressure would be decreased considerably. Thus, for all practical purposes, the force in the connecting rod (F_C) is taken equal to the maximum force on the piston due to pressure of the gas or steam (F_L) neglecting piston inertia effects.

The bending forces were also analysed as follows; Consider a connecting rod PC and a crank OC rotating with uniform angular velocity ω rad/s. In order to find the acceleration of the various points on the connecting rod, draw the Klien's acceleration diagram CQNO as shown in Figure2.3, CO represents the acceleration of C towards O and NO represents the acceleration of P towards O and it continues in that order.

The acceleration of other points such as D, E, F and G etc. on the connecting rod PC may be found by drawing horizontal lines from these points to intersect CN at d, e, f and g respectively. Now dO , eO , fO , and gO represents the acceleration of D, E, F and G all towards O. The inertia force acting on each point will be as follows:

$$\text{inertia force at } C = m \times \omega^2 \times cO$$

$$\text{inertia force at } D = m \times \omega^2 \times dO$$

$\text{inertia force at } E = m \times \omega^2 \times eO$ and so on.

The inertia force will be opposite to the direction of acceleration or centrifugal force. The inertia forces can be resolved into two components, one parallel to the connecting rod and the other perpendicular to the rod. The parallel (or longitudinal) components adds up algebraically to the force acting on the connecting rod (F_C) and produces thrust on the pins. The perpendicular (or transverse) components produces bending action and the stress induced in the connecting rod is called whipping stress.

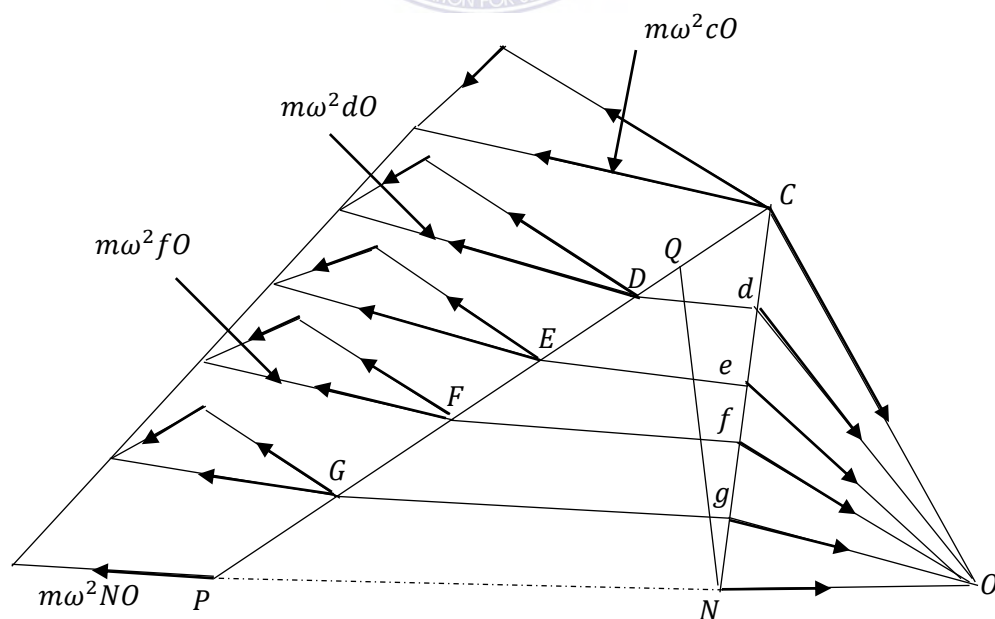


Figure 2.3 Bending forces on the connecting rod)

2.4 The Automotive Industry in Ghana

The Government of Ghana, as part of its transformational agenda has identified Vehicle Assembly and Automotive Components Manufacturing as a strategic anchor industry to be facilitated and supported as part of the Ten Point Plan for industrial development. As a result of this positive signal, Ghana is attracting investment in vehicle assembly from leading Original Equipment Manufacturers (OEMs) and investment partners, with positive projections of spill-overs into local manufacturing. The ministry of trade and industry of the Republic of Ghana in August, 2019 developed the Ghana automotive policy. The policy document seeks to guide potential investors in the automotive industry. According to the policy (2019), the vision is to make Ghana a fully integrated and competitive industrial hub for the Automotive Industry in the West Africa sub-region. The government through the policy seeks to provide opportunities for higher value addition and highly skilled employment, the Ministry of Trade and Industry has developed a comprehensive package of incentives and policy measures to support the establishment of an automotive assembly and component manufacturing industry, as a strategic anchor of industrialisation and a new pillar of growth in Ghana. The strategic objectives of the Ghana Automotive Development Policy (GADP) 2019, clearly stated as follows:

1. To establish a fully integrated and competitive industrial hub for automotive manufacturing in collaboration with the private sector – global, regional and domestic;
2. To generate highly skilled jobs in automotive assembly and the manufacture of components and parts, with spill over effects into other sectors of the economy;
3. To establish an asset-based vehicle financing scheme for locally manufactured vehicles to ensure affordability for vehicle buyers;

4. To improve balance of payments through competitive import substitution and export market development;
5. To improve vehicle safety and environmental standards; and
6. To transform the quality of the national road transport fleet and safeguard the natural environment.

The objective 2 of the policy is one of the reasons for this research. This objective clearly indicated government of Ghana intention to promote the manufacturing of automotive components and parts to feed the local automotive industry. Government of Ghana planned to establish a multi purpose-built Automotive Park.

Scope of the Auto Policy (2019), indicated that the initial scope of the Ghana Automotive Development Policy (hereafter referred to as “the Auto Policy”) is to provide the necessary framework to establish assembly and manufacturing capacity in Ghana. The initial coverage of vehicles to be assembled under the policy includes new passenger cars, SUVs and light commercial vehicles which would include pickups, minibuses and cargo vans. The ministry of trade and industry (2019) went further to state that, additional policy interventions will be introduced in the course of implementation for assembling medium and heavy-duty commercial vehicles, and for the assembly of buses. For the purpose of policy implementation and effective regulation of incentives, Ghana has categorized auto assembly into Semi-Knocked-Down (SKD), Enhanced SKD and Completely-Knocked-Down (CKD), based on the qualifying list of local or foreign assembly, and Fully-Built- Units (FBUs). Each category is defined according to place of assembly or manufacture.

With regards to automotive component supply chain, the policy objective is to establish and implement a comprehensive Supplier Development Programme to create viable

domestic enterprises capable of supplying components for local assembly and the global supply chain and also to transfer the skills and technology needed by existing SMEs to find their niche in the automotive supply chain. The policy seeks to develop a comprehensive programme of support to upgrade the Local Supply Chain, particularly in respect of:

- a. Parts and Accessories;
- b. Component manufacturing;
- c. Equipment manufacturing;
- d. Logistics and
- e. Support services.

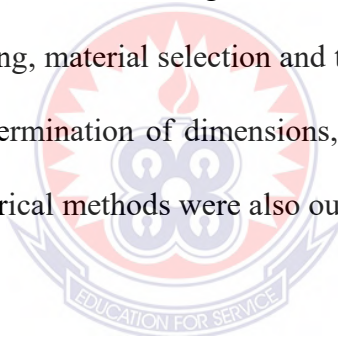


CHAPTER THREE

METHOD AND MATERIALS

3.0 Introduction

This chapter outlines and describes the design considerations necessary for connecting rod design and manufacturing, material selection and the mechanical properties of some selected materials. The determination of dimensions, modelling of the connecting rod and the procedure for numerical methods were also outlined in this chapter.



3.1 Material Selection

Wrought Aluminium alloy (Al7075 T6) has been selected for the manufacturing of the connecting rod. Aluminium 7075 is composed of 90.0% Al, 5.6% Zn, 2.5% Mg, 0.23% Fe, and 1.6% Cu, though these percentages nominally fluctuate depending upon manufacturing factors. The material has a density of 2.81 g/cm^3 , which is relatively light compared to metals such as structural steel, grey cast iron and Titanium alloy for the purpose of weight and cost optimisation. Aluminium alloy 7075 is one of the strongest aluminium alloys available, making it valuable in high-stress situations. The copper content in aluminium 7075 increases its susceptibility to corrosion, but this sacrifice is necessary to make such a strong-yet-workable material. The measure of a

material's resistance to deformation is given by its modulus of elasticity (E) and shear modulus (G). The modulus of elasticity for aluminium 7075 is 71.7 GPa , and its shear modulus is 26.9 GPa . Generally, this alloy is strong and resists deformation well, which makes it suitable for applications which needed a tough-yet-light metal. When specifying an alloy, one of the most important measures is its yield strength. The yield strength of a material is defined as the maximum amount of stress (or force over some area) that will not permanently deform a material. The yield stress indicates the maximum amount of bending that can be done before the metal stays permanently bent. Aluminium 7075 alloy has a tensile yield strength of 480 MPa , which means it takes 480 MPa of stress on a piece of 7075 alloy before it cannot return to its original shape. This value shows the huge benefit of alloying aluminium, and why aluminium 7075 is the best material for structural designs. Table 3.1 shows the properties of the selected material (Aluminium Al7075 T6).

Table 3.1 Properties of the Material (Al 7075 T6)

Parameters	Value	SI Unit
Density	2.81	g/cm^3
Ultimate Tensile Strength	572	MPa
Tensile Yield Strength	480	MPa
Compressive yield Strength	607.9	MPa
Poisson's Ratio	0.33	
Young's Modulus	71.7	GPa
Shear Modulus	26.9	GPa
Shear strength	331	MPa
Thermal Conductivity	196	W/m. K
Fatigue Strength	159	MPa

The commonly known materials for connecting rod manufacturing are; steel and its alloys, cast iron, Titanium and its alloys and aluminium alloys. For the purpose of this research, analysis of the connecting rod has been based on comparing connecting rod made of gray cast iron, titanium and structural steel to a connecting rod made with aluminium alloy 7075. The parameters that were considered for this study were: Equivalent Von Mises stress, Equivalent elastic strain, factor of safety, Total deformation, Directional deformation and the Principal stresses. The Table 3.2 below shows the mechanical properties of the three other materials.

Table 3.2 Properties of Cast Iron, Titanium Alloy and Structure Steel

Materials	Tensile Yield strength (MPa)	Compressive Yield Strength	Tensile strength (MPa)	Density (Kg/m ³)	Poisson's ratio	Young's Modulus (MPa)
Grey Cast Iron	130	943 MPa	200	7196	0.3	170
Titanium Alloy	1207	848 MPa	1276	4840	0.31	116
Structural Steel	540	720 MPa	845	7900	0.3	210

3.2 Method of Manufacturing

Connecting rod as stated earlier is one of the most important components in an internal combustion engine. The component is supposed to be designed to be very strong since the compressive forces acting on the connecting rod through the piston is massive. The connecting rod can be manufactured by three manufacturing methods. These are;

casting, forging and powdermetallurgy. For the purpose of this study, casting as a manufacturing method has been employed to manufacture the connecting rod made with aluminium 7075 alloy. This method has been selected because, its able to refined the grain structure of the material to improve the strength of the connecting rod. The method does not also necessary need very complex or sophisticated equipment to set up and such shops are readily available everywhere, hence its selection. The material selected is wrought aluminium alloy 7075 and the manufacturing process suitable for this material is casting, as a result the research employed casting as a manufacturing method for producing the connecting rod.

3.3 Theoretical Design Calculations

The theoretical design calculations of the I-section connecting rod are outlined as shown below:

A connecting rod is a machine member which is subjected to alternating direct compressive and tensile forces. Since the compressive forces are much higher than the tensile forces, therefore the cross-section of the connecting rod is design as a strut and the Rankine's formula is used.

A connecting rod subjected to an axial load W may buckle with X-axis as neutral axis (i.e., in the plane of motion of the connecting rod) or Y- axis as neutral axis (i.e., in the plane perpendicular to the plane of motion). The connecting rod is considered like both ends hinged for buckling about X-axis and both ends fixed for buckling about Y-axis. A connecting rod should be equally strong in buckling about either axes.

Taking,

$A =$ cross – sectional area of the connecting rod

$l =$ Length of the connecting rod

$\sigma_c =$ Compressive yield stress of connecting rod material

$W_B =$ buckling load

I_{xx} and $I_{yy} =$ Moment of inertia of the section about $x -$ axis and y

– axis respectively

k_{xx} and $k_{yy} =$ Radius of gyration of the section about $x -$ axis and y

– axis respectively

3.3.1 Determination of buckling load of the connecting rod

According to Rankine's formula

$$W_B \text{ (about } x - \text{ axis)} = \frac{\sigma_c \times A}{I + a\left(\frac{L}{K_{xx}}\right)^2} = \frac{\sigma_c \times A}{I + a\left(\frac{l}{K_{xx}}\right)^2}$$

$$W_B \text{ about } y - \text{ axis} = \frac{\sigma_c \times A}{I + a\left(\frac{L}{K_{yy}}\right)^2} = \frac{\sigma_c \times A}{I + a\left(\frac{l}{2K_{yy}}\right)^2}$$

For both ends fixed, $L = \frac{l}{2}$

In order to have a connecting rod equally strong in buckling about both the axes, the buckling loads must be equal,

$$\frac{\sigma_c \times A}{I + a\left(\frac{l}{K_{xx}}\right)^2} = \frac{\sigma_c \times A}{I + a\left(\frac{l}{2K_{yy}}\right)^2}$$

$$K_{xx}^2 = 4K_{yy}^2 \text{ or } I_{xx} = 4I_{yy}$$

The connecting rod design is considered to be satisfactory if $\frac{I_{xx}}{I_{yy}} = 3.2$.

3.3.2 Dimensioning of the I-Section of the connecting rod

Consider a Cross-Section of an I-section of a connecting rod as shown Figure 3.1

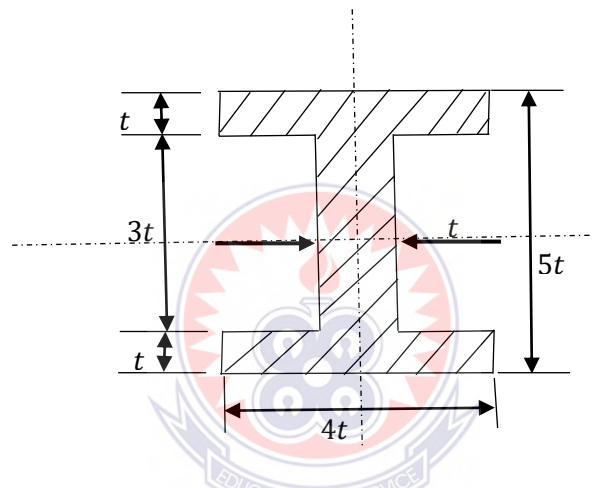


Figure 3.1 Cross -Section of an I-Section Connecting Rod

The flange and web thickness of the section = t

Width of the section, $B = 4t$

Depth or height of the section $H = 5t$

The area of the I-section is given as

$$A = 2(4t \times t) + (3t \times t) = 11t^2$$

$$I_{xx} = \frac{bh^3}{12} = \frac{1}{12} [(4t \times (5t^3)) - 3t \times (3t)^3] = \frac{419}{12} t^4$$

$$I_{yy} = \frac{b^3h}{12} = [2 \times \frac{1}{12} \times t((4t)^3) + \frac{1}{12} \times 3t \times t^3] = \frac{131}{12} t^4$$

Therefore,

$$\frac{I_{xx}}{I_{yy}} = \frac{419}{12} \times \frac{12}{131} = 3.2$$

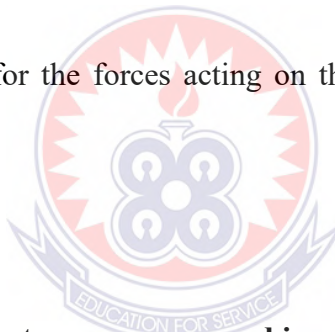
Since $\frac{I_{xx}}{I_{yy}} = 3.2$, therefore, the section chosen is quite satisfactory.

3.3.3 Forces acting on a connecting rod

A connecting rod is subjected to the following forces.

1. Force due to gas or steam pressure and inertia of reciprocating parts, and
2. Inertia bending forces.

Deriving the expressions for the forces acting on the connecting rod is as discussed below.



3.3.3.2 Force due to gas or steam pressure and inertia of reciprocating parts.

Consider a connecting rod PC as shown in the Figure 3.2.

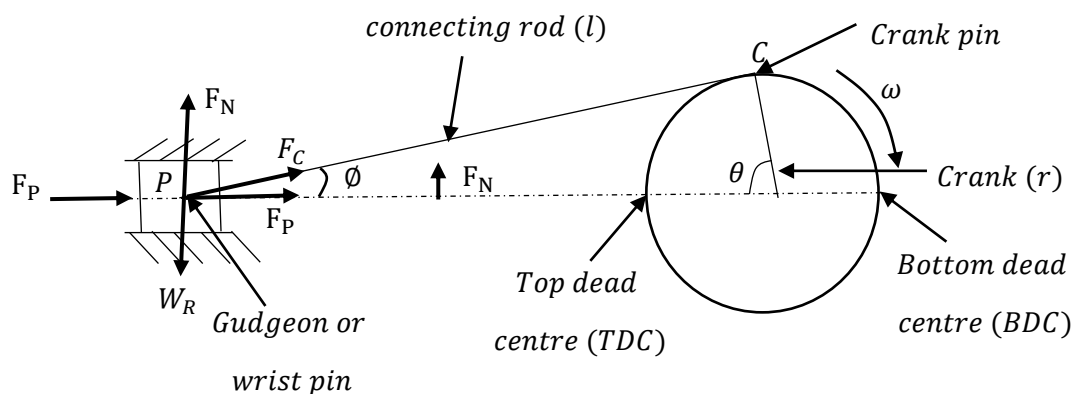


Figure 3.2 Forces on a Connecting Rod

$P = \text{pressure of gas or steam}$

$A = \text{Area of piston}$

$M_R = \text{mass of reciprocating parts}$

$\omega = \text{Angular speed of crank}$

$\phi = \text{Angle of inclination of the connecting rod with the line of stroke}$

$\theta = \text{Angle of inclination of the crank from inner dead centre}$

$r = \text{Radius of crank}$

$l = \text{Length of connecting rod and}$

$n = \text{Ratio of length of connecting rod to radius of the crank} = \frac{l}{r}$

The force on the piston due to pressure of gas or steam is given as:

$$F_p = \text{pressure} \times \text{Area} = P \times A$$

The inertia force of reciprocating parts is also given as:

$$F_I = \text{mass} \times \text{Acceleration} = m_g \times \omega^2 \times r \left[\cos\theta + \frac{\cos 2\theta}{n} \right]$$

Net force acting on the piston pin (or gudgeon or wrist pin)

$$F_p = \text{force due to pressure of gas or steam} \pm \text{inertia force} = F_p \pm F_I$$

The +ve sign is used when the piston is accelerated and –ve sign is used when the piston is retarded.

$$\text{Acceleration of reciprocating parts} = \omega^2 r \left(\cos\theta + \frac{\cos 2\theta}{n} \right)$$

The force F_p gives rise to a force F_C in the connecting rod and a thrust F_N on the sides of the cylinder walls.

$$F_C = \frac{F_P}{\cos\theta} = \frac{F_P}{\sqrt{1 - \frac{\sin^2\theta}{n^2}}}$$

The force in the connecting rod will be maximum when the crank and the connecting rod are perpendicular to each other (i.e., when $\theta = 90^\circ$). But at this position, the gas pressure would be decreased considerably. Thus, for all practical purposes, the force in the connecting rod (F_C) is taken equal to the maximum force on the piston due to pressure of the gas or steam (F_p) neglecting piston inertia effects.

3.3.3.2 Inertia bending forces

Consider a connecting rod PC and a crank OC rotating with uniform angular velocity ω rad/s. In order to find the acceleration of the various points on the connecting rod, draw the Klien's acceleration diagram CQNO as shown in Figure 3.3 (a). CO represents the acceleration of C towards O and NO represents the acceleration of P towards O.

The acceleration of other points such as D, E, F and G etc. on the connecting rod PC may be found by drawing horizontal lines from these points to intersect CN at d, e, f and g respectively. Now dO , eO , fO , and gO represents the acceleration of D, E, F and G all towards O.

The inertia force acting on each point on the connecting rod will be calculated as:

$$\text{inertia force at C} = m \times \omega^2 \times cO$$

$$\text{inertia force at D} = m \times \omega^2 \times dO$$

inertia force at $E = m \times \omega^2 \times eO$ and so on.

The inertia force will be opposite to the direction of acceleration or centrifugal force. The inertia forces can be resolved into two components, one parallel to the connecting rod and the other perpendicular to the rod. The parallel (or longitudinal) components adds up algebraically to the force acting on the connecting rod (F_C) and produces thrust on the pins.

The perpendicular (or transverse) components produces bending action and the stress induced in the connecting rod is called whipping stress.

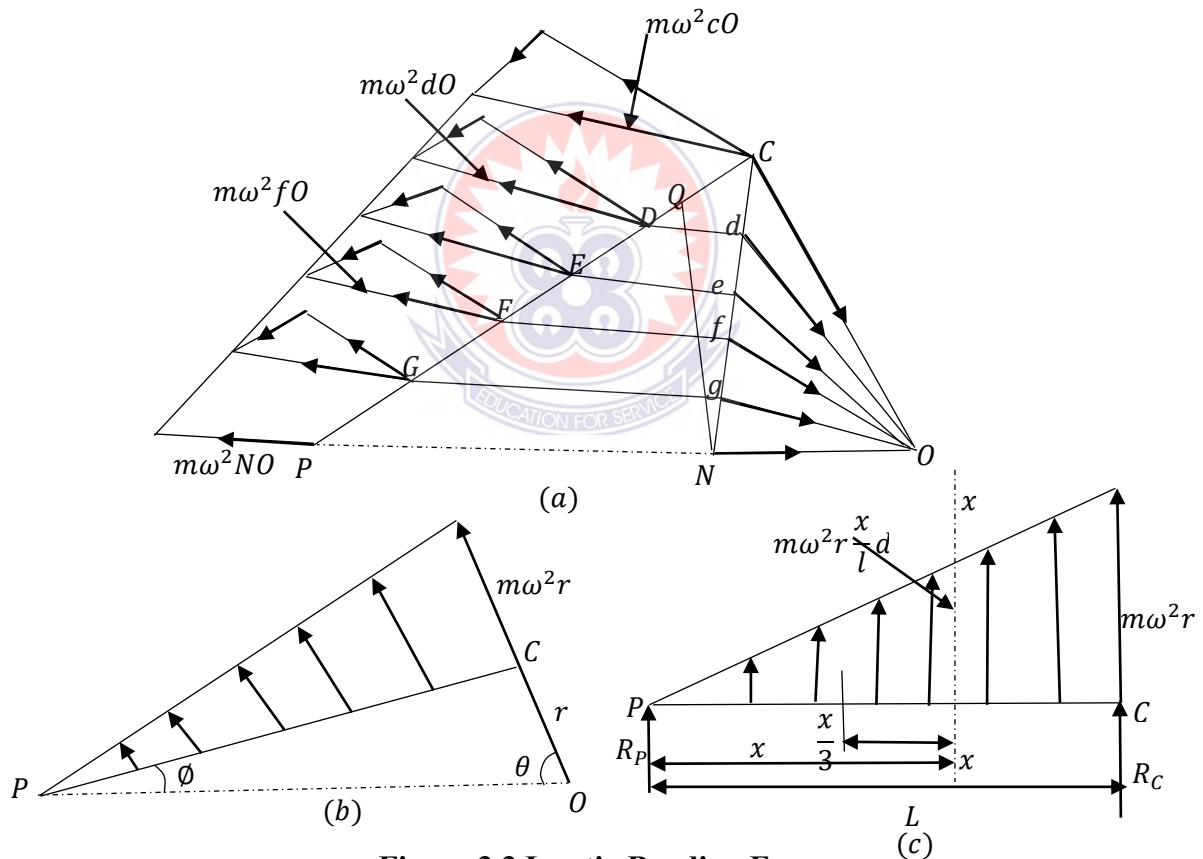


Figure 3.3 Inertia Bending Forces

A little consideration will show that, the perpendicular components will be maximum, when the crank and connecting rod are at right angles to each other. The variation of the

inertia force on the connecting rod is linear and is like a simple supported beam of variable loading as shown in Figure 3.3 (b) and (c). Assuming that the connecting rod is of uniform cross section and has mass m kg per unit length, therefore,

$$\text{Inertia force per unit length at the crank pin} = m_1 \times \omega^2 r$$

$$\text{and inertia force per unit length at the gudgeon pin} = 0$$


Inertia force due to small element of the length dx at a distance x from the gudgeon pin.

$$dF_I = m_1 \times \omega^2 r \times \frac{x}{l} \times dx$$

Therefore,

Resultant inertia force,

$$F_I = \int_0^l m_1 \times \omega^2 r \times \frac{x}{l} \times dx = \frac{m_1 \omega^2 r}{l} \left[\frac{x^2}{2} \right]_0^l$$

$$= \frac{m_1 \times l}{2} \omega^2 r$$


Substituting $m_1 l = m$ gives

$$= \frac{m}{2} \times \omega^2 r$$

This resultant inertia force acts at a distance of $\frac{2l}{3}$ from the gudgeon pin P. since it has been assumed that $\frac{1}{3}rd$ mass of the connecting rod is concentrated at gudgeon pin P (i.e., small end of the connecting rod) and $\frac{2}{3}rd$ at the crank pin (big end of the connecting rod), therefore the reactions at these two ends will be in the same proportion, i.e.,

$$R_P = \frac{1}{3}F_I \text{ and } R_C = \frac{2}{3}F_I$$

Now the bending moment acting on the rod at section x-x at a distance x from P,

$$M_x = R_p \times x - m_1 \omega^2 r \times \frac{x}{l} \times \frac{1}{2} x \times \frac{x}{3} = \frac{1}{3} F_l \times x - \frac{m_1 l}{2} \times \omega^2 r \times \frac{x^3}{3l^2}$$

$$= \frac{F_l \times x}{3} - \frac{F_l \times x^3}{3l^2} = \frac{F_l}{3} \left[x - \frac{x^3}{l^2} \right]$$

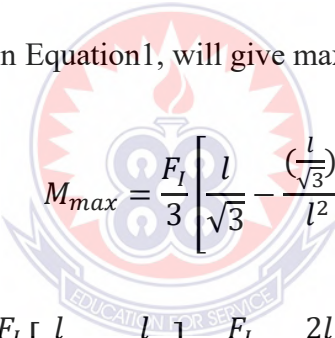
For maximum bending moment, differentiate M_x with respect to x and equate to zero,

i.e.

$$\frac{dM_x}{dx} = 0 \text{ or } \frac{F_l}{3} \left[x - \frac{3x^2}{l^2} \right] = 0 \quad 1$$

$$1 - \frac{3x^2}{l^2} = 0 \text{ or } 3x^2 = l^2 \text{ or } x = \frac{l}{\sqrt{3}}$$

Substituting this value of x in Equation 1, will give maximum bending moment as,



$$M_{max} = \frac{F_l}{3} \left[\frac{l}{\sqrt{3}} - \frac{\left(\frac{l}{\sqrt{3}}\right)^3}{l^2} \right]$$

$$= \frac{F_l}{3} \left[\frac{l}{\sqrt{3}} - \frac{l}{3\sqrt{3}} \right] = \frac{F_l}{3} \times \frac{2l}{3\sqrt{3}} = \frac{2F_l l}{9\sqrt{3}}$$

$$= 2 \times \frac{m}{2} \times \omega^2 r \times \frac{l}{9\sqrt{3}} = m\omega^2 r \frac{l}{9\sqrt{3}}$$

$F_l = \frac{m}{2} \omega^2 r$ and the maximum bending stress due to inertia of the connecting rod,

$$\sigma_{max} = \frac{M_{max}}{Z}$$

where $Z = \text{section modulus}$

From above we see that the maximum bending moment varies as the square of speed, therefore, the bending stress due to high speed will be dangerous. It may be noted that,

the maximum axial force and the maximum bending stress do not occur simultaneously. In an I.C engine, the maximum gas load occurs close to top dead centre whereas the maximum bending stress occurs when the crank angle $\theta = 65^{\circ}$ to 70° from top dead centre. The pressure of the gas falls suddenly as the piston moves from top dead centre.

3.4 Engine Specification and Pressure Calculations

Vehicle Model: Nissan NP 300 Pickup Double Cab 2.5 litres

Displacement: 2488 cc (cm^3)

$$\text{Volume per cylinder} = \frac{2488}{4} = 622 \text{ cm}^3 = 622 \times 10^3 \text{ mm}^3$$

Fuel type: Diesel

Maximum power: 98 Kw at 3600 r.p.m

Maximum Torque: 304 Nm at 2000 r.p.m

Compression ratio: 16.5: 1

Number of Cylinders: 4

Cylinder bore and Stroke: 100 mm \times 114 mm

Gearbox: 5 Speed, manual

3.4.1 Pressure developed by the engine

Engine: 2488 cc Diesel 4 in line cylinder (water cooled)

$$\text{Volume per cylinder} = \frac{2488}{4} = 622 \text{ cm}^3 = 622 \times 10^3 \text{ mm}^3$$

$$\text{Density of diesel: } 832 \times 10^{-9} \text{ kg/mm}^3$$

$$\text{Operating temperature}(T) = 210^\circ\text{C}$$

$$\text{Molecular weight of diesel} = 230 \text{ g/mole} = 230 \times 10^{-3} \text{ kg/mole}$$

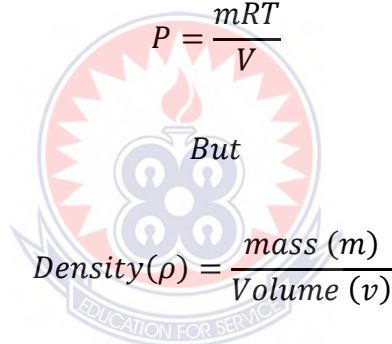
$$\text{Gas constant (R) of diesel} = \frac{\text{Universal gas constant}}{\text{Molecular weight of diesel}}$$

$$= \frac{8314.3}{230 \times 10^{-3}} = 36.15 \times 10^3 \text{ J/kgmol}$$

From the ideal gas equation

$$PV = mRT$$

$$P = \frac{mRT}{V}$$



$$\text{Density}(\rho) = \frac{\text{mass (m)}}{\text{Volume (v)}}$$

$$\text{Mass (m)} = \text{density of diesel} \times \text{volume per cylinder}$$

$$= 832 \times 10^{-9} \times 622 \times 10^3 = 0.517504\text{kg} = \mathbf{51.7504 \times 10^{-2}\text{kg}}$$

$$\text{Pressure developed in a cylinder (P)} = \frac{51.7504 \times 10^{-2} \times 36.15 \times 10^3 \times 210}{622 \times 10^3}$$

$$= \frac{3928631.616}{622 \times 10^3} = \mathbf{6.32 \text{ N/mm}^2}$$

3.5 Forces Acting on the Connecting Rod

The connecting rod is designed by taking the force of the connecting rod (F_C) equal to

the maximum force on the piston (F_P) due to gas pressure.

$$F_C = F_P = \frac{\pi D^2}{4} \times p = \frac{\pi(100)^2}{4} \times 6.32 = 49637.2 \text{ N}$$

The connecting rod is designed for buckling about x-axis. The factor of safety is taken as 5.5, therefore the buckling load,

$$W_B = F_C \times F.S = 49637.2 \times 5.5 = 273005 \text{ N}$$

The radius of gyration of the section about x-axis is;

$$K_{xx} = \sqrt{\frac{I_{xx}}{A}}$$

$$K_{xx} = \sqrt{\frac{419t^4}{12} \times \frac{1}{11t^2}} = 1.78t$$

$$\text{Length of crank, } r = \frac{\text{Stroke of Piston}}{2} = \frac{114}{2} = 57 \text{ mm}$$

Length of the connecting rod is 2 × times the stroke, $l = 228 \text{ mm}$

According to Rankine's formula, the buckling load about x-axis is:

$$W_B = \frac{\sigma_c \times A}{1 + a \left(\frac{l}{K_{xx}} \right)^2}$$

The compressive yield strength of the Aluminium alloy (Al7075) = 607.9 MPa

The Young's modulus of the material (Al 7075) = 71.7 GPa

$$a = \frac{\sigma_c}{\pi^2 \times E} = \frac{607.9 \times 10^6}{\pi^2 \times 71.7 \times 10^9} = \frac{607.9 \times 10^6}{7.0765 \times 10^{11}} = 8.59 \times 10^{-4} = 0.000859$$

$$273005 = \frac{607.9 \times 11t^2}{1 + 0.000859 \left(\frac{228}{1.78t} \right)^2}$$

$$\frac{273005}{607.9} = \frac{11t^2}{1 + 0.000859 \left(\frac{51984}{3.1684t^2} \right)} = \frac{11t^2}{1 + \frac{44.654}{3.1684t^2}}$$

$$449 = \frac{11t^2}{1 + \frac{14.09}{t^2}}$$

$$449 = \frac{11t^2}{\frac{t^2 + 14.095}{t^2}}$$

$$449 = \frac{11t^2 \times t^2}{t^2 + 14.095}$$

$$449(t^2 + 14.095) = 11t^4$$

$$449t^2 + 6328.66 = 11t^4$$

Dividing through by 11 and rearranging the equation gives:

$$t^4 - 40.82t^2 - 575.33 = 0$$

Using the formula to solve the quadratic equation gives:

$$t^2 = \frac{40.82 \pm \sqrt{(40.82)^2 + 4 \times 575.33}}{2} = \frac{40.82 \pm 62.99}{2}$$

$$= 51.905 \text{ (taking + ve sign)}$$

$$t = \sqrt{51.905} = 7.2 \text{ mm say } 7\text{mm}$$

3.5.1 Dimensions of the I-Section of the connecting rod

Thickness of the flange and web of the section $t = 7 \text{ mm}$

Width of the section, $B = 4t = 4 \times 7 = 28 \text{ mm}$

Depth of the section $H = 5t = 5 \times 7 = 35 \text{ mm}$

These dimensions are at the middle of the connecting rod. The width (B) is kept constant throughout the length of the rod, but the depth (H) varies.

The depth near the big end or crank end is kept as 1.1H to 1.25H

$$H_1 = 1.2H = 1.2 \times 35 = \mathbf{42 \text{ mm}}$$

The depth near the small end or piston end is kept as 0.75H to 0.9H.

$$H_2 = 0.85H = 0.85 \times 35 = \mathbf{29.75 \text{ mm say } 30\text{mm}}$$

Therefore,

Dimensions of the section near the big end = **42 mm × 28 mm and**

Dimensions of the section near the small end = **30 mm × 28 mm**

Since the connecting rod is manufactured by forging or casting, therefore, the sharp corners are rounded off.

To determine whether the section chosen is satisfactory, then, $\frac{I_{xx}}{I_{yy}} = 3.2$.

$$I_{xx} = \frac{419}{12}t^4 = \frac{419}{12} \times 7^4 = 83834.92 \text{ mm}^4$$

$$I_{yy} = \frac{131}{12}t^4 = \frac{131}{12} \times 7^4 = 26210.92 \text{ mm}^4$$

$$\frac{I_{xx}}{I_{yy}} = \frac{83834.92 \text{ mm}^4}{26210.92 \text{ mm}^4} = 3.198 = \mathbf{3.2}$$

This is an indication that the section chosen is satisfactory.

3.7.2 Dimensions of the crankpin or the big end bearing

Taking,

d_c = Diameter of the crankpin or big end bearing

l_c = Length of the crankpin or big end bearing = $1.3d_c$

P_{bc} = bearing pressure = 10.8 to 12.6 N/mm²

The load on the crank pin or big end bearing = Projected area \times Bearing pressure

$$= d_c \times l_c \times P_{bc} = d_c \times 1.3d_c \times 12 = 15.6(d_c)^2$$

The crankpin or the big end bearing is designed for maximum gas force (F_p), therefore, equating the load on the crankpin or big end bearing to the maximum gas force gives;

$$15.6 (d_c)^2 = F_p = 49637.2$$

$$(d_c)^2 = \frac{49637.2}{15.6} = 3182$$

Therefore,

$$d_c = \sqrt{3182} = 56.4 \text{ mm} \approx \mathbf{56 \text{ mm}}$$

The length of the crankpin is given as;

$$l_c = 1.3d_c = 1.3 \times 56 = 72.8 \text{ mm} \approx \mathbf{73 \text{ mm}}$$

The big end has a removable precision bearing shells or brass or bronze or steel with a thin lining (1 mm or less).

3.7.3 Dimensioning of the piston pin or small end bearing.

Taking

d_p = Diameter of the piston pin or small end bearing

$$l_p = \text{length of the piston pin or small end bearing} = 2d_p$$

$$P_{bp} = \text{Bearing pressure} = 15 \text{ N/mm}^2$$

The load on piston pin or small end bearing = Projected area \times Bearing pressure

$$= d_p \times l_p \times P_{bp} = d_p \times 2d_p \times 15 = 30(d_p)^2$$

The piston pin or the small end bearing is designed for the maximum gas force (F_p), therefore, equating the load on the piston pin or the small end bearing to the maximum gas force,

$$30(d_p)^2 = 49637.2$$

$$(d_p)^2 = \frac{49637.2}{30} = 1654.573333$$

$$d_p = \sqrt{1654.6} = 40.7 \approx \mathbf{41 \text{ mm}}$$

$$l_p = 2d_p = 2 \times 41 = \mathbf{82 \text{ mm}}$$

The small end bearing is usually a phosphor bronze bush of about 3 mm thickness.

3.7.4 Size of bolts for securing the big end cap

Taking

$$d_{cb} = \text{core diameter of the bolts}$$

σ_t = allowable tensile stress of the material of the bolts = 80 N/mm²

n_b = Number of bolts.

The force or load on the bolts

$$= \frac{\pi(d_{cb})^2}{4} \times \sigma_t \times n_b = \frac{\pi(d_{cb})^2}{4} \times 80 \times 2 = 125.66(d_{cb})^2$$

The bolts and the big end cap are subjected to tensile force which corresponds to the inertia force of the reciprocating parts at the top dead centre on the exhaust stroke. The inertia force of the reciprocating parts is;

$$F_1 = M_R \times \omega^2 r \left(\cos\theta + \frac{\cos 2\theta}{l/r} \right)$$

But at the top dead centre on the exhaust stroke, $\theta = 0$.

Therefore,

$$F_1 = M_R \times \omega^2 r \left(1 + \frac{r}{l} \right) = 2.5 \times \left(\frac{2\pi \times 3600}{60} \right)^2 \times 0.057 \left(1 + \frac{0.057}{0.228} \right)$$

$$= 2.5 \times 376.99^2 \times 0.057 \times 1.25 = \mathbf{25315.5 \text{ N}}$$

Equating the inertia force to the force on the bolts, gives;

$$25315.5 = 125.66(d_{cb})^2$$

$$(d_{cb})^2 = \frac{25315.5}{125.66} = 201.5$$

$$d_{cb} = \sqrt{201.5} = \mathbf{14.2 \text{ mm}}$$

The nominal diameter of the bolt,

$$d_b = \frac{d_{cb}}{0.84} = 1.2d_{cb} = 1.2 \times 14.2 = \mathbf{17 \text{ mm}}$$

3.7.5 The thickness of the big end cap

Taking

t_c = thickness of the big end cap

b_c = Width of the big end cap. It is taken equal to the length of the crankpin or

big end bearing (l_c) = 73 mm

σ_b = allowable bending stress for the material of the cap = 100 N/mm²

The big end cap is designed as a beam freely supported at the cap bolt centres and loaded by the inertia force at the top dead centre on the exhaust stroke (*i.e.*, F_1 when $\theta = 0$). Since the load is assumed to act in between the uniformly distributed load and the centrally concentrated load, therefore, maximum bending moment is taken as $M_C = \frac{F_1 \times x}{6}$

Where,

x = Distance between the bolt centres

= Diameter of crankpin or big end bearing + 2 × thickness of the bearing liner + Nominal diameter of bolt + clearance.

$$= (d_c + 2 \times 3 + d_b + 3) \text{mm} = 56 + 6 + 17 + 3 = \mathbf{82 \text{ mm}}$$

Therefore, maximum bending moment acting on the cap,

$$M_C = \frac{F_1 \times x}{6} = \frac{25315.5 \times 82}{6} = \mathbf{345978.5 \text{ Nmm}}$$

Section modulus for the cap

$$Z_c = \frac{b_c(t_c)^2}{6} = \frac{73 \times (t_c)^2}{6} = 12.17(t_c)^2$$

Bending stress (σ_b),

$$100 = \frac{M_c}{Z_c} = \frac{345978.5}{12.17(t_c)^2} = \frac{28428.8}{(t_c)^2}$$

$$(t_c)^2 = \frac{28428.8}{100} = 284.288$$

$$t_c = \sqrt{284.288} = 16.9 \text{ mm} \approx \mathbf{17 \text{ mm}}$$

Let us now check the design for the induced bending stress due to inertia bending forces on the connecting rod (i.e., whipping stress).

The mass of the connecting rod per meter length,

$$m_1 = \text{Volume} \times \text{density} = \text{Area} \times \text{length} \times \text{density}$$

The density of A7075 T651 is $2.81 \text{ g/cm}^3 = 2810 \text{ kg/m}^3$

$$m_1 = A \times l \times \rho = 11t^2 \times l \times \rho = 11(0.007)^2 \times (0.228) \times 2810 = 0.345 \text{ kg}$$

Maximum bending moment,

$$M_{max} = m \times \omega^2 r \times \frac{l}{9\sqrt{3}} = m_1 \times \omega^2 r \times \frac{l^2}{9\sqrt{3}}$$

$$= 0.345 \left(\frac{2 \times \pi \times 3600}{60} \right)^2 (0.057) \frac{(0.228)^2}{9\sqrt{3}}$$

$$= 0.345 \times 376.99^2 \times 0.057 \times \frac{0.051984}{9\sqrt{3}} = \frac{145.29}{15.588} = 9.32 \text{ Nm} = \mathbf{9320.63 \text{ Nmm}}$$

and section modulus,

$$Z_{xx} = \frac{I_{xx}}{5t/2} = \frac{419t^4}{12} \times \frac{2}{5t} = 13.97t^3 = 13.97 \times 7^3 = \mathbf{4792 \text{ mm}^3}$$

Therefore, maximum bending stress (induced) due to inertia bending forces or whipping

$$\text{stress, } \sigma_b = \frac{M_{max}}{Z_{xx}} = \frac{9320.63}{4792} = \mathbf{1.95 \text{ N/mm}^2}$$

Since the maximum bending stress induced (1.95 N/mm^2) is less than the allowable bending stress of 100 N/mm^2 , therefore the design is very safe.

3.7.6 Determination of the outer diameters of big end and small end

The inner diameter of the Big End (D_{in})

$$= \text{The diameter of crankpin } (d_c) + \text{Thickness of the bush } (t_b)$$

$$\text{The inner diameter of the Big End } (D_{in}) = 56 + 2 = \mathbf{58 \text{ mm}}$$

$$\text{Marginal thickness } (t_m) = 5 \text{ to } 15 \text{ mm}$$

$$\text{Bolt diameter } (d_b) = 17 \text{ mm}$$

$$\text{Thickness of the bush } (t_b) = 2 \text{ to } 5 \text{ mm}$$

$$\text{Diameter of the crankpin } (d_c) = 56 \text{ mm}$$

$$\text{The outer diameter of the big end } (D_{out}) = d_c + 2t_b + 2d_b + 2t_m$$

$$= 56 + 2 \times 2 + 2 \times 17 + 2 \times 5 = 56 + 4 + 34 + 10 = \mathbf{104 \text{ mm}}$$

The inner diameter of the Small End (d_{in})

$$= \text{The diameter of piston pin } (d_p) + \text{Thickness of the bush } (t_b)$$

$$\text{The inner diameter of the Small End } (d_{in}) = 41 + 2 = \mathbf{43 \text{ mm}}$$

$$\text{Thickness of the bush } (t_b) = 2 \text{ to } 5 \text{ mm}$$

$$\text{Marginal thickness } (t_m) = 5 \text{ to } 15 \text{ mm}$$

The diameter of piston pin (d_p) =

$$\begin{aligned} \text{The outer diameter of the small end } (d_{out}) &= d_p + 2t_b + 2t_m = 41 + 2 \times 2 + 2 \times 5 \\ &= 41 + 4 + 10 = \mathbf{55 \text{ mm}} \end{aligned}$$

Table 3.3 Specifications of the connecting rod

serial No.	Connecting Rod Parameters (mm)
1	Thickness of the connecting rod (t) = 7
2	Width of the section ($B = 4t$) = 28
3	Height of the section ($H = 5t$) = 35
4	Height at the Big End ($H_1 = 1.2H$) = 42
5	Height at the small end ($H_2 = 0.85H$) = 30
6	Inner diameter of the Small End = 43
7	Outer diameter of the Small End = 55
8	Inner diameter of the Big End = 58
9	Outer diameter of the Big End = 104
10	Diameter of the bolt = 17
11	Thickness of the big end cap = 17
12	<i>Length of connecting rod</i> = 228
13	<i>Crank pin diameter</i> = 56
14	Length of crank pin = 73
15	Piston pin diameter = 41
16	Length of piston pin = 81

3.8 Modelling of Component in Autodesk Inventor 2017

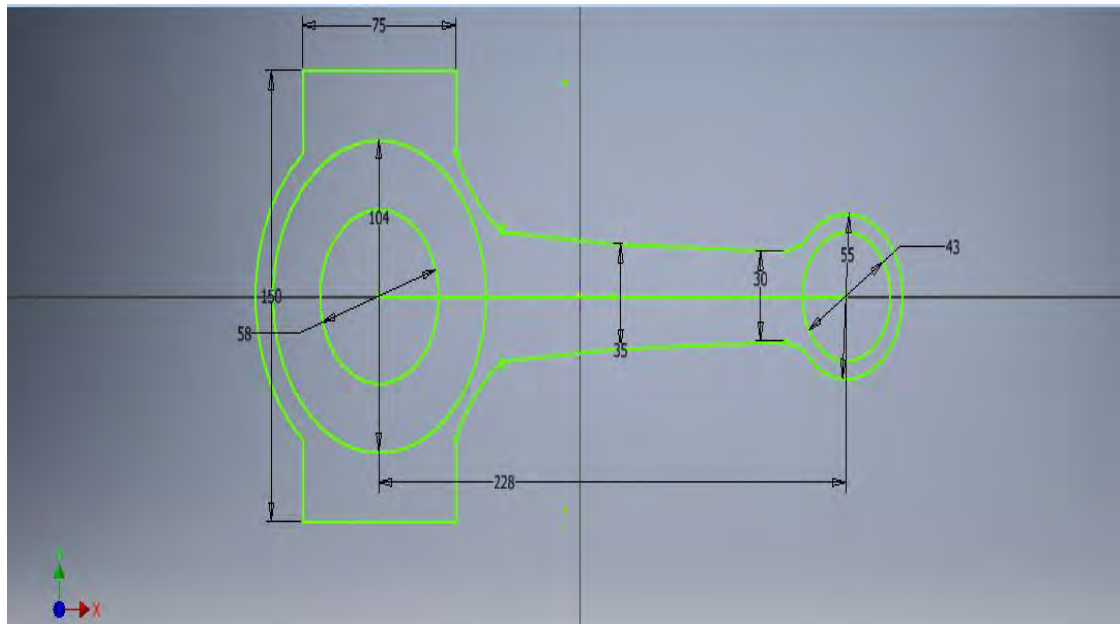


Figure 3.4 Dimensioning of the Connecting Rod

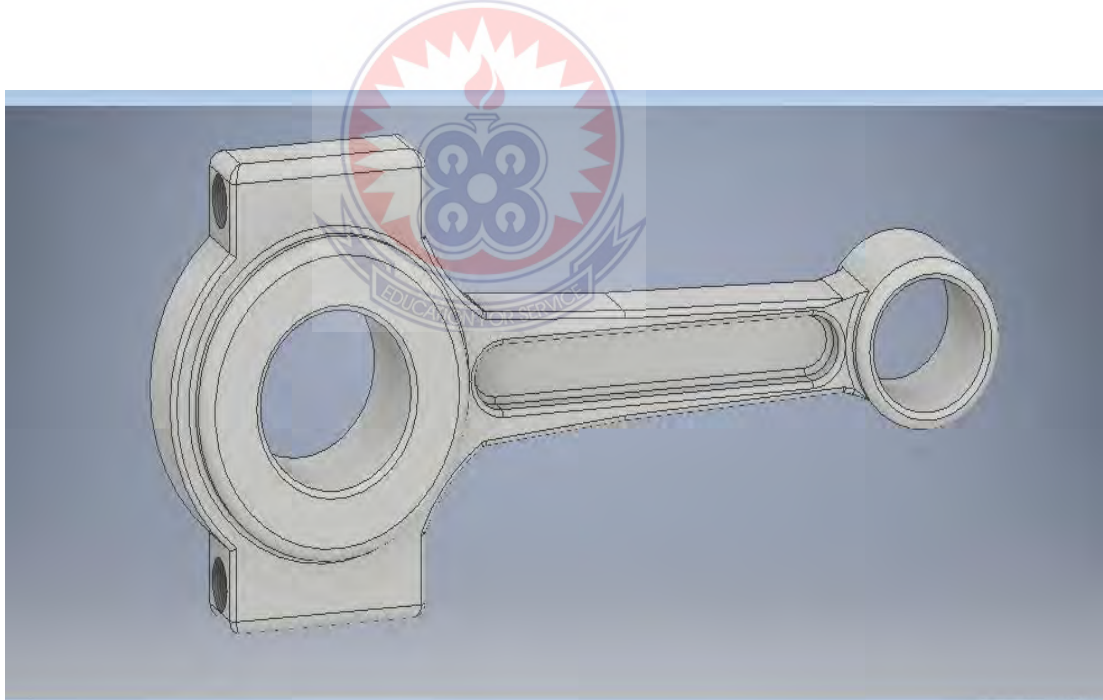


Figure 3.5 Connecting Rod with the Big End Cap and Bottom End Joined

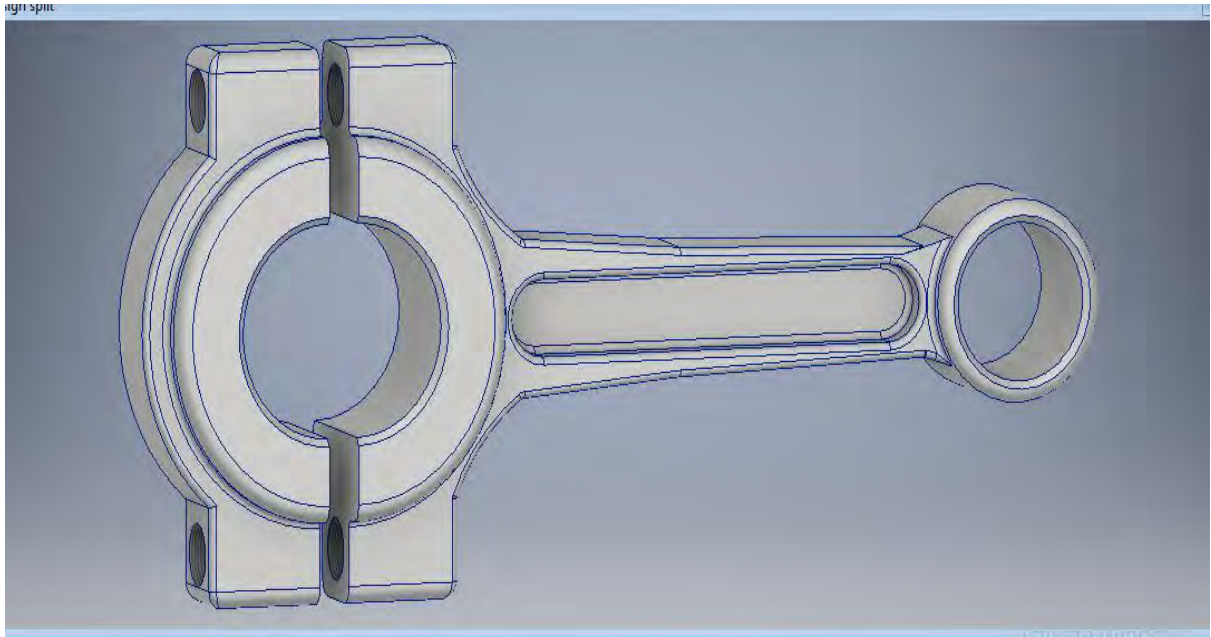


Figure 3.6 The Connecting Rod with the Big End Cap Splitted from the Bottom



Figure 3.7 Bolt of the Connecting Rod

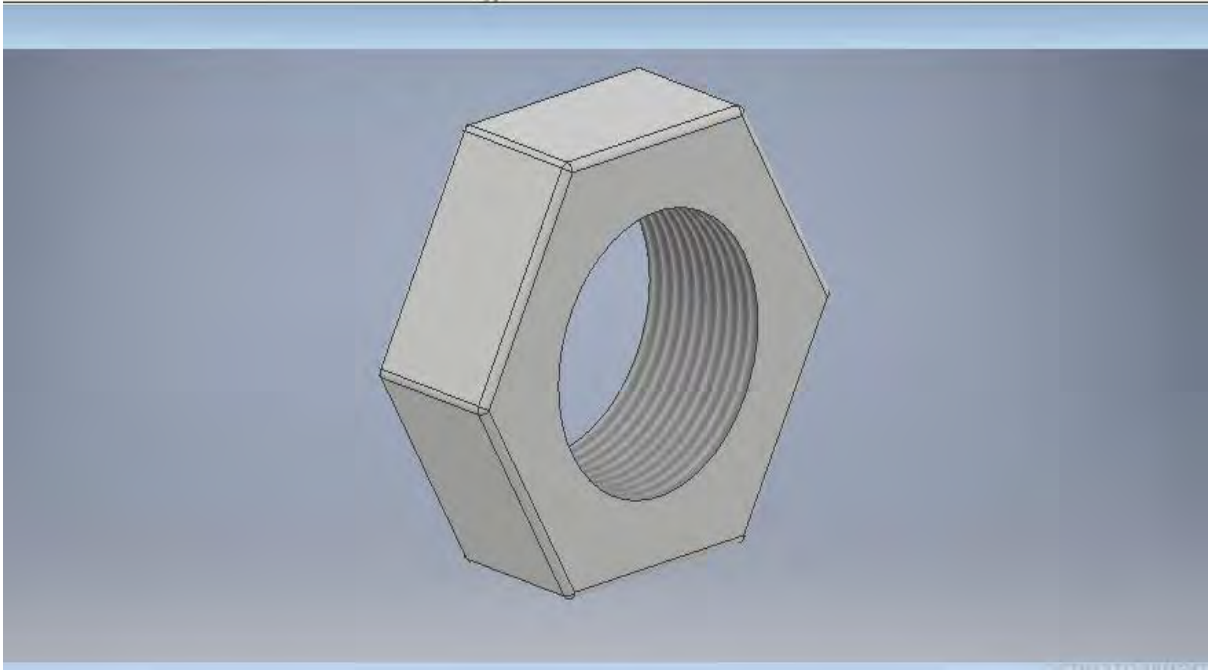


Figure 3.8 Nut of the Connecting Rod

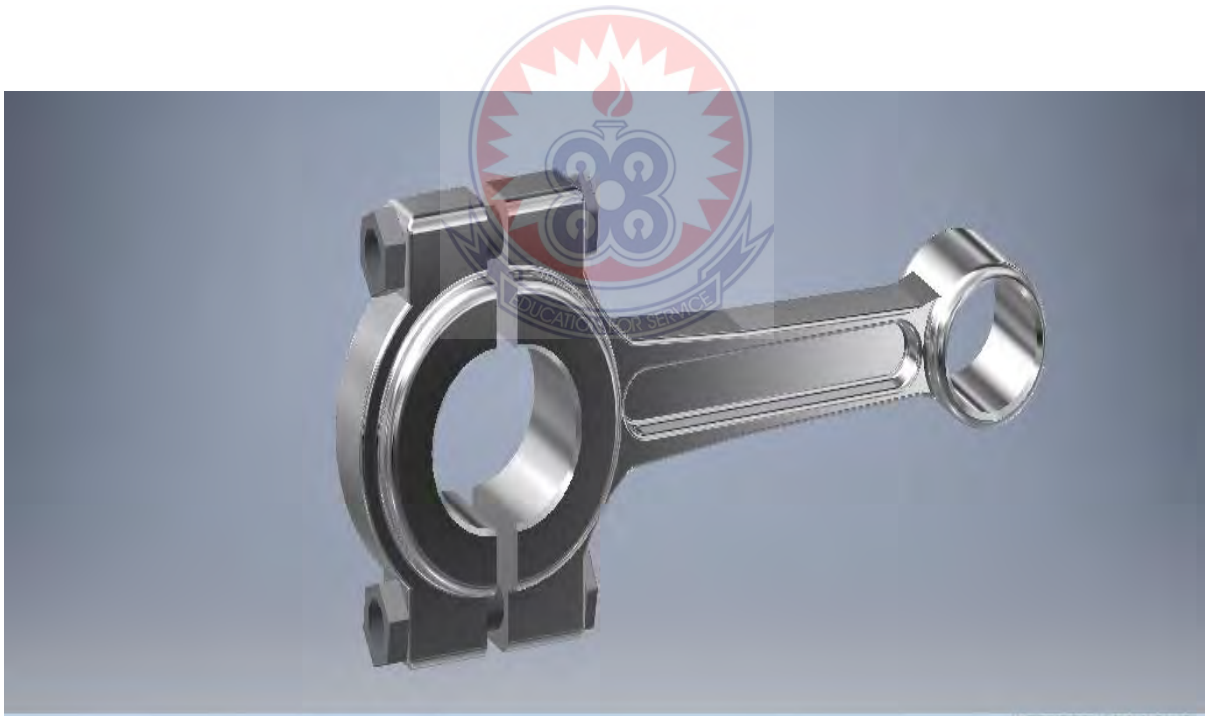


Figure 3.9 Assembly of the Connecting Rod after Al7075 was Applied

3.9 Procedure for the Numerical Methods

This section of the study presents the procedure for the numerical methods which includes: meshing of the component, grid independence test and the boundary conditions set for this study.

3.9.1 Meshing of Component

Meshing is very important step in static structural and modal analysis process. Meshing is an integral part of the engineering simulation process where complex geometries are divided into simple elements that can be used as discrete local approximations of the larger domain. The mesh influences the accuracy, convergence and speed of the simulation. If meshing is accurate, then the results are also anticipated to be feasible. The meshing details of the model connecting rods are: number of nodes 22570 and element size 12764. The meshing of the Nissan Pickup connecting rod is as shown in

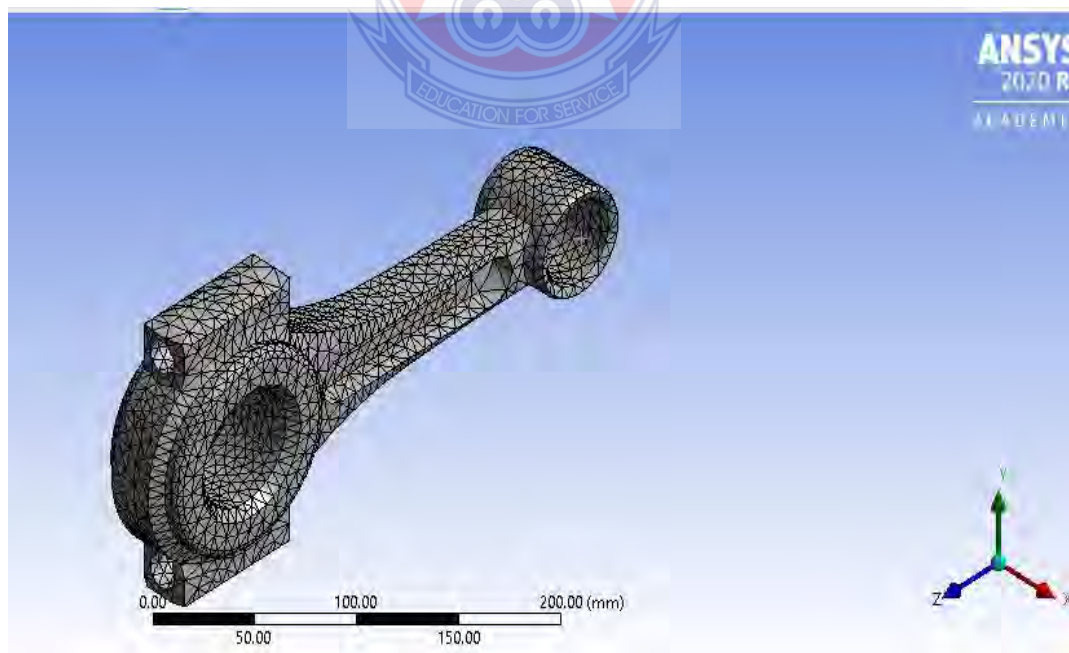


Figure 3.10.

Figure 3.10 Connecting rod Meshed in Ansys

3.9.2 Grid Independence Test

The mesh size of the connecting rod was carefully selected since the validity of the mesh can influence the results. Independent test for four (4) iterations were conducted with mesh sizes 2 mm, 3 mm 4 mm and 5 mm and the best iteration number was selected as the mesh size. The results of the independent tests with a resolution of six (6) are as summarise in Table 3.4.

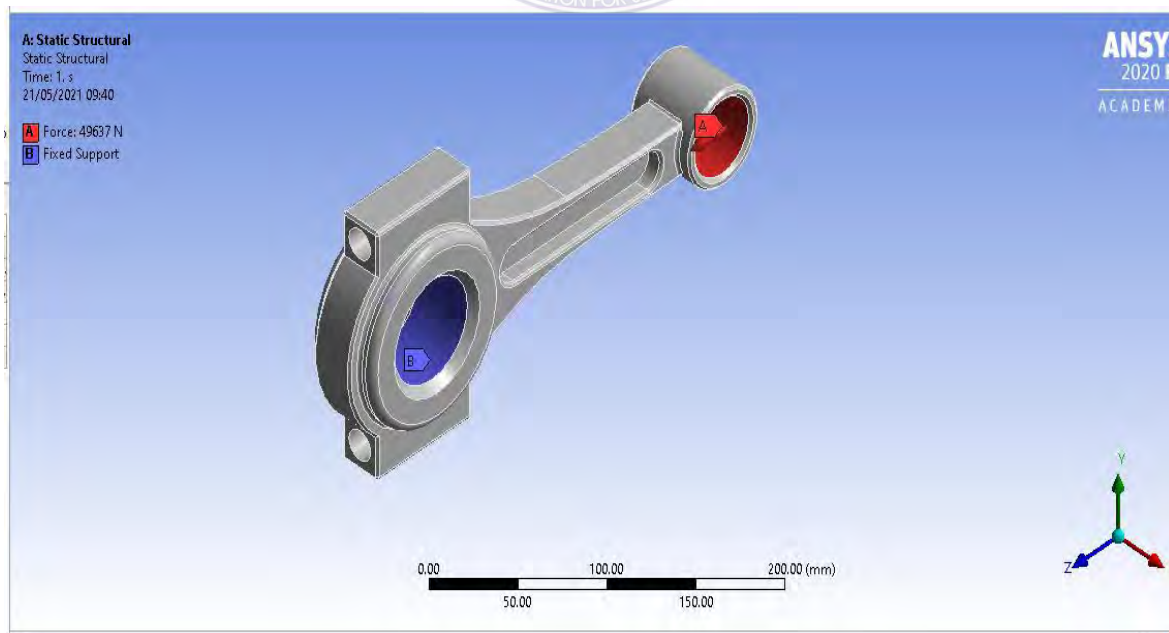
Table 3.4 Grid Independence Test Results

Mesh Size	Number of Nodes	Von Mises Stress	Deformation
2 mm	31835	411.78 MPa	0.216 mm
3 mm	22570	378.75 MPa	0.227 mm
4 mm	22621	420.67 MPa	0.225 mm
5 mm	21450	429.72 MPa	0.221 mm

From Table 3.4 it is evident that the mesh size that yielded the best induced Von Mises stress is mesh size 3 mm. It can be observed from Table 3.4 that all the mesh sizes yielded almost the same magnitudes of deformation with an approximation of 0.23 mm with the exception of mesh size 2 mm which produced a deformation of approximately 0.22 mm. The highest deformation of 0.23 was adopted for this experiment to ensure that the result is closer to reality. Based on Table 3.4 the mesh size that yielded the lowest induced Von Mises stress of 378.75 MPa and a deformation of approximately 0.23 mm is mesh size 3 mm. Hence, the model connecting rods of the four different materials were analysed in Ansys by using mesh size of 3.0 mm with 22570 nodes at a resolution of six (6).

3.7.3 The Boundary Conditions Set for the Analysis

Analysis of the connecting rods made with four different materials was done in Ansys software version 2020 R2 using static structural analysis. The big end of the connecting rod was constraint (fixed) and a compressive load of 49637.2 N was applied at the small end portion of the connecting rod. Compressive load was considered because, connecting rods are designed for the maximum gas load acting on the piston. This load subject the connecting rod to compression, the connecting rod comes under tension due to the inertial of the reciprocating and rotating parts of the engine. The calculated maximum gas load for the engine which connecting rod is under consideration is 49637.2N. The parameters that were considered during the static structural analysis were: total deformation, directional deformation, equivalent elastic strain, equivalent (Von Mises) stress, maximum principal stress, minimum principal stress and safety



factor of the four (4) materials assigned to the model.

Figure 3.11The boundary condition for the analysis

3.8 Fabrication of the Connecting Rod

Forging is a manufacturing process involving the shaping of metal using localized compressive forces. Forging is often classified according to the temperature at which it is performed: "cold", "warm", or "hot" forging. Wrought Aluminium alloy 7075 was chosen for fabricating the connecting rod due to its low cost, weight and high strength. The fabrication of the connecting rod was started by preparing the aluminium alloy block. The chemical composition of the aluminium alloy 7075 comprised, 90% Aluminium, 5.6% Zinc, 2.5% Magnesium, 0.23% Iron and 1.6% Copper. The metals were heated in a crucible furnace to various degrees of temperature until the solid metals were converted to semi-solid. The mixture of the semi-solid aluminium and the aforementioned metals were mixed proportionally according to the percentages given. The mixture was stirred in the crucible furnace until a homogeneous mixture was achieved. The mixture was then poured into a sand-casting mould and was allowed to naturally cool to solidification. The cast aluminium 7075 alloy block was fabricated in the cool state to refine the grain structure of the metal as shown in Figure 3.12.



Figure 3.12 Sand Cast Rectangular Al7075 T6 Block



Figure 3.13 Crucible Furnace

The sand-cast rectangular aluminium 7075 alloy block was cast to a thickness of 35mm.

The block was then fabricated to take the shape of the connecting rod shown in Figure

3.14

taking

cognis

ance



of the design dimensions. The big end and the small end holes were drilled using pillar drilling machine and later milled with a milling machine to their required diameters. The big end cap was sawed from the bottom end of the connecting rod. The fabricated connecting rod was heat treated to increase the strength of the connecting rod to be able to endure the high compressive load as a result of the gas pressure acting on the piston.

Figure 3.14 Fabrication of Al 7075 T6 connecting rod

CHAPTER FOUR

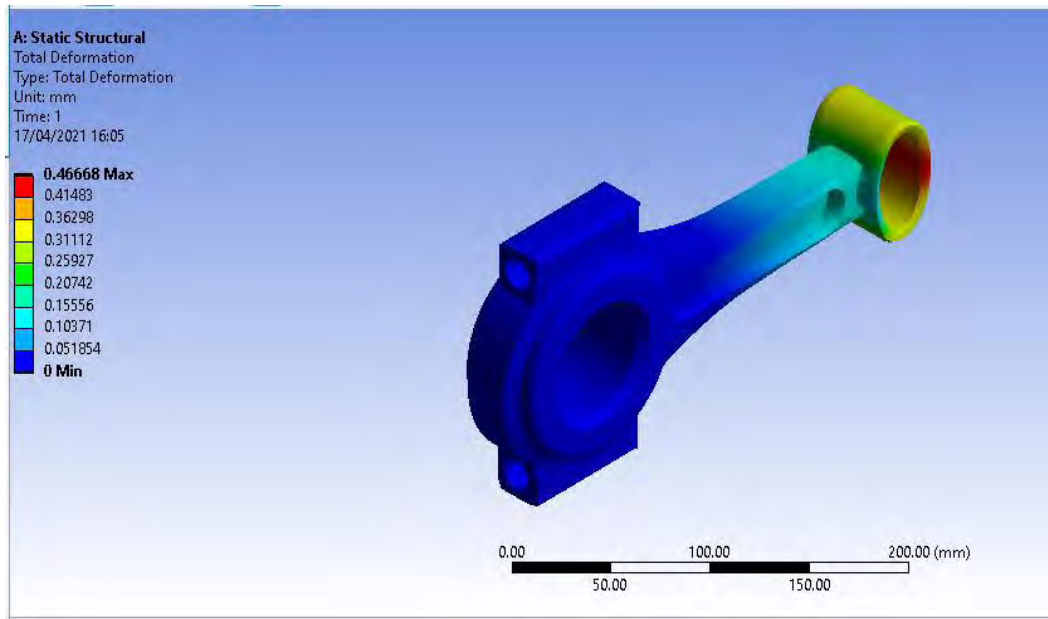
PRESENTATION OF RESULTS AND ANALYSIS

4.0 Introduction

This chapter presents the simulated results on the static structural and the modal analysis for all the four (4) connecting rod materials, namely: titanium alloy, structural steel, grey cast iron and aluminium 7075 T6 alloy used in this work. The chapter also discusses and compared the results obtained from the simulation. The weight of the connecting rods of titanium alloy, structural steel, grey cast iron and aluminium 7075 T6 alloy materials were also compared.

4.1 Static Structural Analysis of the Connecting Rod

a. T

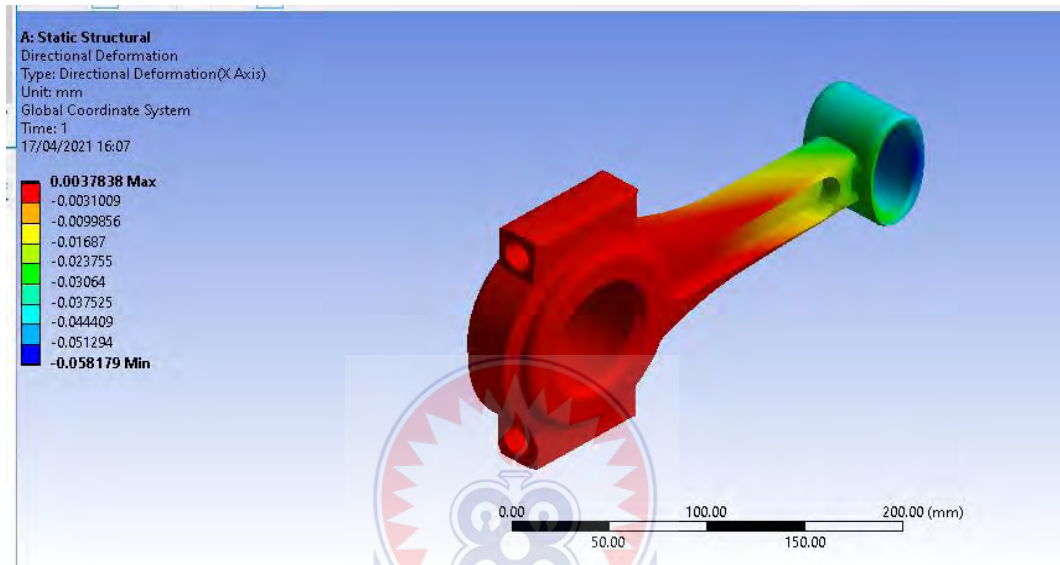


itan
ium
allo
y
mat
eria
l



Figure 4.1 Total Deformation of Titanium Alloy Material

The Total maximum deformation induced in the titanium alloy connecting rod when a compressive load of 49637.2N was applied is 0.46668 mm. Titanium has a percentage reduction of 23% which is far greater than the induced deformation when the load was applied. So, the model will remain safe with the induced deformation in the titanium alloy connecting rod. The maximum deformation was observed to have occurred at the



small end of the titanium alloy connecting rod where the load was applied. The big end of the connecting rod did not suffer any visible form of deformation as shown in Figure 4.1.

Figure 4. 2 Directional Deformation of Titanium Alloy Material

The maximum directional deformation induced in the x direction is with the magnitude of 0.0037838 mm and a minimum directional deformation of -0.058179 mm. Titanium has a percentage reduction of 23% which is far greater than the induced directional deformation when the compressive load was applied. The directional deformation in the x direction was observed to be more pronounced at the big end of the connecting rod spreading through the shank towards the small end of the connecting rod as shown in Figure 4.2. The connecting rod is noted to buckle in the x direction more than the y

direction. Since the deformation in the x direction was insignificant, the model will remain safe with the induced directional deformation in the connecting rod

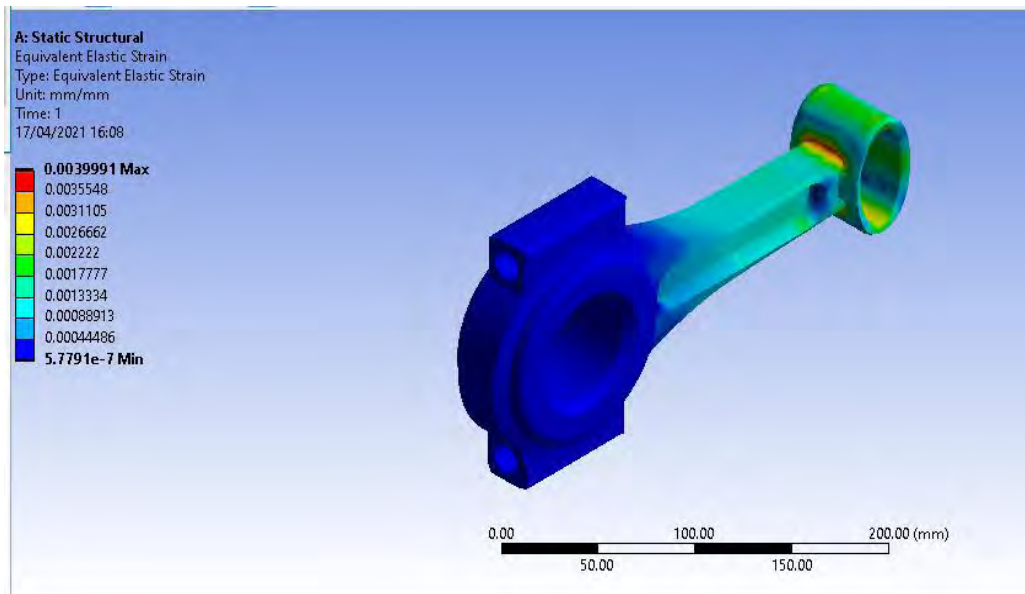


**Fig
 ure
 4.3
 Eq
 uiv
 ale
 nt**

Elastic Strain of Titanium Alloy Material

The magnitudes of the maximum and minimum equivalent elastic strain induced in the model titanium alloy connecting rod are 0.0039991 and 5.779×10^{-7} respectively for the given loading condition. It was observed that the equivalent elastic strain in the model connecting rod was more pronounced at the piston end of the connecting rod. The big end of the connecting rod experienced the minimum elastic strain as shown in Figure 4.3.

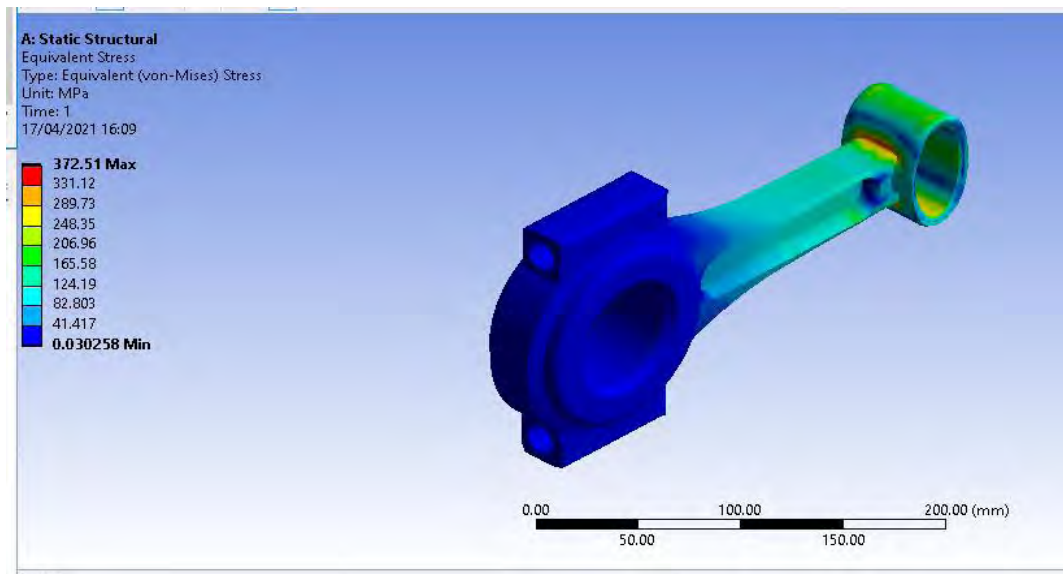


Figure 4.4 Equivalent (Von Mises) Stress of Titanium Alloy Material

The maximum equivalent (Von Mises) stress induced in the titanium alloy connecting rod has a magnitude of 372.57 MPa for the given loading condition. The compressive yield strength of titanium alloy is 848 MPa. The stress distribution in the titanium alloy connecting rod was observed to be high at the piston end of the connecting rod and reduces gradually towards the big end of the connecting rod. The big end of the connecting rod was observed to have the minimum induced Von Mises stress as shown in Figure 4.4. The induced stresses in the titanium alloy connecting rod are far lower compared to compressive yield strength of the titanium alloy material. The model can therefore be considered to be fit for purpose since it can withstand the given load imposed on the connecting rod.

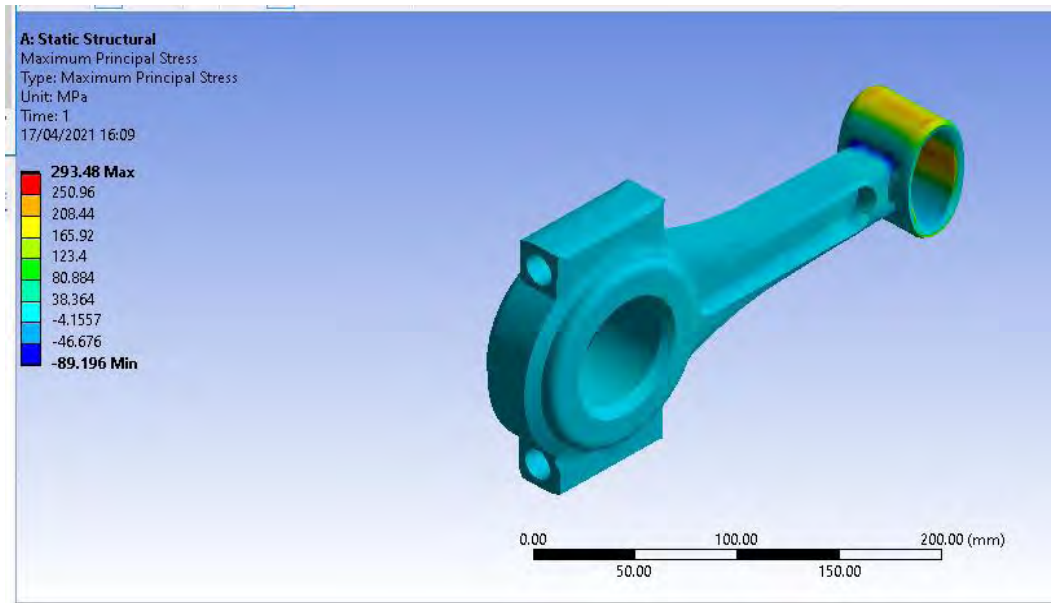


Figure 4.5 Maximum Principal Stress of Titanium Alloy Material

The maximum principal stress induced in the titanium alloy connecting rod was of a magnitude of 293.48 MPa for the given loading condition. The compressive yield strength of titanium alloy is 848 MPa. The maximum principal stress was observed to be more pronounced at the circumference of the piston end. It was also observed from Figure 4.5 that, the maximum principal stress was distributed evenly from the piston end through the shank to the big end of the titanium alloy connecting rod with a minimum stress of -46.676 MPa as shown in Figure 4.5. The induced maximum principal stress is far lower compared to the compressive yield strength of the titanium alloy material. The model can therefore be considered to be fit for purpose since it can withstand the given loading condition.

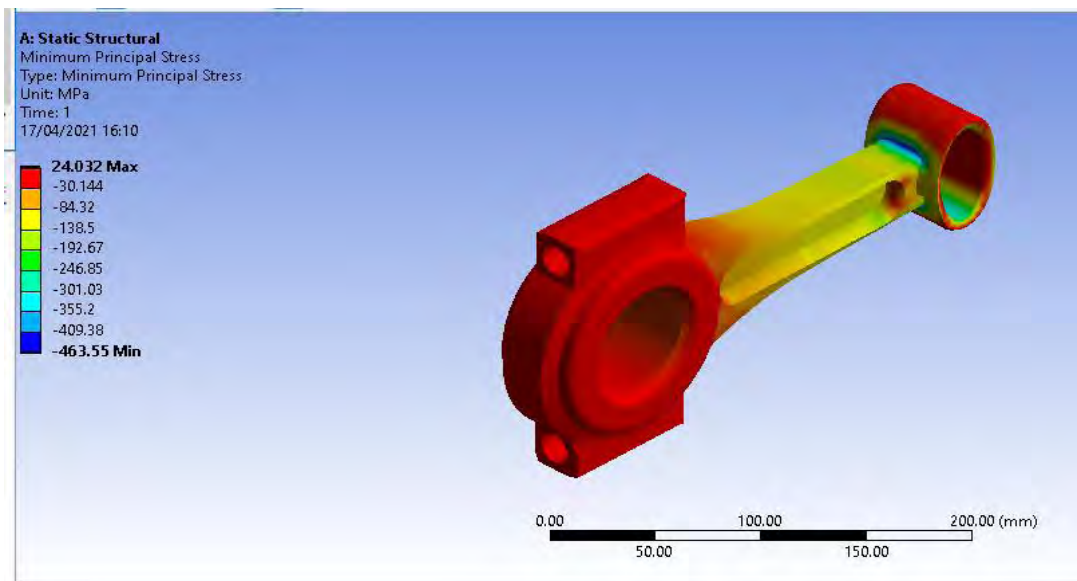


Figure 4.6 Minimum Principal Stress of Titanium Alloy Material

The minimum principal stress induced in the titanium alloy connecting rod has a maximum magnitude of 24.67 MPa for the given loading condition. The induced minimum principal stress was observed to be maximum at the big end of the connecting rod. The minimum principal stress induced in the shank portion of the connecting rod ranges from -84.32 MPa to -192 MPa as shown in Figure 4.6. The induced minimum principal stress is far lower compared to the compressive yield strength of 848 MPa of the titanium alloy material. The model can therefore be considered to be fit for purpose since it can withstand the given load condition.

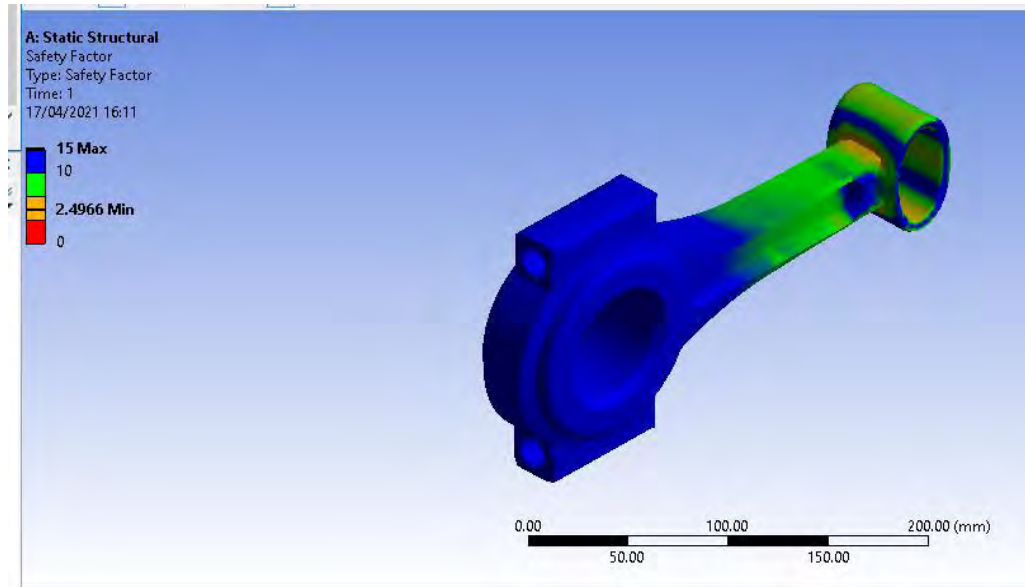


Figure 4.7 Factor of Safety of Titanium Alloy Material

The theoretical factor of safety value for connecting rods is 5.5. The Ansys generated factor of safety for titanium alloy connecting rod model has a maximum and minimum factor of safety range magnitudes of 15 and 2.4966 respectively. The big end of the titanium alloy connecting rod was observed to have a higher factor of safety than the small end of the connecting rod where the load was applied as shown in Figure 4.7. The theoretical factor of safety value of 5.5 was found to be within the range of factor of safety values generated by Ansys. The model is therefore very safe.

Table 4.1 Summary Results for Titanium Alloy material

Parameters	Maximum	Minimum
Total deformation	0.46668 mm	0.051854 mm
Directional deformation	0.0037838 mm	-0.058179 mm
Equivalent Elastic Strain	0.0039991	5.779×10^{-7}
Equivalent Von Mises Stress	372.57 MPa	0.030258 MPa
Maximum Principal Stress	293.48 MPa	89.196 MPa
Minimum Principal Stress	24.032 MPa	-463.55 MPa
Factor of Safety	15	2.4966

Table 4.1 shows a summary of the results obtained when static structural analysis was conducted on the model titanium alloy connecting rod.

b. Structural Steel material

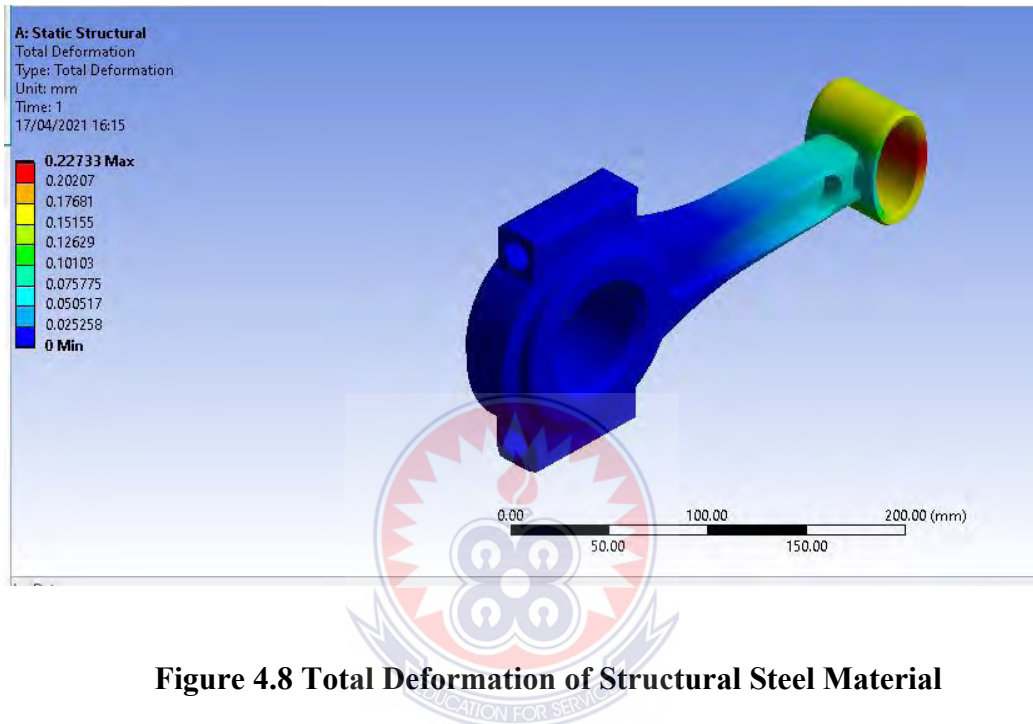


Figure 4.8 Total Deformation of Structural Steel Material

The Total maximum deformation induced in the model structural steel connecting rod when a compressive load of 49637.2N was applied at the small end is 0.22733 mm. Structural Steel has a percentage elongation or reduction of 21% which is far greater than the induced deformation of the connecting rod when the compressive load was applied. It was observed from Figure 4.8 that, minimum deformation occurred at the big end of the structural steel connecting rod. The deformation was pronounced at the small end of the structural steel connecting rod where the compressive load was applied. So, the structural steel connecting rod will remain safe with the induced total deformation.

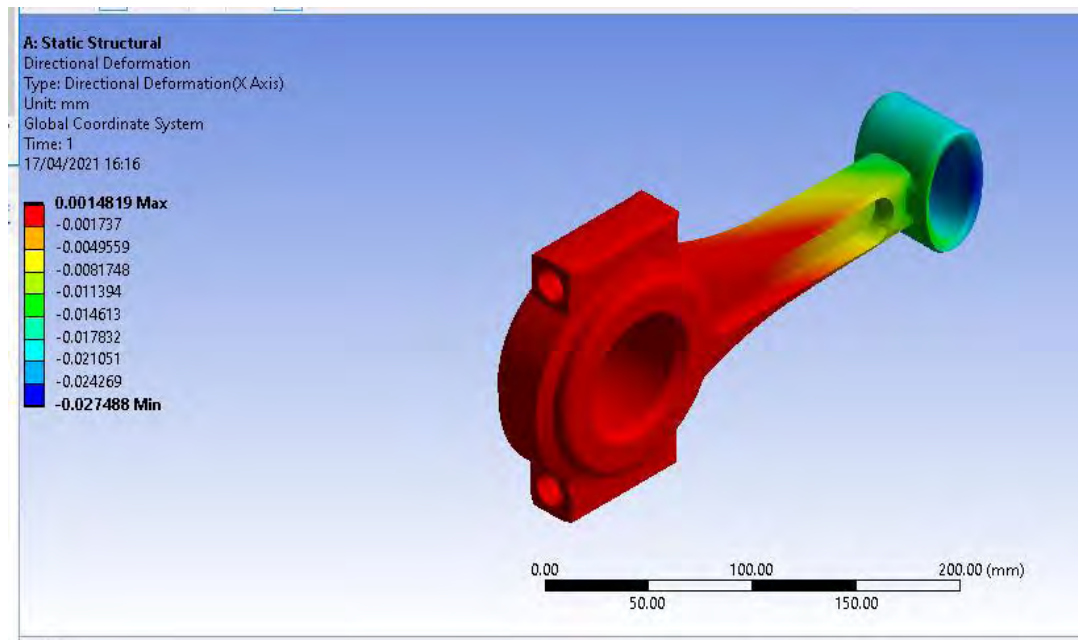


Figure 4.9 Directional Deformation of Structural Steel Material

The maximum directional deformation induced in the x direction of the structural steel connecting rod has a magnitude of 0.0014819mm. Structural Steel has a percentage elongation or reduction of 21% which is far greater than the induced maximum directional deformation when the compressive load was applied. Figure 4.9 shows that maximum directional deformation occurred at the big end of the structural steel connecting rod. Part of the shank of the connecting rod also suffered maximum directional deformation but the directional deformation was minimum at the piston end of the connecting rod as shown in Figure 9.

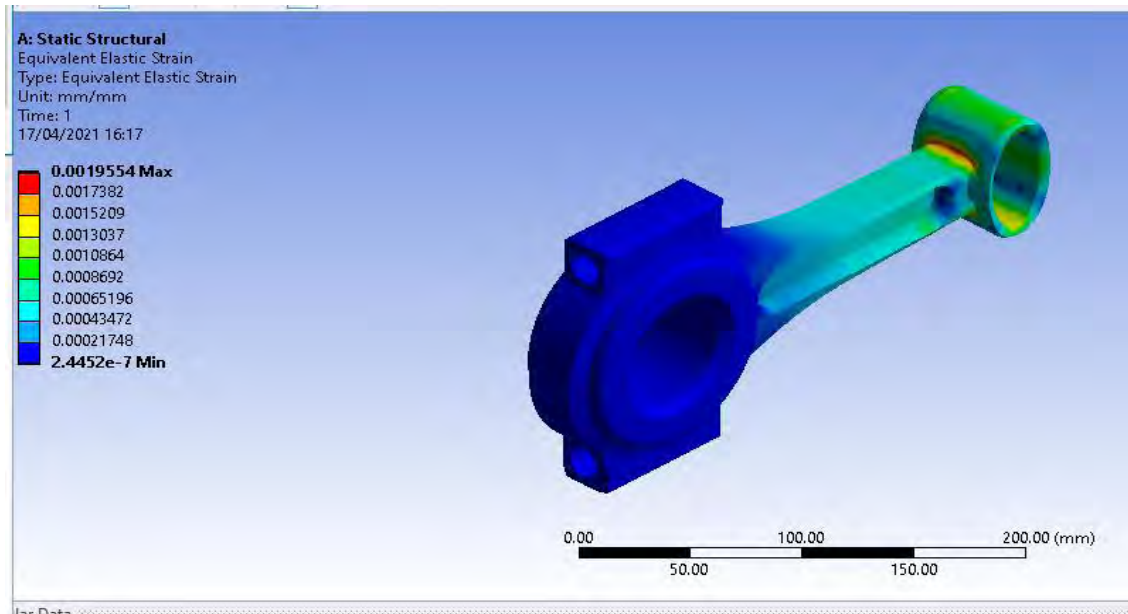
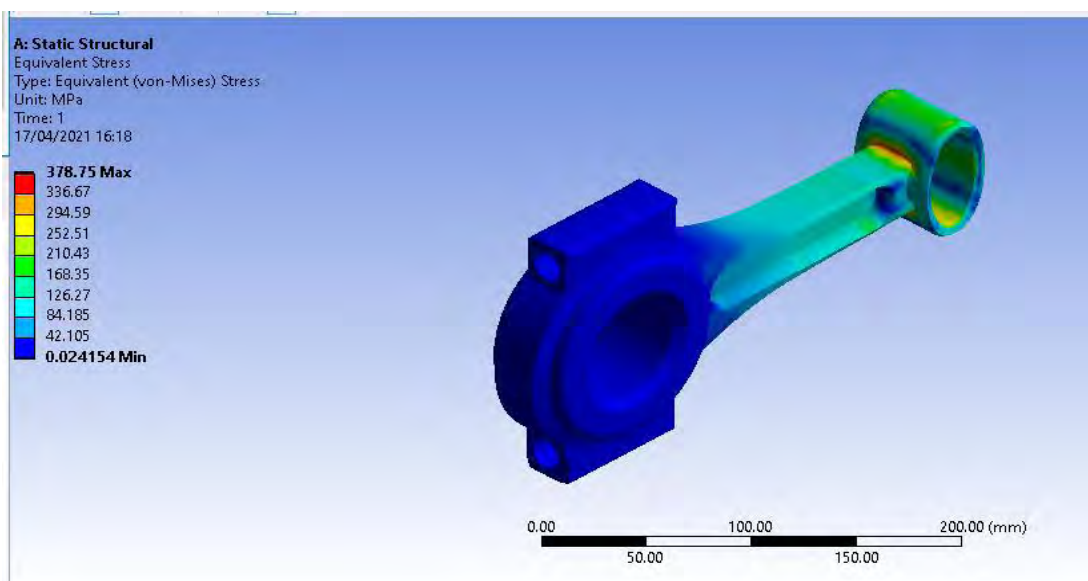


Figure 4.10 Equivalent Elast Strain of Structural Steel Material

The magnitudes of maximum and minimum equivalent elastic strain induced in the model structural steel connecting rod are 0.001955 and 2.4452×10^{-7} respectively for the given loading condition. It was observed that the equivalent elastic strain was more pronounced at the small end of the connecting rod. The big end of the structural steel connecting rod was observed to have suffered the least equivalent elastic strain as



shown in Figure 4.10.

Figure 4.11 Equivalent (Von Mises) Stress of Structural Steel Material

The maximum equivalent (Von Mises) stress induced in the structural steel connecting rod has a maximum magnitude of 378.75 MPa for the given loading condition. The compressive yield strength of Structural Steel is 920 MPa. The stress distribution in the structural steel connecting rod was lower at the big end of the connecting rod. It was observed that the maximum stress occurred at the small end of the connecting rod where the compressive load was applied as shown in Figure 4.11. The induced Von Mises stress is lower compared to the compressive yield strength of the Structural Steel material. For material optimisation, material can be removed from the big end of the structural steel connecting rod for improve weight and cost reduction. The model can therefore be considered to be fit for purpose since it can withstand the given loading condition.

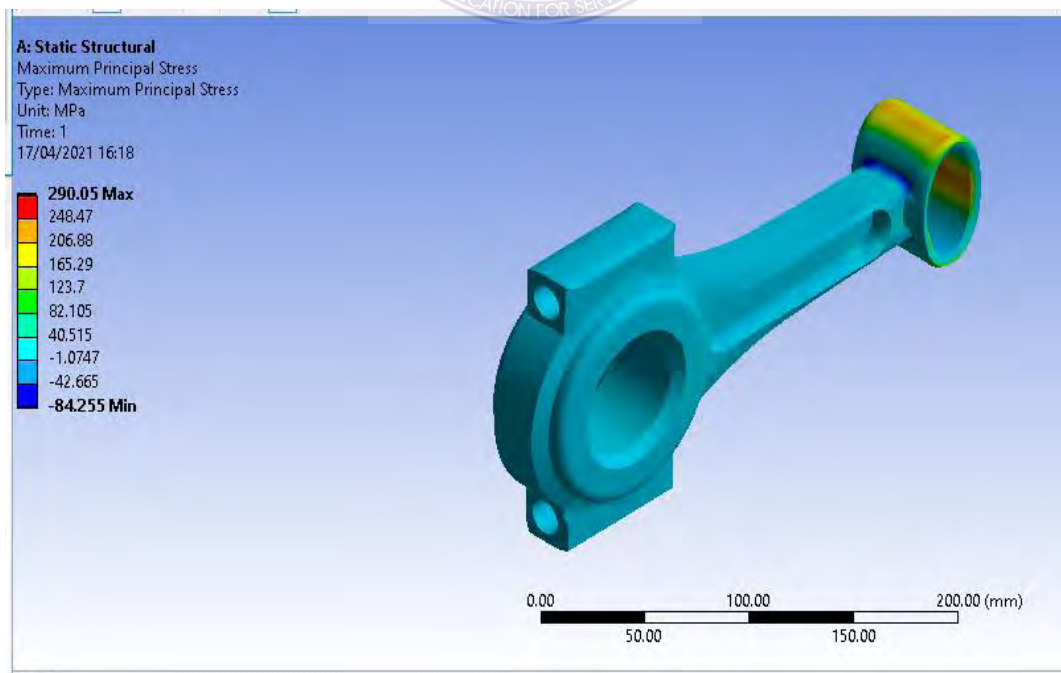
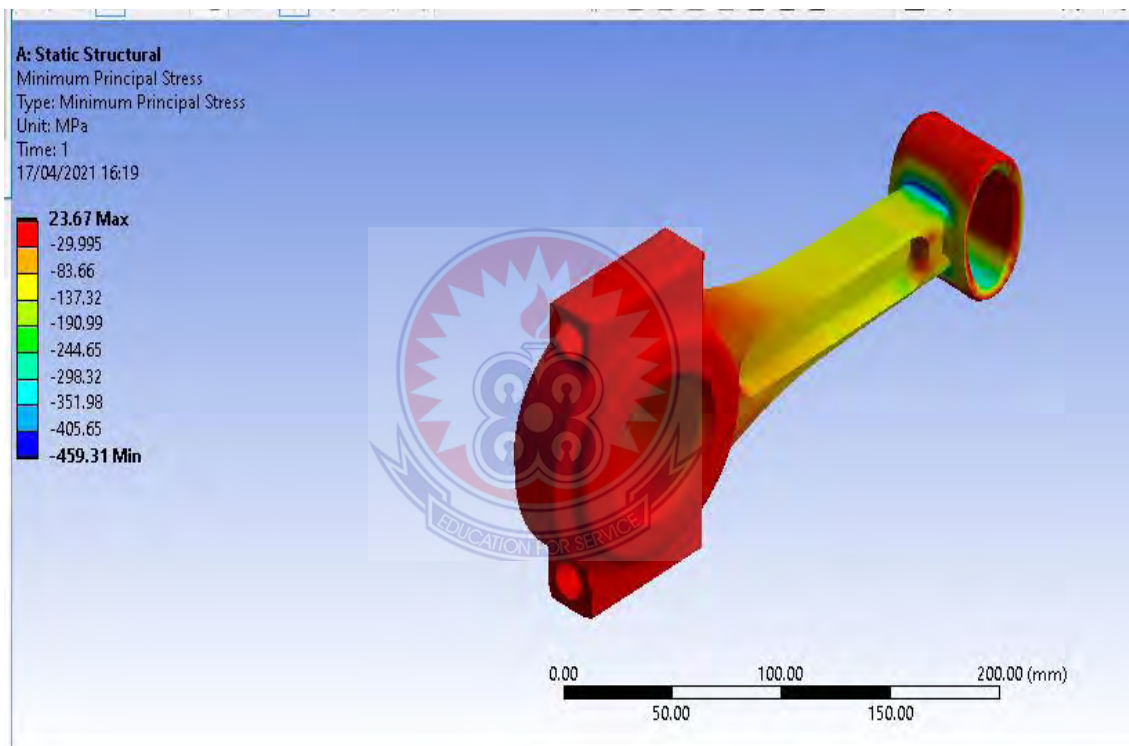


Figure 4.12 Maximum Principal Stress of Structural Steel Material

The maximum principal stress induced in the structural steel connecting rod has a maximum magnitude of 290.05 MPa for the given loading condition. The compressive yield strength of structural steel is 920 MPa. It was observed that, the maximum principal stress was evenly distributed from the big end to the end of the shank towards the piston pin end of the connecting rod with a uniform stress distribution of -42.665 MPa. The maximum value of the maximum principal stress was observed at the small end of the connecting rod as shown in Figure 4.12. The induced maximum principal



stress in the structural steel connecting rod is far lower compared to the compressive yield strength of the structural steel material. The model can therefore be considered to be safe since it can withstand the given loading condition.

Figure 4.13 Minimum Principal Stress of Structural Steel Material

The minimum principal stress induced in the structural steel connecting rod has a maximum magnitude of 23.67 MPa for the given loading condition. The compressive yield strength of structural steel is 920 MPa. Maximum value of the minimum principal

stress occurred at the big end and part of the small end of the connecting rod as shown in Figure 4.13. The induced minimum principal stress is far lower compared to the compressive yield strength of the structural steel material. The model can therefore withstand the given loading condition.

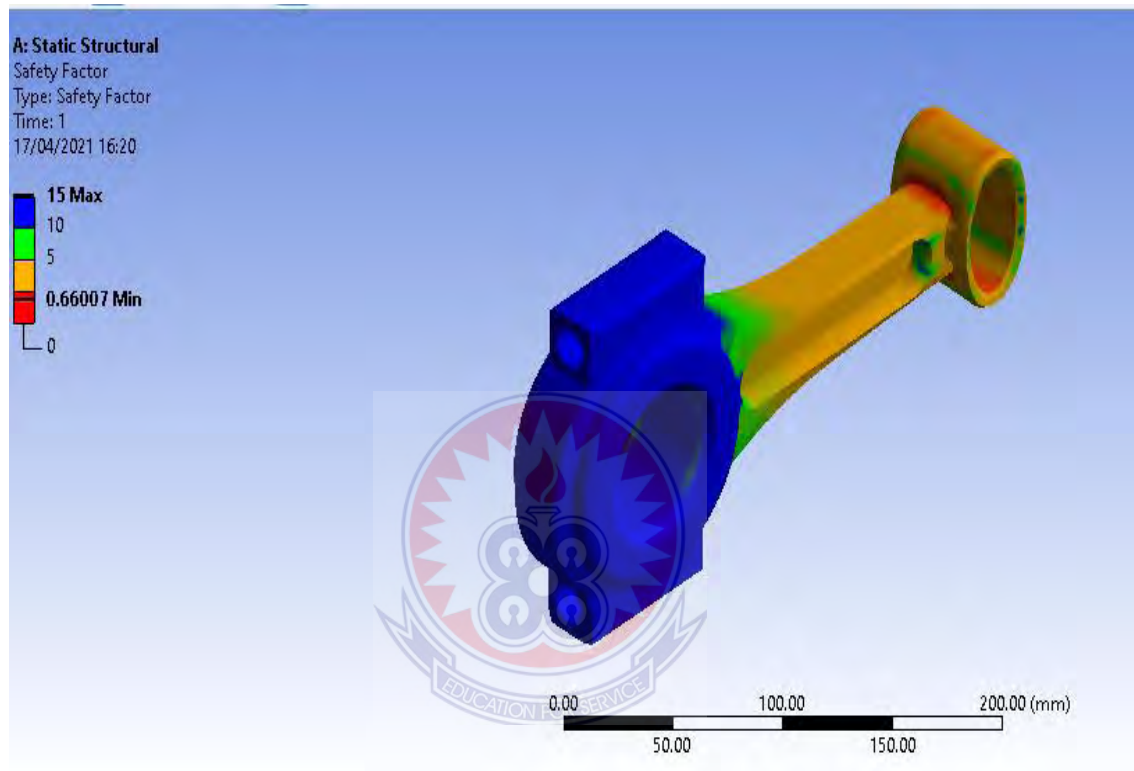


Figure 4.14 Safety Factor of Structural Steel Material

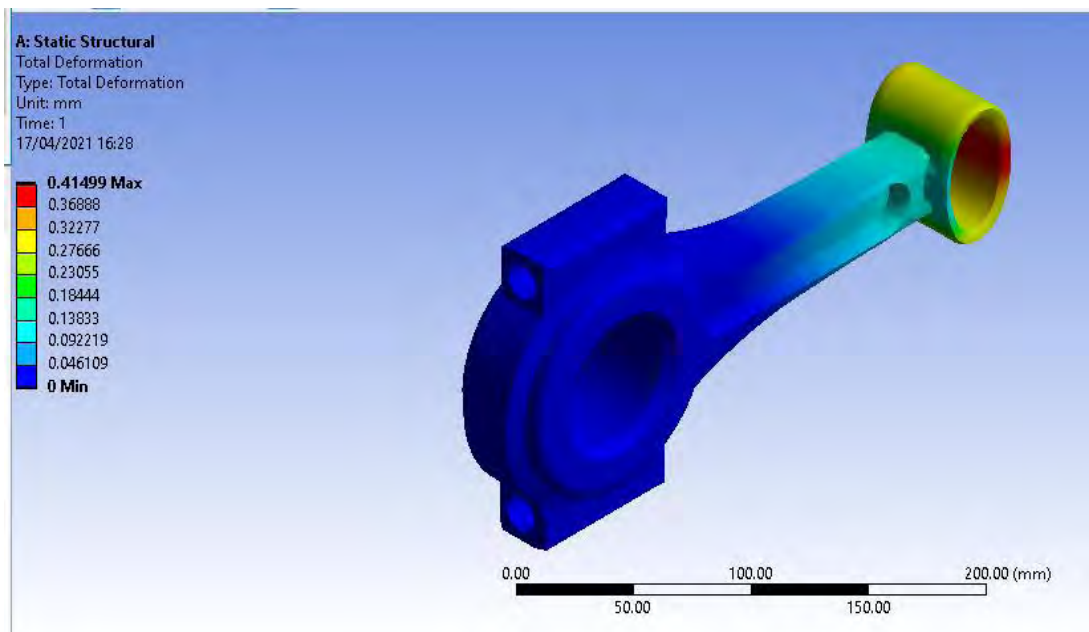
Generally, the theoretical factor of safety value for connecting rod is 5.5. The Ansys generated factor of safety of the structural steel connecting rod model has a maximum and minimum factor of safety magnitudes of 15 and 0.66007 respectively. The maximum factor of safety was observed to be more pronounced at the big end of the connecting rod as shown in Figure 4.14. The theoretical factor of safety value of 5.5 is within the range of factor of safety of the model structure steel connecting rod generated by the Ansys. The model is therefore very safe.

Table 4.2 Results for Structural Steel material

Parameters	Maximum	Minimum
Total deformation	0.22733 mm	0.025258 mm
Directional deformation	0.0014819 mm	-0.027488
Equivalent Elastic Strain	0.001955	2.4452×10^{-7}
Equivalent Von Mises Stress	378.75 MPa	0.024154 MPa
Maximum Principal Stress	290.05 MPa	-84.255 MPa
Minimum Principal Stress	23.67 MPa	-459.31 MPa
Factor of Safety	15	0.66007

Table 4.2 shows a summary of the results obtained when static structural analysis was conducted on the model structural steel connecting rod.

c. Gray Cast Iron material

**Figure 4.15 Total Deformation of Gray Cast Iron Material**

The total maximum deformation induced in the gray cast iron connecting rod when a compressive load of 49637.2N was applied is 0.41499 mm. Gray cast iron has a percentage reduction of 15% which is greater than the induced total deformation when the compressive load was applied. So, the model gray cast iron connecting rod will remain safe with the induced total deformation in the connecting rod. The maximum deformation was observed to have occurred at the small end of the gray cast iron connecting rod where the compressive load was applied. The big end of the gray cast iron connecting rod suffered the least deformation as shown in Figure 4.15.

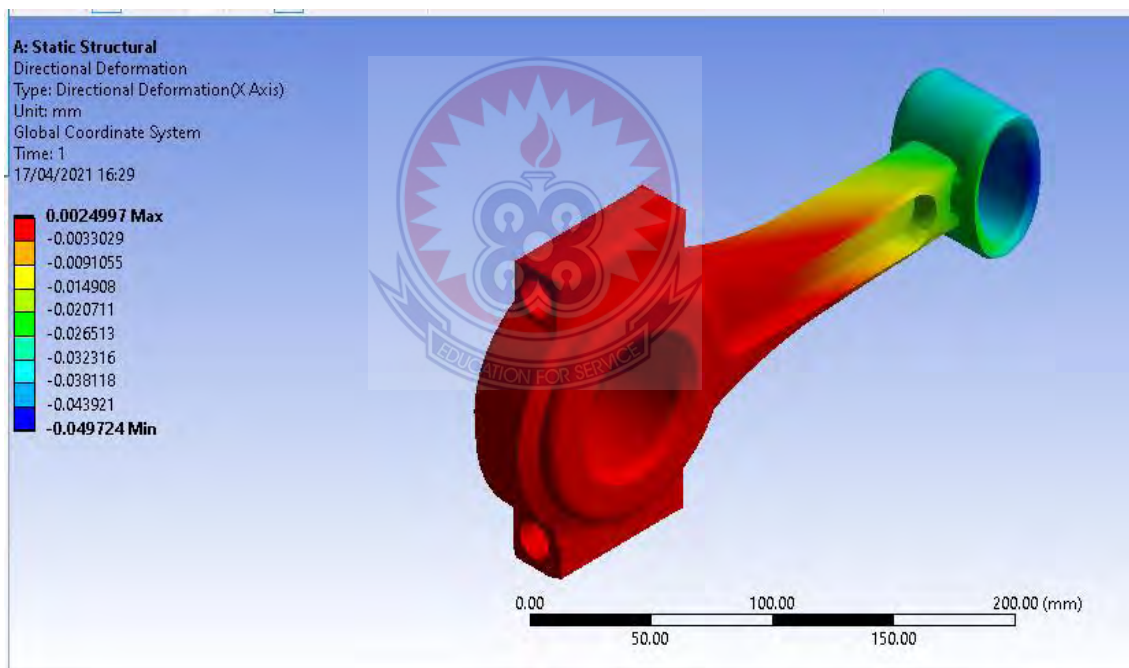


Figure 4.16 Directional Deformation of Gray Cast Iron Material

The maximum directional deformation induced in the x direction of a gray cast iron connecting rod has a maximum magnitude of 0.0024997mm. Gray cast iron has a percentage reduction of 15 % which is greater than the induced maximum directional deformation when the compressive load was applied. The directional deformation in the

x direction was observed to be more pronounced at the big end of the gray cast iron connecting rod. The directional deformation was also observed to be minimum at the piston end of the connecting rod as shown in Figure 4.16. Since the deformation in the x direction was insignificant, the model will therefore remain safe with the induced deformation in the gray cast iron connecting rod.

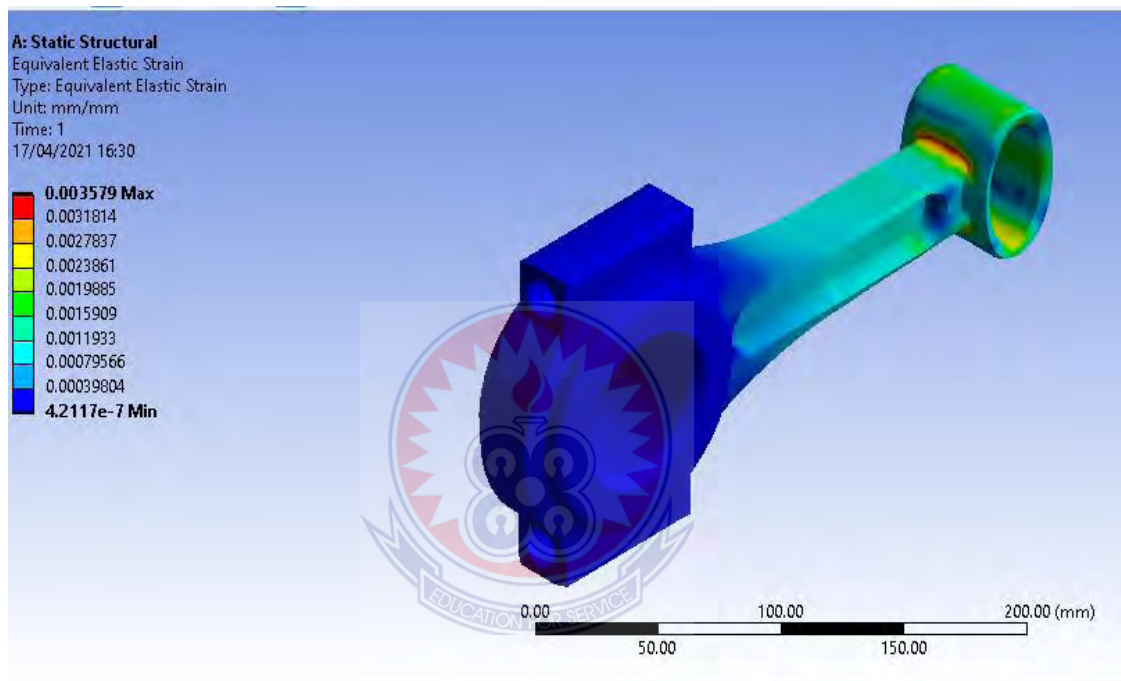


Figure 4.17 Equivalent Elastic Strain of Gray Cast Iron material

The magnitudes of maximum and minimum equivalent elastic strain induced in the model gray cast iron connecting rod are 0.003579 and 4.2117×10^{-7} respectively for the given loading condition. It was observed that the equivalent elastic strain in the model connecting rod was lower at the big end of the gray cast iron connecting rod. The piston pin end of the connecting rod was observed to have suffered the greatest equivalent elastic strain as shown in Figure 4.17.

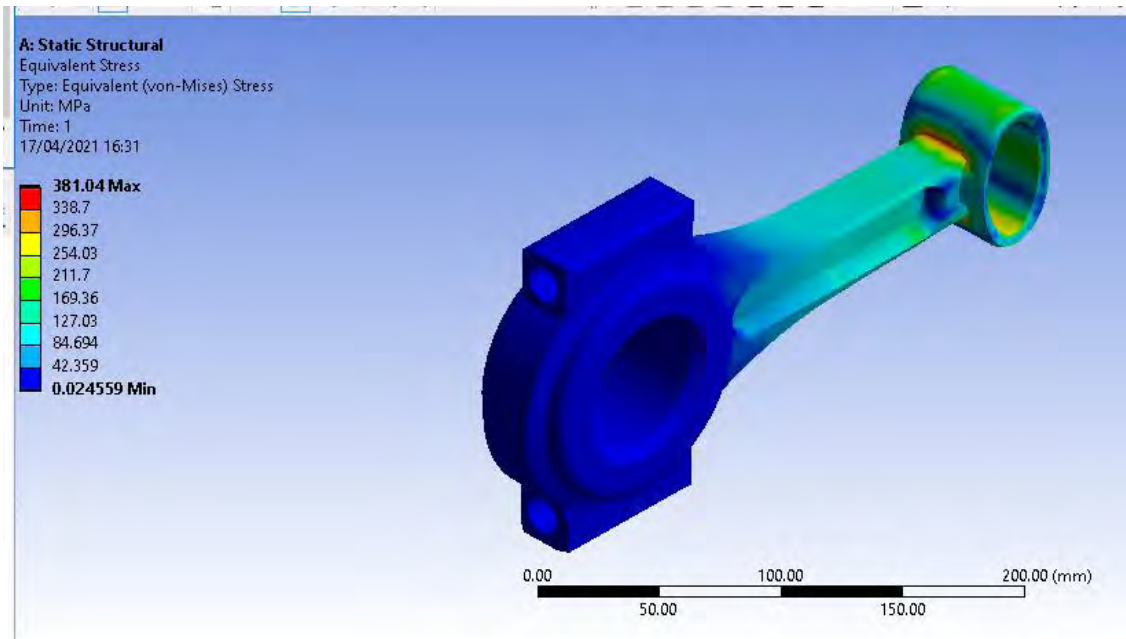


Figure 4.18 Equivalent (Von Mises) Stress of Gray Cast Iron Material

The maximum equivalent (Von Mises) stress induced in the gray cast iron connecting rod has a maximum magnitude of 381.04 MPa for the given loading condition. The average compressive yield strength of gray cast iron is 943 MPa. The induced Von Mises stress in the gray cast iron connecting rod is lower compared to the average compressive yield strength of the gray cast iron material. It was also observed that the induced Von Mises stress was maximum at the piston pin end while the big end of the connecting rod suffered the least inducement of Von Mises stress as shown in Figure 4.18. The big end of the gray cast iron connecting rod was not greatly affected by the compressive load imposed on the connecting rod. For material optimisation, material can be removed from the big end of the gray cast iron connecting rod for improve weight and cost reduction. The model can therefore be considered to be fit for purpose since it can withstand the given loading condition.

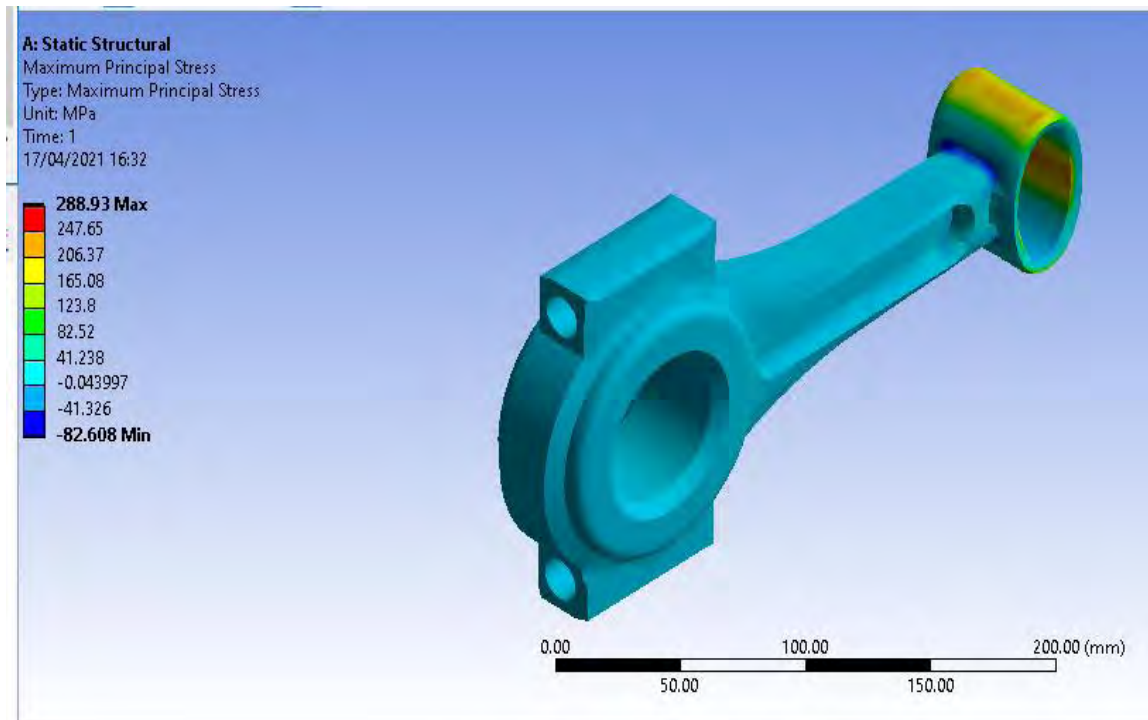


Figure 4.19 Maximum Principal Stress of Gray Iron Material

The maximum principal stress induced in the gray cast iron connecting rod has a maximum value of 288.93 MPa for the given loading condition. The average compressive yield strength of gray cast iron is 943 MPa. The maximum principal stress was observed to be uniformly distributed in the connecting rod as shown in Figure 4.19. The induced maximum principal stress in the gray cast iron connecting rod is far lower compared to the average compressive yield strength of the gray cast iron material. The model can therefore be considered to be fit for purpose since it can withstand the given loading condition.

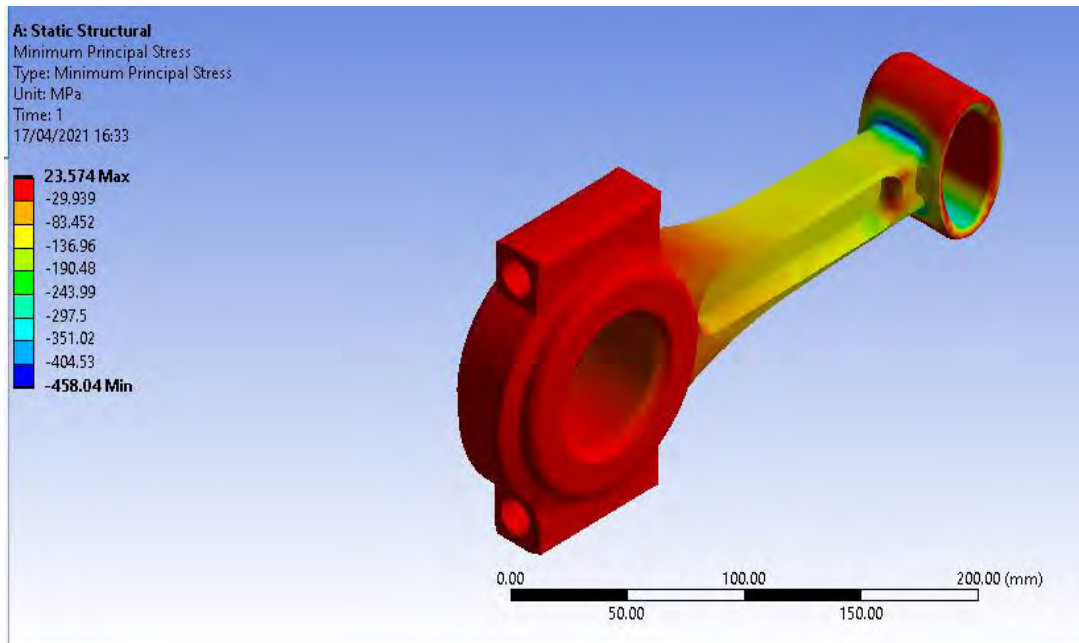
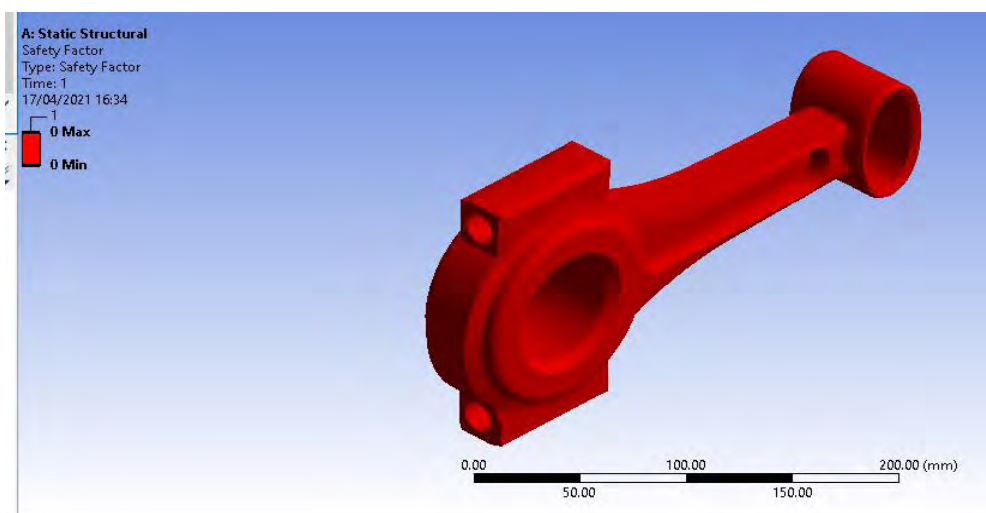


Figure 4.20 Minimum Principal Stress of Gray Cast Iron Material

The minimum principal stress induced in the gray cast iron connecting rod has a maximum magnitude of 23.574 MPa for the given loading condition. The average compressive yield strength of gray cast iron material is 943 MPa. It was observed that, the big end and part of the small end of the gray cast iron connecting rod was worst affected by the minimum principal stress compared to the shank as shown in Figure 4.20. The induced minimum principal stress in the gray cast iron connecting rod is far lower compared to the average compressive yield strength of the gray cast iron material. The model can therefore withstand the given loading condition.



**Fig
 ure
 4.2**

1 Safety Factor of Gray Cast Iron Material

Connecting rods are designed to have a theoretical factor of safety value of 5.5. The Ansys generated factor of safety of the modal gray cast iron connecting rod has a maximum and minimum factor of safety magnitudes of 0 and 0 respectively. It was observed that, the entire connecting rod has no factor of safety as shown in Figure 21. The theoretical factor of safety value of connecting rod of 5.5 is greater than the range of factor of safety generated by Ansys. The model is therefore not safe if the factor of safety of the model gray cast iron connecting were to be considered.



Table 4.3 Results for Grey Cast Iron Material

Parameters	Maximum	Minimum
Total deformation	0.41499 <i>mm</i>	0.046109 <i>mm</i>
Directional deformation	0.0024997 <i>mm</i>	-0.049724 <i>mm</i>
Equivalent Elastic Strain	0.003579	4.2117×10^{-7}
Equivalent Von Mises Stress	381.04 <i>MPa</i>	0.024559 <i>MPa</i>

Maximum Principal Stress	288.93 MPa	-82.608 MPa
Minimum Principal Stress	23.574 MPa	-458.04 MPa
Factor of Safety	0	0

Table 4.3 shows a summary of the results obtained when static structural analysis was conducted on the model gray cast iron connecting rod of a Nissan pick up engine.

d. Aluminium 7075 T6 Alloy Material

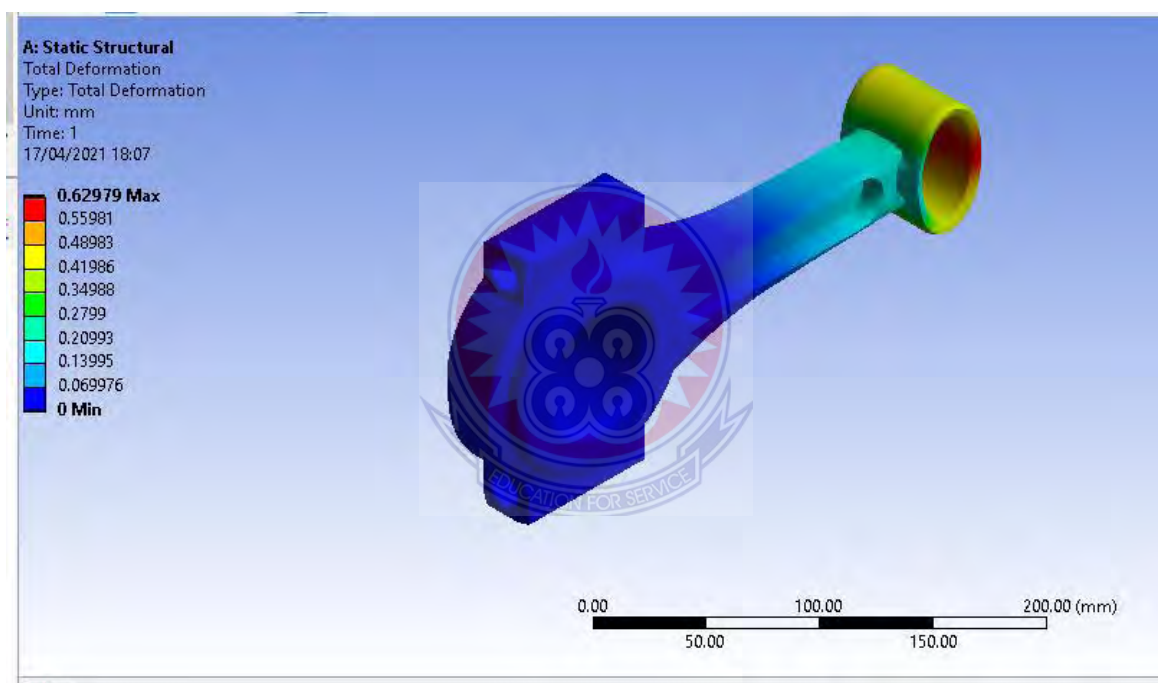


Figure 4.22 Total Deformation of Aluminium 7075 T6 Alloy Material

The total maximum deformation induced in the aluminium 7075 T6 alloy connecting rod when a compressive load of 49637.2N was applied is 0.62979 mm. Aluminium 7075 T6 alloy material has a maximum percentage reduction of 25% which is far greater than the induced deformation in the connecting rod when the compressive load was applied. Figure 4.22 shows that the induced deformation was maximum at the piston pin end of the connecting rod. The big end of the aluminium 7075 T6 alloy connecting

rod suffered the minimum deformation as shown in Figure 4.22. The total deformation suffered by the connecting rod when the compressive load was applied was less than the percentage reduction of aluminium 7075 T6 alloy material. Hence, the model will remain safe with the induced total deformation in the aluminium 7075 T6 alloy connecting rod.

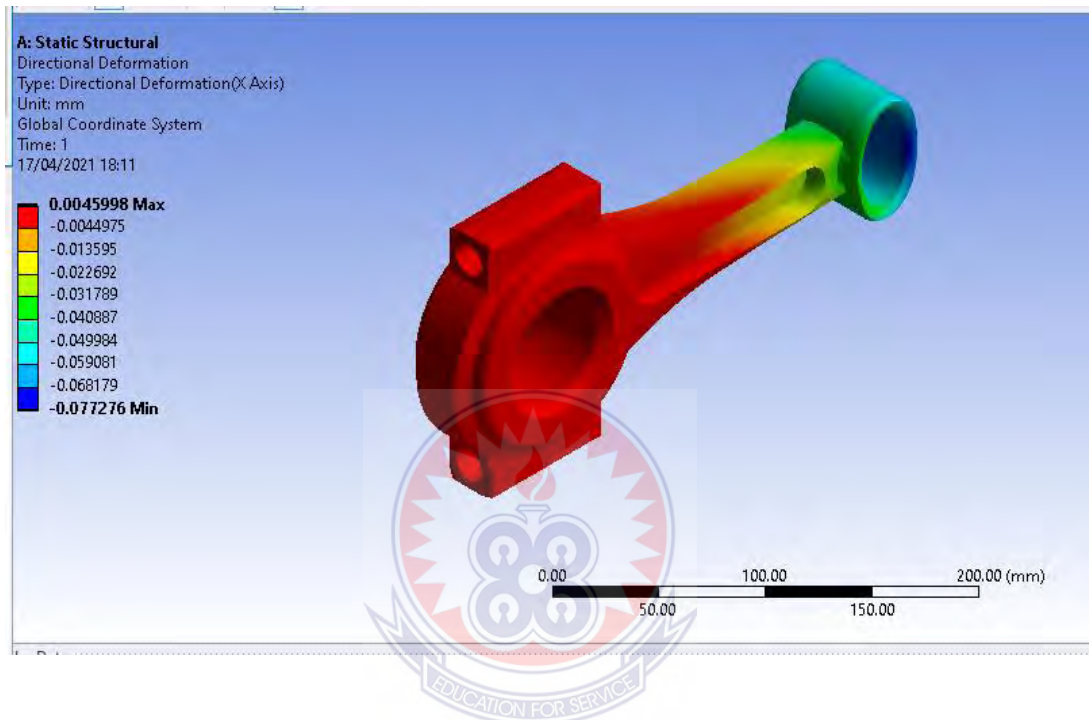


Figure 4.23 Directional Deformation of Aluminium 7075 T6 Alloy Material

The maximum directional deformation induced in the x direction of the aluminium 7075 T6 alloy connecting rod has a maximum magnitude of 0.0045998mm. Aluminium 7075 T6 alloy material has a maximum percentage reduction of 25 % which is far greater than the induced maximum directional deformation when the compressive load was applied. The directional deformation in the x direction was observed to be more pronounced at the big end of the aluminium 7075 T6 alloy connecting rod. The piston pin end where the compressive load was applied suffered the minimum directional deformation as shown in Figure 4.23. The connecting rod is noted to buckle in the x direction more than the y direction. Since the directional deformation in the x direction

was below the percentage reduction of the material, the model aluminium 7075 T6 alloy connecting rod will therefore remain safe with the induced directional deformation.

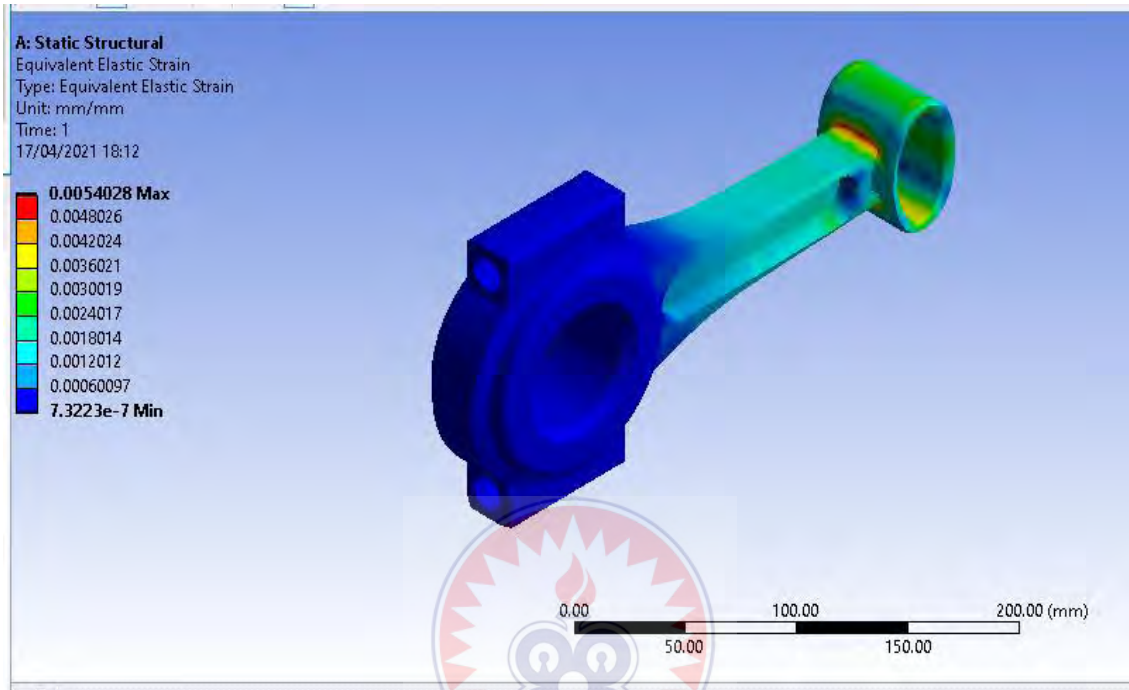


Figure 4.24 Equivalent Elastic Strain of Aluminium 7075 T6 Alloy

The magnitudes of maximum and minimum equivalent elastic strain induced in the model aluminium 7075 T6 alloy connecting rod are 0.0054028 and 7.3223×10^{-6} respectively for the given loading condition. It was observed that the equivalent elastic strain in the model aluminium 7075 T6 alloy connecting rod was maximum at the piston pin end of the connecting rod as shown in Figure 4.24. This was anticipated since it was the piston pin end that suffered the maximum deformation. The big end of the connecting rod suffered the minimum equivalent elastic strain as shown in Figure 4.24.

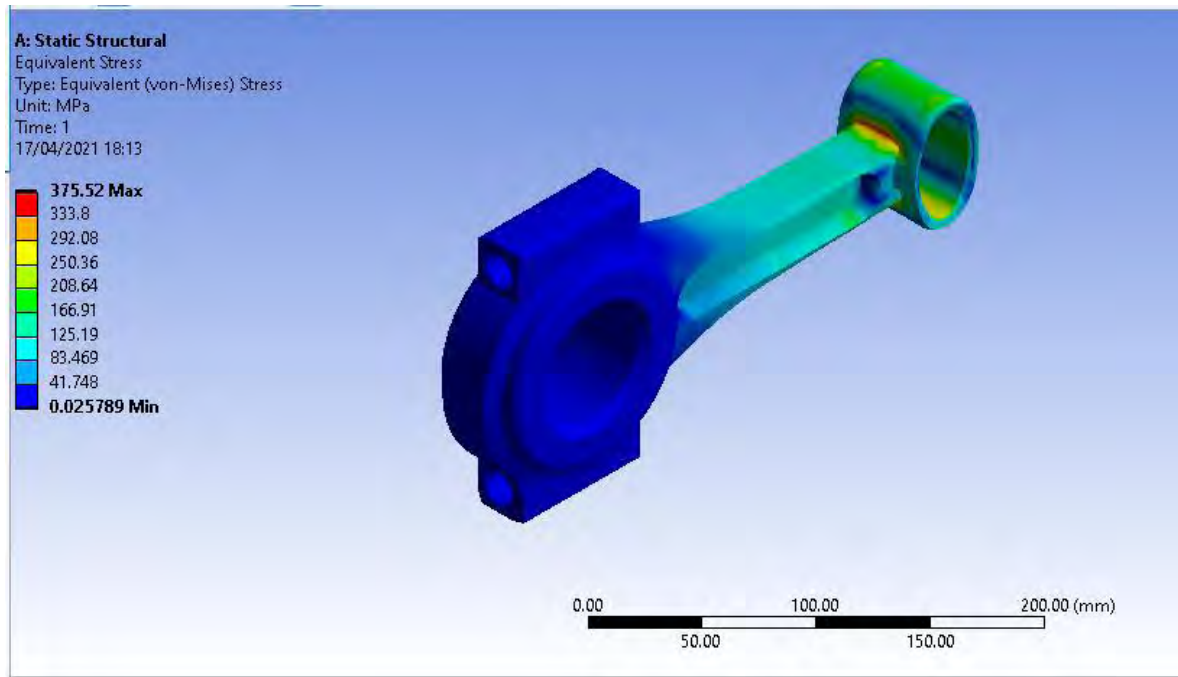


Figure 4.25 Equivalent Stress of Aluminium 7075 T6 Alloy Material

The maximum equivalent (Von Mises) stress induced in the aluminium 7075 T6 alloy connecting rod has a maximum magnitude of 375.52 MPa for the given loading condition. The compressive yield strength of aluminium 7075 T6 alloy material is 607.9 MPa. The induced Von Mises stress is lower compared to the compressive yield strength of the aluminium 7075 T6 alloy material. It was also observed that the induced Von Mises stress was only experienced at the small end where the compressive load was applied through to the shank of aluminium 7075 T6 alloy connecting rod. The big end of the connecting rod was not greatly affected by the compressive load imposed on the connecting rod as shown in Figure 4.25. For material optimisation, material can be removed from the big end of the aluminium 7075 T6 alloy connecting rod for improved weight and cost reduction. The model aluminium 7075 T6 alloy connecting rod can therefore be considered to be safe since it can withstand the given loading condition.

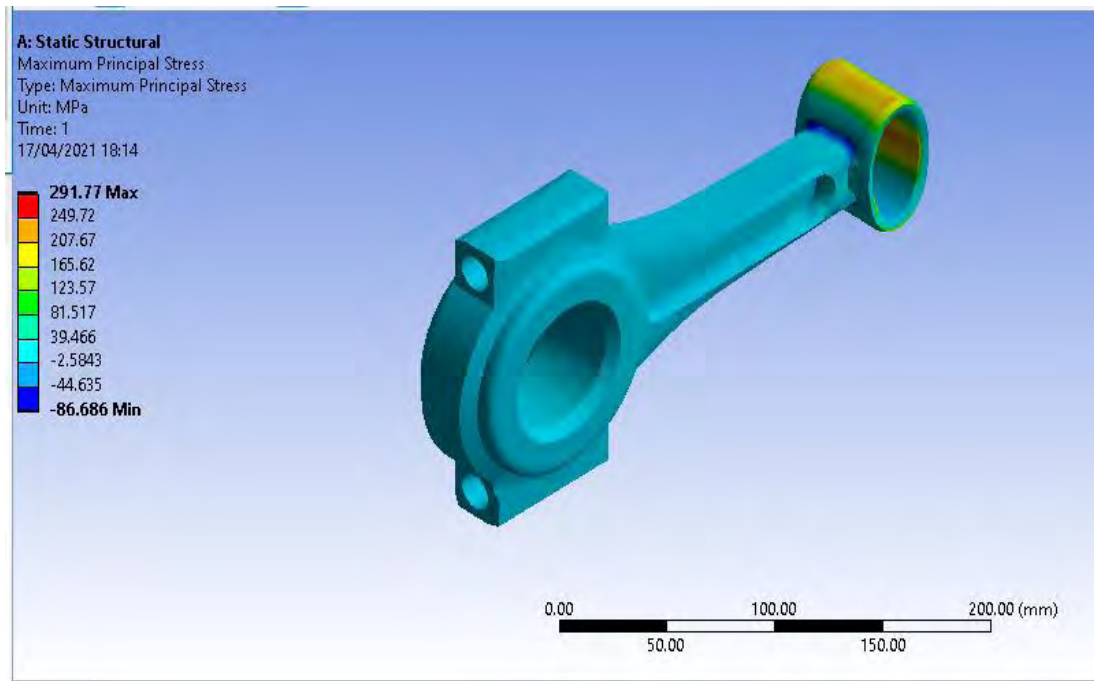


Figure 4.26 Maximum Principal Stress of Aluminium 7075 T6 Alloy Material

The maximum principal stress induced in the aluminium 7075 T6 alloy connecting rod has a maximum value of 291.77 MPa for the given loading condition. The compressive yield strength of aluminium 7075 T6 alloy is 607.9 MPa. It was observed that the maximum principal stress is more pronounced at the piston pin end of the connecting rod while the big end through to the shank of the connecting rod suffered the least maximum principal stress as shown in Figure 4.26. The induced maximum principal stress is far lower compared to the compressive yield strength of the aluminium 7075 T6 alloy material. The model aluminium 7075 T6 alloy connecting rod can therefore be considered to be fit for purpose since it can withstand the given loading condition.

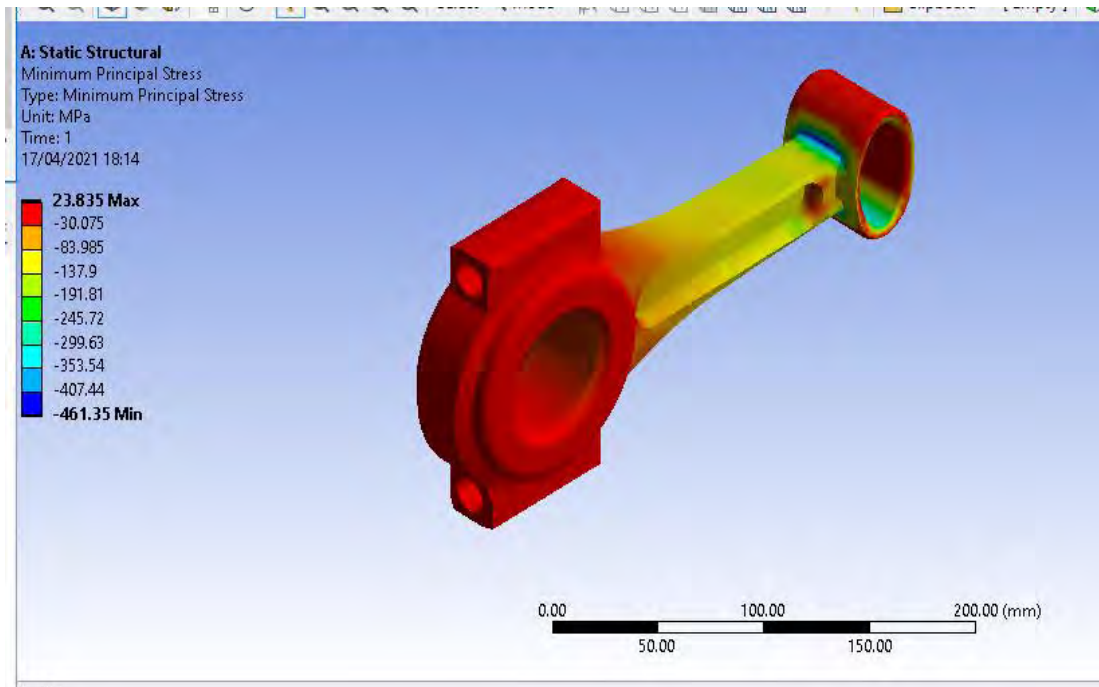


Figure 4.27 Minimum Principal Stress of Aluminium 7075 T6 Alloy

The minimum principal stress induced in the aluminium 7075 T6 alloy connecting rod has a maximum magnitude of 23.835 MPa for the given loading condition. The compressive yield strength of aluminium 7075 T6 alloy material is 607.9 MPa. The induced minimum principal stress is far lower compared to the compressive yield strength of the aluminium 7075 T6 alloy material. It was observed that, the maximum minimum principal stress occurred at the big end of the connecting rod as shown in Figure 4.27. The model aluminium 7075 T6 alloy connecting rod can therefore withstand the given loading condition.

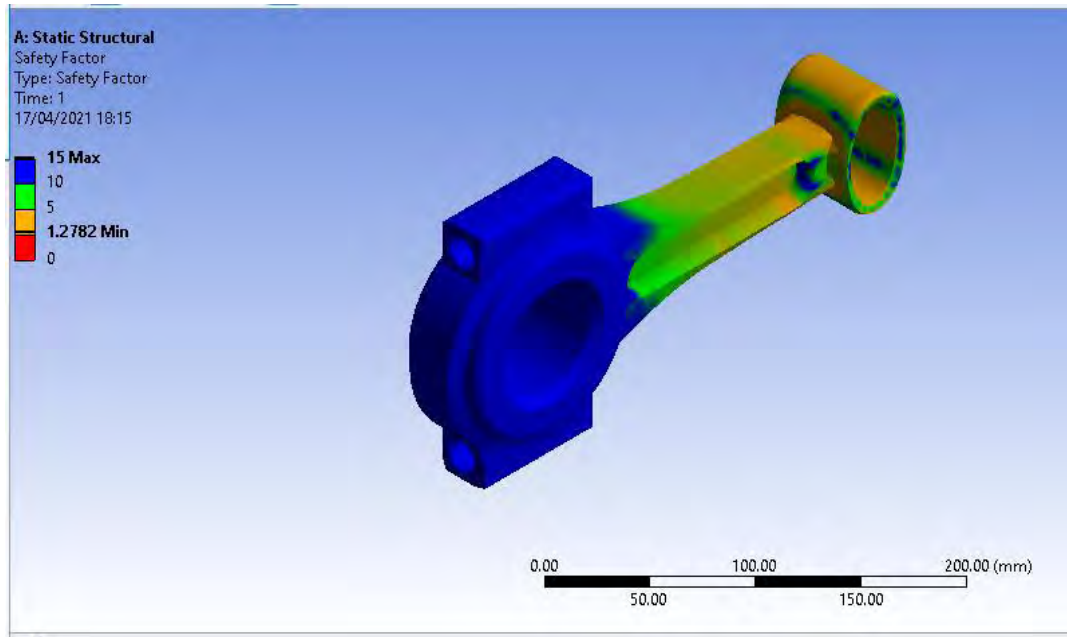


Figure 4.28 Safety Factor of Aluminium 7075 T6 Alloy Material

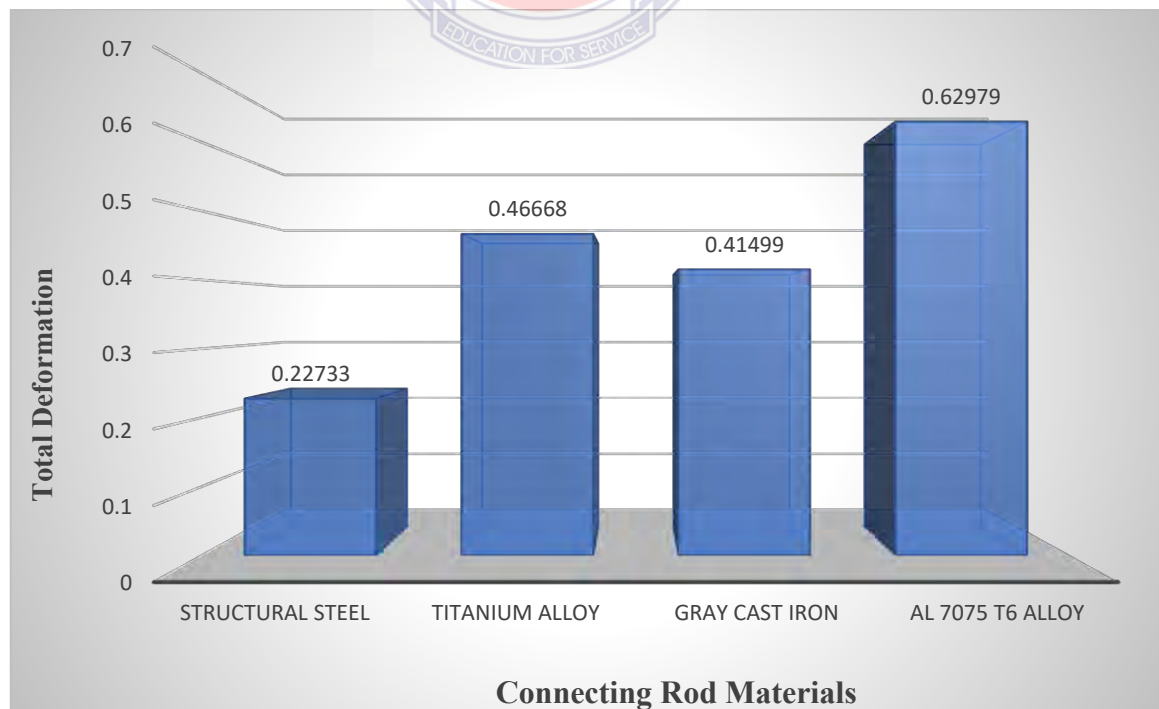
Theoretical value of factor of safety for Connecting rods design is 5.5. The Ansys generated factor of safety of the modal aluminium 7075 T6 alloy connecting rod has a maximum and minimum factor of safety magnitudes of 15 and 1.2782 respectively. It was observed that the maximum factor of safety occurred at the big end of the connecting rod while the small end and the shank of the connecting rod was observed to have lower factor of safety as shown in Figure 4.28. The theoretical factor of safety value of connecting rod of 5.5 falls within the range of factor of safety values generated by Ansys. The modal aluminium 7075 T6 alloy connecting rod is therefore safe if the factor of safety of the material were to be considered.

Table 4.4 Results for Aluminium 7075 T6 Material

Parameters	Maximum	Minimum
Total deformation	0.62979 mm	0.069976 mm
Directional deformation	0.0045998 mm	-0.077276 mm
Equivalent Elastic Strain	0.0054028	7.3223×10^{-7}
Equivalent Von Mises Stress	375.52 MPa	0.025789 MPa
Maximum Principal Stress	291.77 MPa	-86.656 MPa
Minimum Principal Stress	23.835 MPa	-461.35 MPa
Factor of Safety	15	1.2782

Table 4.4 shows a summary of the results obtained when static structural analysis was conducted on the model Al 7075 T6 alloy connecting rod of a Nissan pick up engine.

4.2 Discussion of static structural analysis results

**Figure 4.29 Summarised Results for Total Deformation**

The total deformation results of the static structural analysis of the connecting rods of the four different materials are as shown in Figure 4.29. The static structural results presented in Figure 4.29 shows a total deformation for Structural Steel connecting rod as 0.22733 mm, Titanium alloy connecting rod 0.46668 mm, gray cast iron connecting rod 0.41499 mm and aluminium 7075 T6 alloy connecting rod 0.62979 mm. It was observed that, structural steel connecting rod deformed less compared to the other three connecting rods of the four different materials. Aluminium 7075 T6 alloy (implementing material) connecting rod was observed to have deformed more than all the other connecting rods of the three different materials and in all cases as shown in Figure 4.29, it was also observed that minimum deformation occurred at the big end of the connecting rods. Maximum deformation was observed to be more pronounced at the piston end of the connecting rods where the compressive load was applied in all cases.

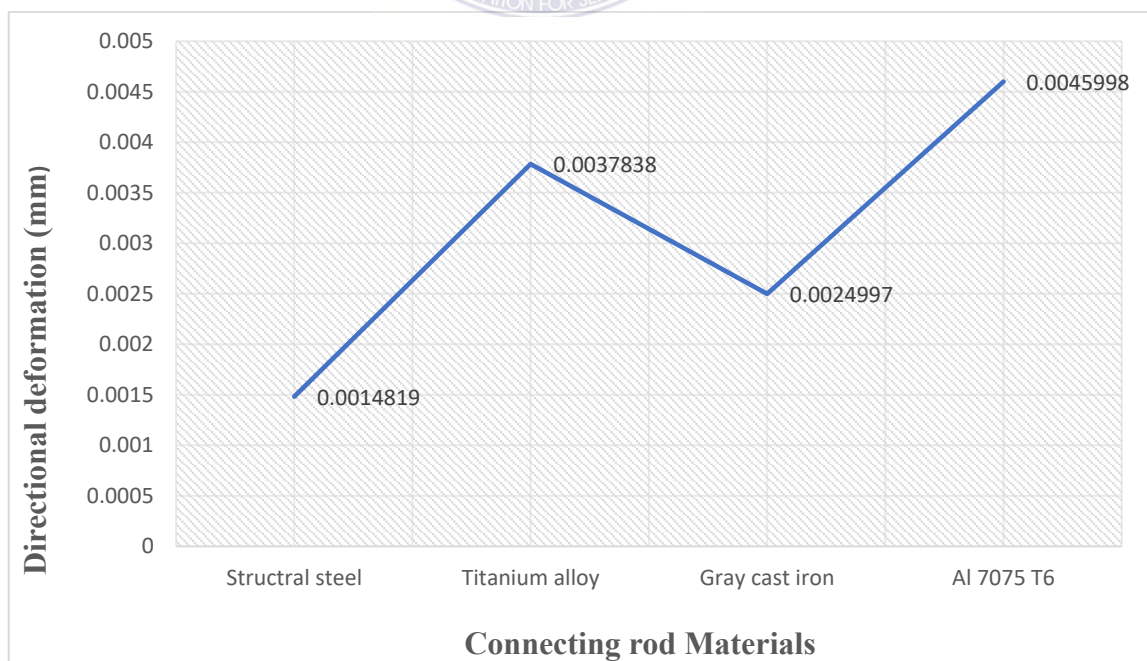


Figure 4.30 Summarised Results for Directional Deformation

The directional deformation results of the static structural analysis of the connecting rods of the four different materials are as shown in Figure 4.30. It was revealed in Figure 4.30 that, structural steel connecting rod has a directional deformation of 0.0014819 mm, titanium alloy connecting rod of 0.0037838 mm, gray cast iron connecting rod of 0.0024997 mm and aluminium 7075 T6 alloy connecting rod of 0.0045998 mm. It was evident again that, structural steel connecting rod has the lowest directional deformation and it was followed closely by gray cast iron connecting rod. Aluminium 7075 T6 alloy connecting rod was observed again to have the highest directional deformation. Results on deformation shows that, structural steel material has superior properties to resist deformation than the other three materials. Aluminium 7075 T6 alloy material has the weakest ability to resist deformation. Hence, the ranking of the materials in terms of deformation superiority is as follows: structural steel, gray cast iron, titanium alloy and aluminium 7075 T6 alloy respectively.

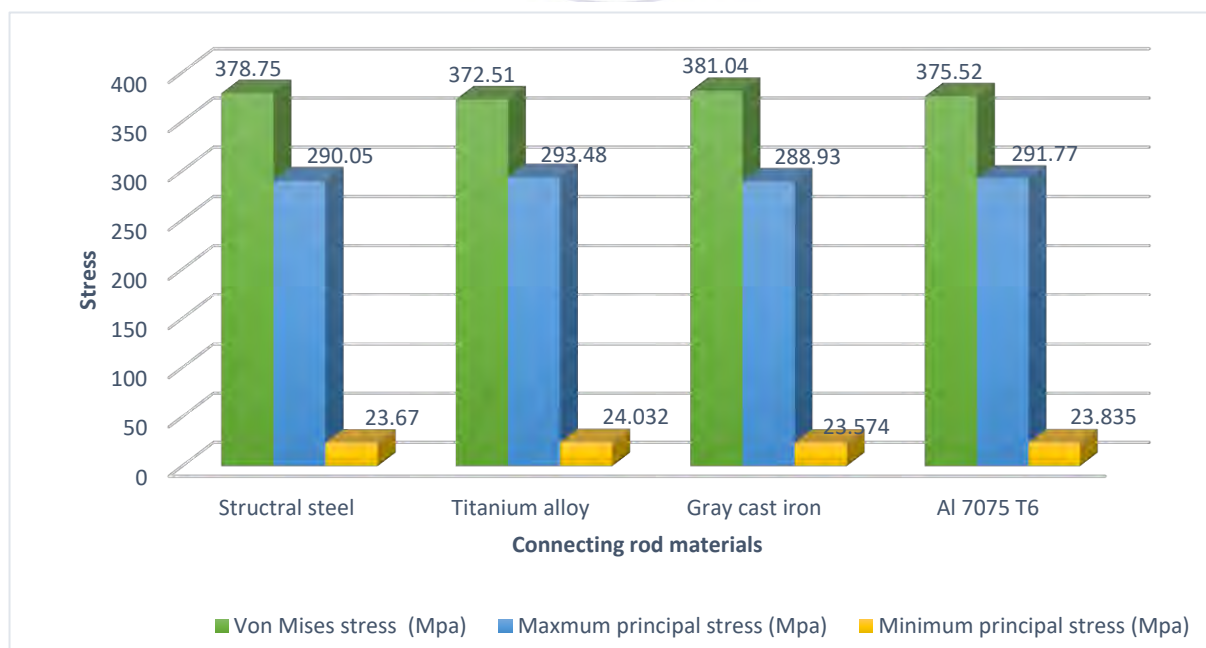


Figure 4.31 Summarised Results for Stresses

Figure 4.31 presents the results of the equivalent Von Mises stresses, maximum principal stresses and minimum principal stresses of the model connecting rods of the four different materials. One of the most critical parameters for this study is the Von Mises stress. This is one of the parameters that was used to determine whether the connecting rods will either fail or not when compared with the yield strengths of the materials. When the induced equivalent (Von Mises) stress is equal or more than the yield strength of the material, then the connecting rod of that material cannot withstand the loading condition, hence the design will fail. From Figure 4.31, when the Von Mises stresses induced in the connecting rods of the four different materials were compared, the figure shows that the induced stresses in the connecting rods are: Structural steel connecting rod yielded 378.75 MPa of stress, Titanium alloy connecting rod yielded 372.51 MPa of stress, Gray cast iron connecting rod yielded 381.04 MPa of stress and Aluminium 7075 T6 alloy connecting rod yielded 375.52 MPa of stress. The compressive yield strengths of the materials are: structural steel material 920 MPa, titanium alloy material 848 MPa, gray cast iron material 943 MPa and aluminium 7075 T6 alloy material 607.9 MPa. In terms of ranking, the results show that, Titanium alloy connecting rod has the least induced equivalent Von Mises stress of 372.51 MPa followed closely by Aluminium 7075 T6 alloy connecting rod of 375.52 MPa, Structural steel connecting rod of 378.75 MPa and Gray cast iron connecting of 381.04 MPa respectively. Titanium alloy connecting rod and aluminium 7075 T6 alloy connecting rod were observed to have the best Von Mises stress than the connecting rods of the two other materials because, titanium alloys and Aluminium alloys are very elastic in nature and has the tendency to distribute the load evenly throughout the connecting rod thereby distributing the induced stress as well, hence their abilities to

endure more stresses than the other two materials. All the connecting rods of the four materials were observed to have their induced Von Mises stresses to be far lower than the yield strengths of the four materials. The maximum principal stress results generated by ANSYS corresponds with the principal stress, σ_1 , that is calculated when determining a stress transformation of a state of stress at a specific point. Typically, σ_2 is also calculated for as a minimum principal stress, but this is provided by ANSYS through a separate viewer. The maximum magnitudes of Major principal stress (Maximum principal stress) and Minor Principal stress (Minimum principal stress) for the connecting rods of the four materials generated by Ansys are: Structural steel connecting rod yielded maximum principal stress of 290.05 MPa and minimum principal stress of 23.67 MPa, Titanium Alloy connecting rod yielded maximum principal stress of 293.48 MPa and minimum principal stress of 24.032 MPa, Gray cast iron connecting rod also yielded maximum principal stress of 288.93 MPa and minimum principal stress of 23.574 MPa and Aluminium 7075 T6 alloy connecting rod yielded a maximum principal stress of 291.77 MPa and a minimum principal stress of 23.835 MPa. From Figure 4.31, it was observed that gray cast iron connecting rod has the least maximum and minimum principal stresses and Titanium alloy connecting rod has the highest values of maximum and minimum principal stresses and was followed closely by structural steel connecting rod. The results when compared to the yield strengths of the materials shows that all the connecting rods have their induced stresses far below than the yield strengths of their individual materials.

Table 4.5 Factor of Safeties for the Connecting Rods of Four Different Materials

Materials	Safety Factor	
	Maximum	Minimum
Structural Steel	15.0000	0.66007
Titanium Alloy	15.0000	2.4966

Gray Cast Iron	00.0000	0.0000
Aluminium 7075 T6 Alloy	15.0000	1.2782

Table 4.5 revealed that, the range of factor of safety values for the connecting rods of the four different materials are: Structural steel connecting rod has the best factor of safety values ranging from 0.66007 to 15 followed by Aluminium 7075 T6 alloy connecting rod which also have factor of safety values ranging from 1.2782 to 15 compared to Titanium alloy which also have very safe factor of safety values ranging from 2.4966 to 15. In terms of factor of safety, gray cast iron is the most dangerous material. The material has zero factor of safety values.

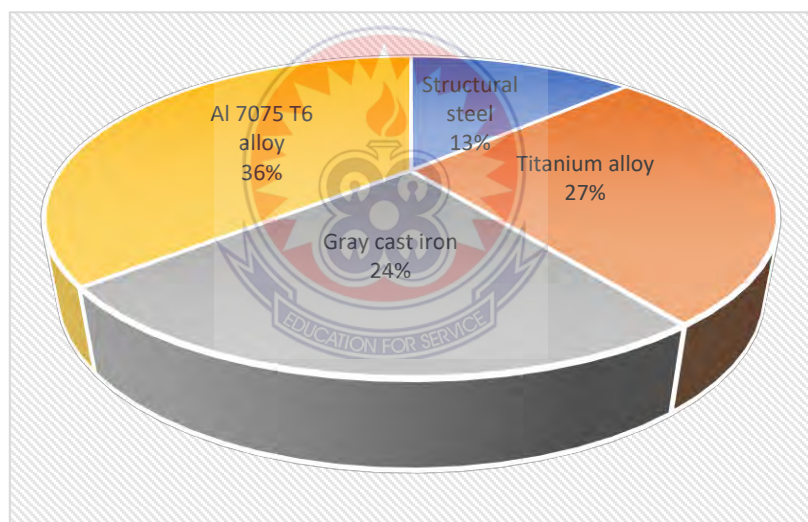


Figure 4.32 Summarised Results for Equivalent Elastic Strains

The results of the equivalent elastic strains of the connecting rod of the four different materials were presented in the pie chart shown in Figure 4.32. When the equivalent elastic strains of the connecting rods of the four different materials were compared in Figure 4.32, the results show that, the equivalent elastic strain for the connecting rods of Structural steel is 0.001955 representing 13% of the total elastic strain of the connecting rod for the four materials, Titanium alloy is 0.0039991 representing 27% of

the total elastic strain of the connecting rod for the four materials, Gray cast iron is 0.003579 representing 24% of the total elastic strain of the connecting rod for the four materials and aluminium 7075 T6 alloy is 0.0054028 representing 36% of the total elastic strain of the connecting rod for the four materials. It was observed from Figure 4.32 that, Structural steel connecting rod has the least equivalent strain followed by Gray cast iron connecting rod, titanium alloy and aluminium 7075 T6 connecting rods respectively. Gray cast iron connecting rod came close to structural steel because the material is brittle and under the given loading condition its deformation and strain will not be visible enough. Since aluminium 7075 T6 alloy connecting rod was the worst affected in terms deformation, it was therefore obvious that it will have the largest strain since strain and deformation are very closely related or strain depends on the extent of deformation.



4.3 Modal Analysis of the Connecting Rod

Modal analysis was run to determine the vibrational frequencies and the extent of deformation of the connecting rods of the four different materials, namely: titanium alloy, structural steel, grey cast iron and aluminium 7075 T6 alloy. The modal analysis of the connecting rod means the free vibration analysis of the connecting rod in which the natural frequencies of vibrations were calculated at no load condition with the help Ansys software version 2020R2. The vibrational mode shapes, deformation and the natural frequencies were presented in graphics and in Tables as shown below.

a. Titanium Alloy material

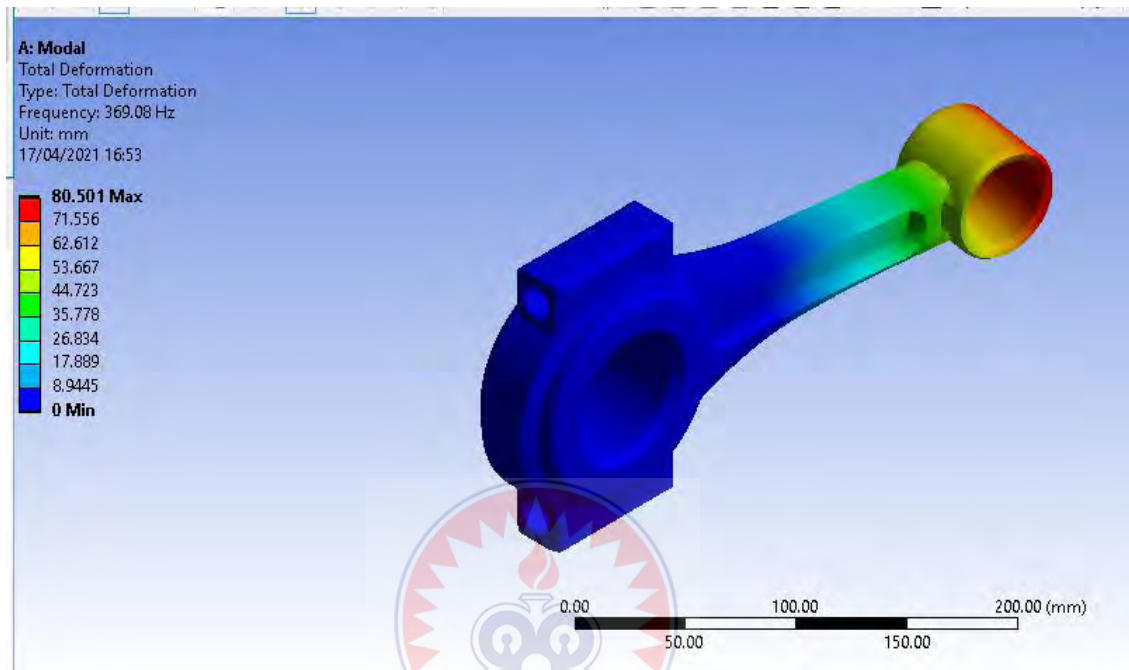


Figure 4.33 Vibration Mode Shape with Natural Frequency 369.08 Hz

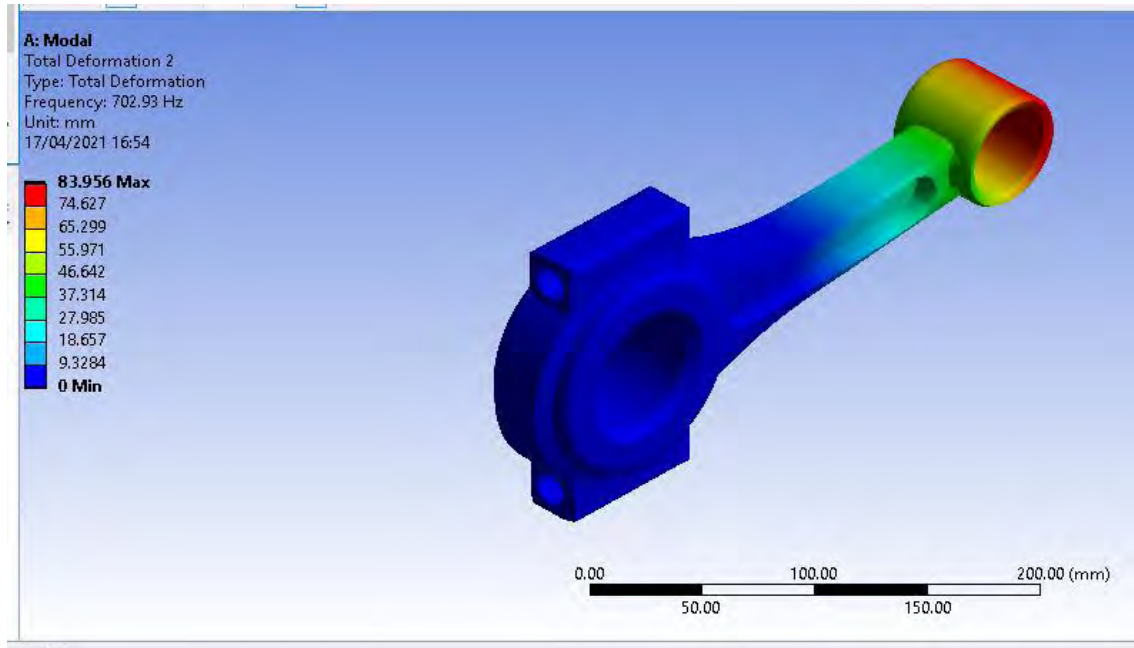


Figure 4.34 Vibration Mode Shape with Natural Frequency 702.93 Hz

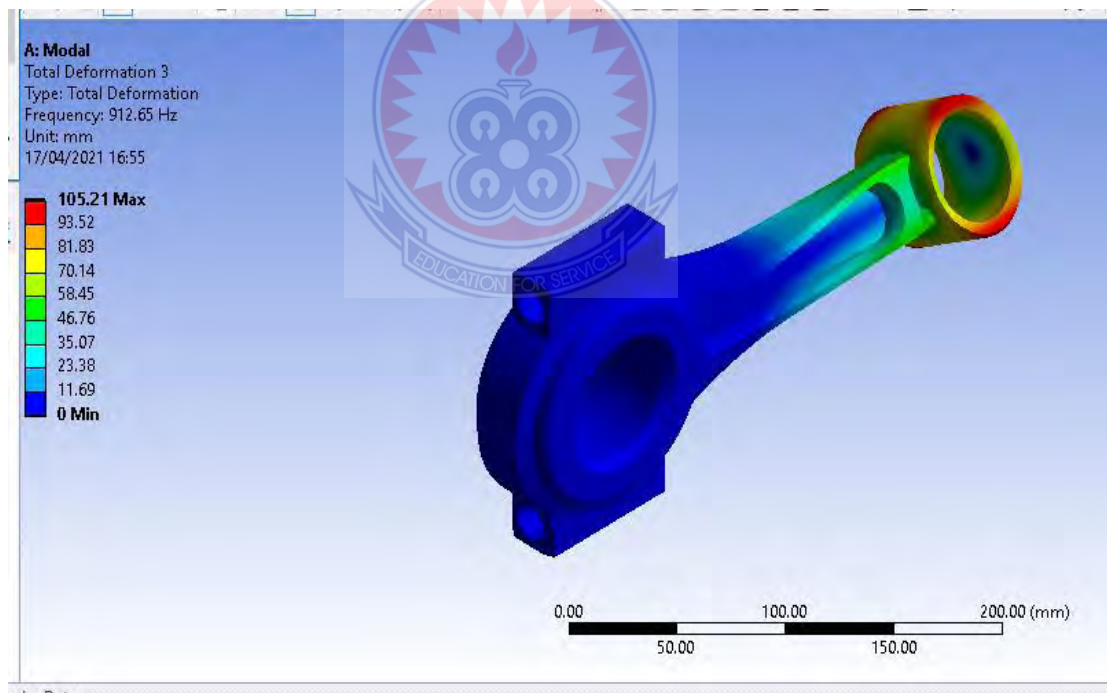


Figure 4.35 Vibration Mode Shape with Natural Frequency 912.65 Hz

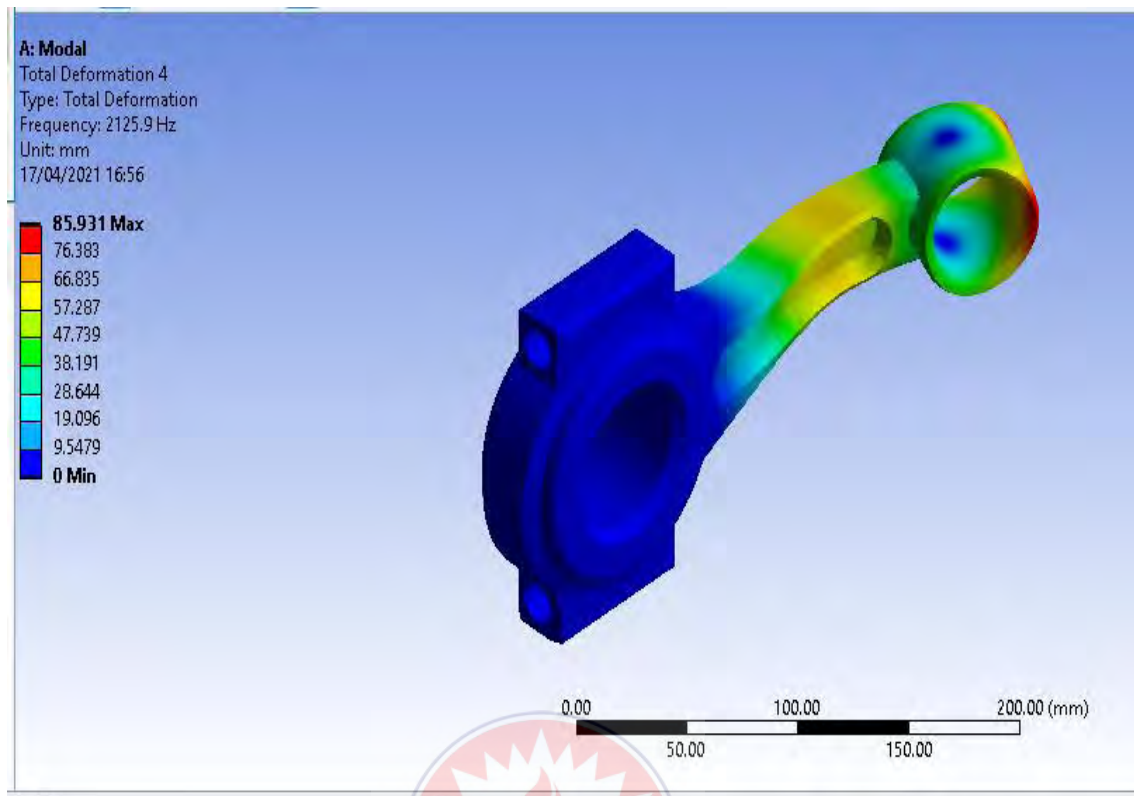


Figure 4.36 Vibration Mode Shape with Natural Frequency 2125.9 Hz

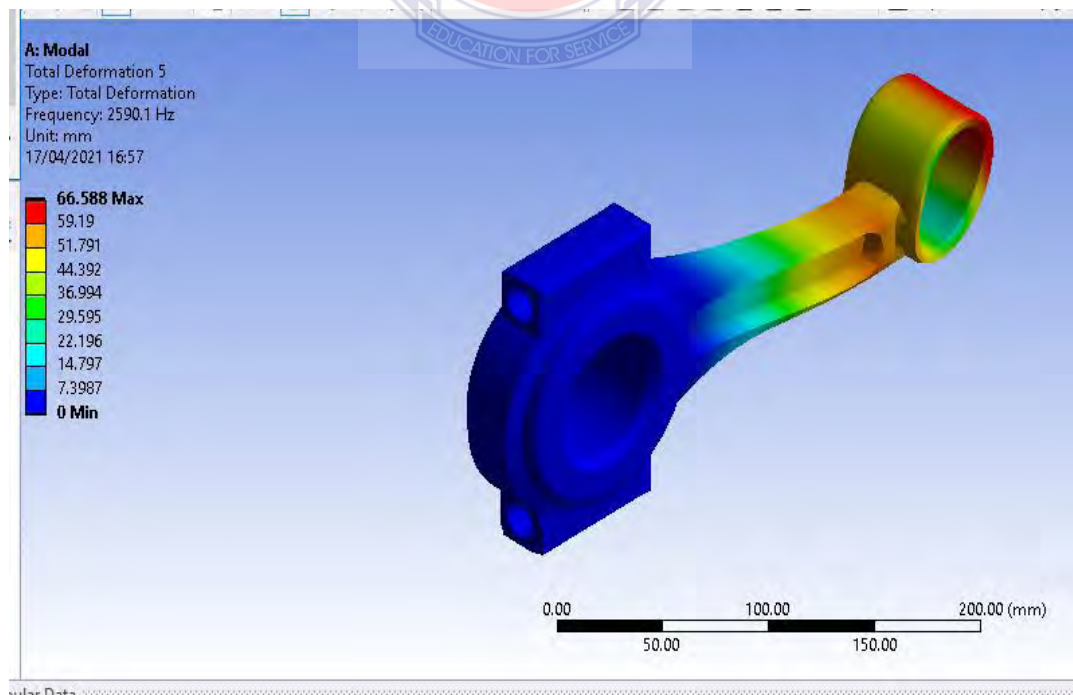


Figure 4.37 Vibration Mode Shape with Natural Frequency 2590.1 Hz

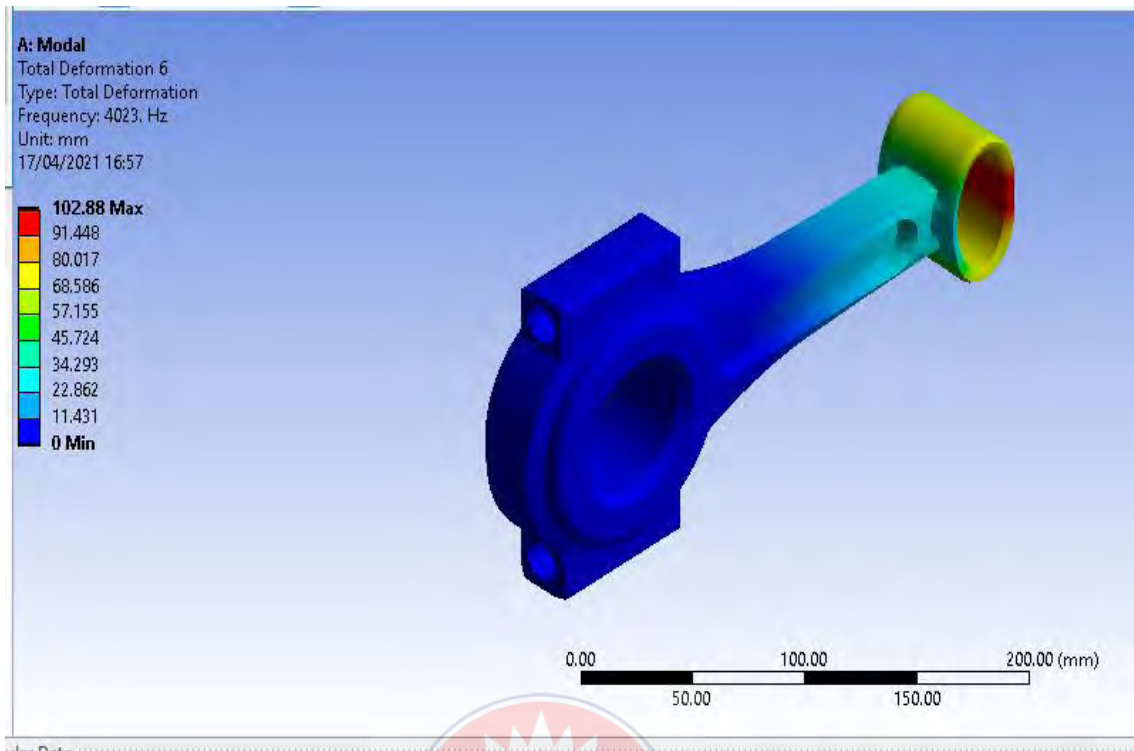


Figure 4.38 Vibration Mode Shape with Natural Frequency 4023.0 Hz

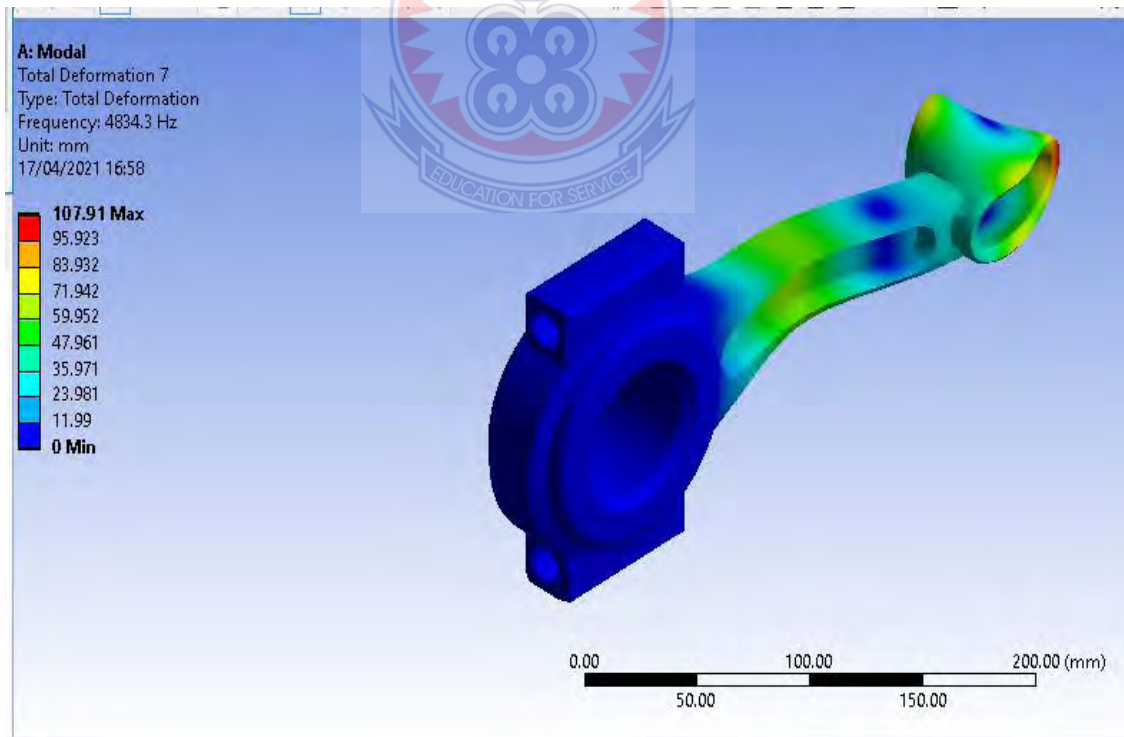


Figure 4.39 Vibration Mode Shape with Natural Frequency 4834.3 Hz

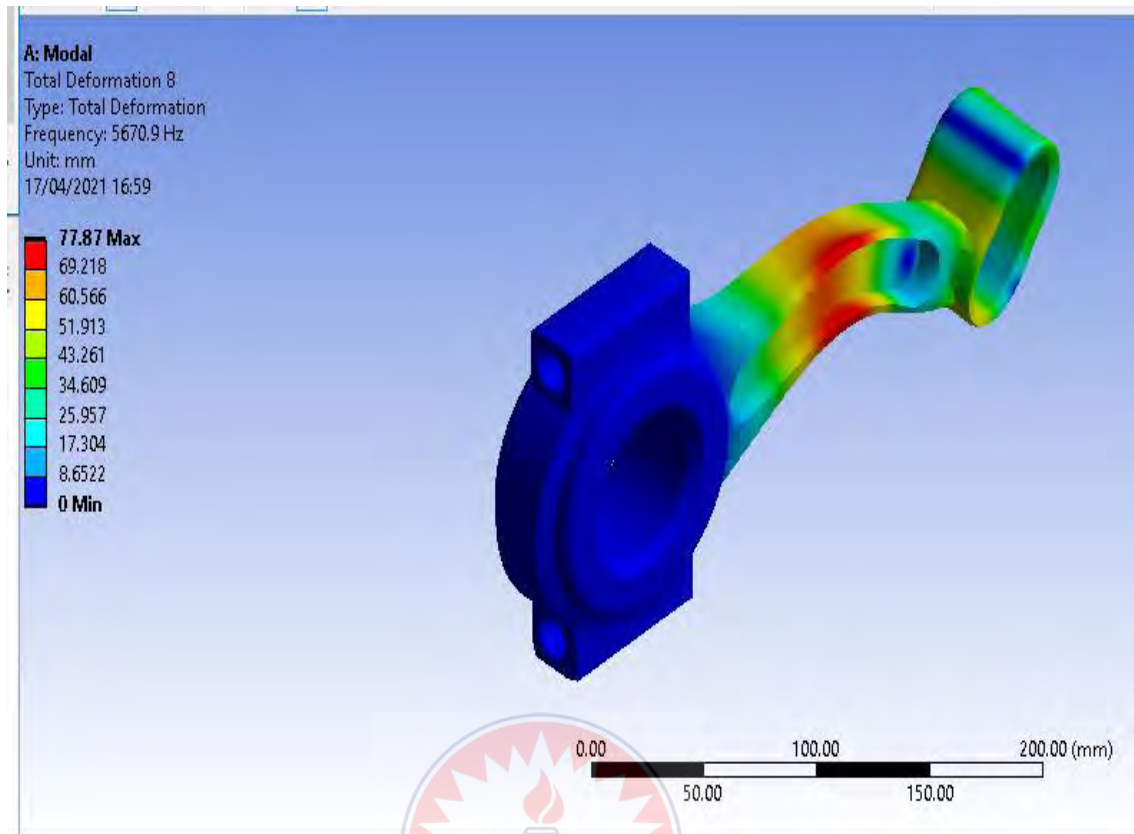


Figure 4.40 Vibration Mode Shape with Natural Frequency 5670.9 Hz

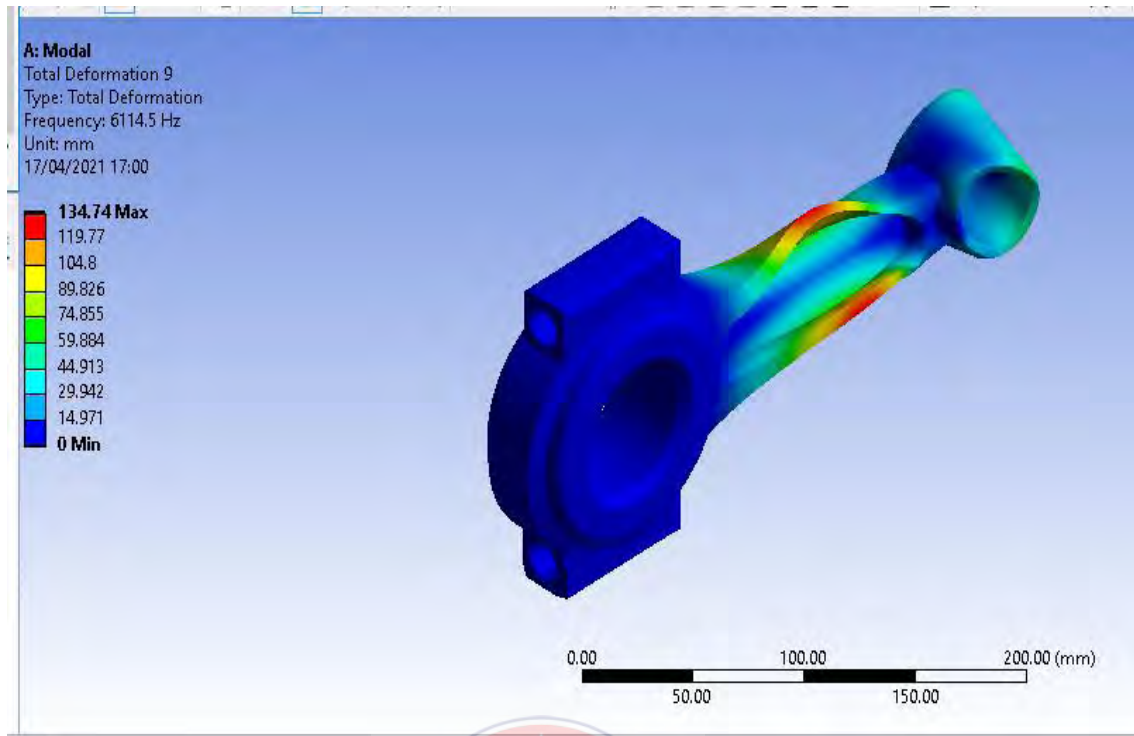


Figure 4.41 Vibration Mode Shape with Natural Frequency 6114.5 Hz

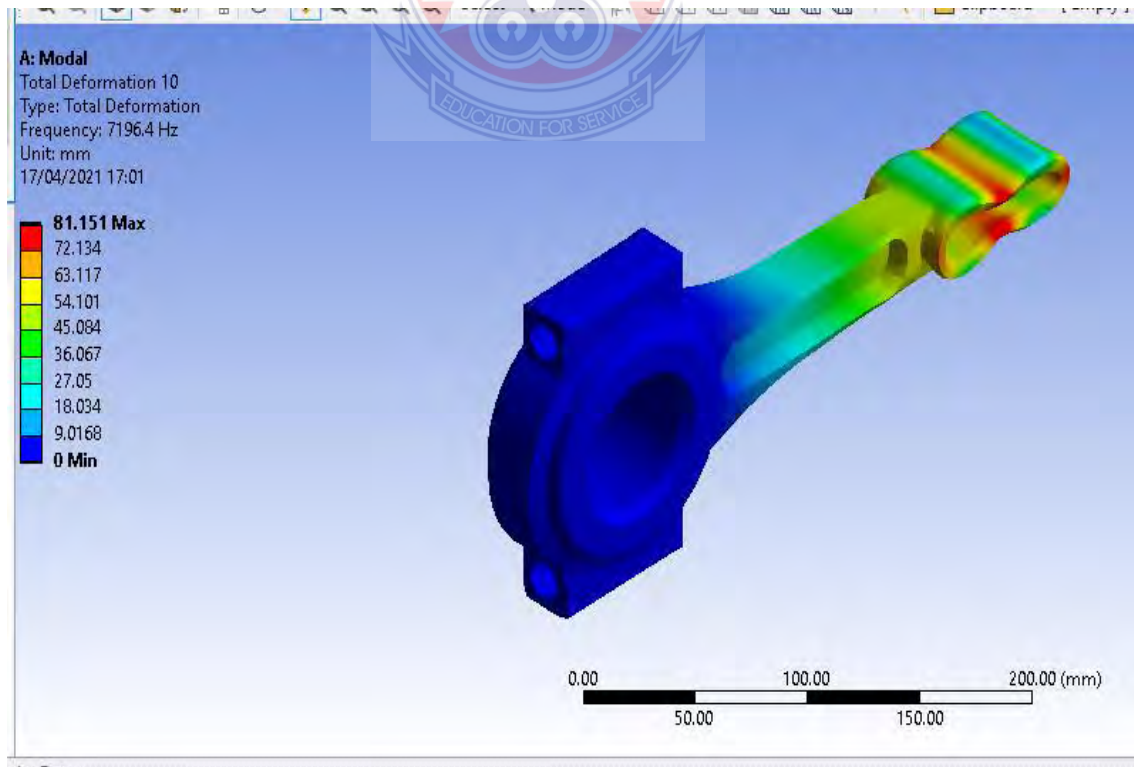


Figure 4.42 Vibration Mode Shape with Natural Frequency 7196.4 Hz

Table 4.6 Deformations and Natural Frequencies of Connecting Rod of Titanium

Mode number	Titanium Alloy Material	
	Deformation (mm)	Natural frequency (Hz)
1	80.501	369.08
2	83.956	702.93
3	105.210	912.65
4	85.951	2125.90
5	66.588	2590.10
6	102.88	4023.00
7	107.91	4834.30
8	77.87	5670.90
9	134.74	6114.50
10	81.151	7196.40

Table 4.6 shows the deformations and the natural frequencies when modal analysis was performed on the connecting rod of titanium alloy material. It was observed from Table 4.6 that the modal number with the highest deformation of 134.74 mm occurred in mode 9 corresponding to a natural frequency of 6114.5 Hz. It was also observed that mode 5 has the least deformation of 66.588 mm corresponding to a natural frequency of 2590.10 Hz. From Table 4.6, it was clear that, the highest vibrational frequency of 7196.40 Hz corresponding to mode 10 has a low deformation of 81.151 mm compared to some of the modes with lower frequencies. It was again observed that the

deformation of the connecting rod of titanium alloy material is not proportional to the magnitudes of the natural frequencies.

b. Structural Steel Material

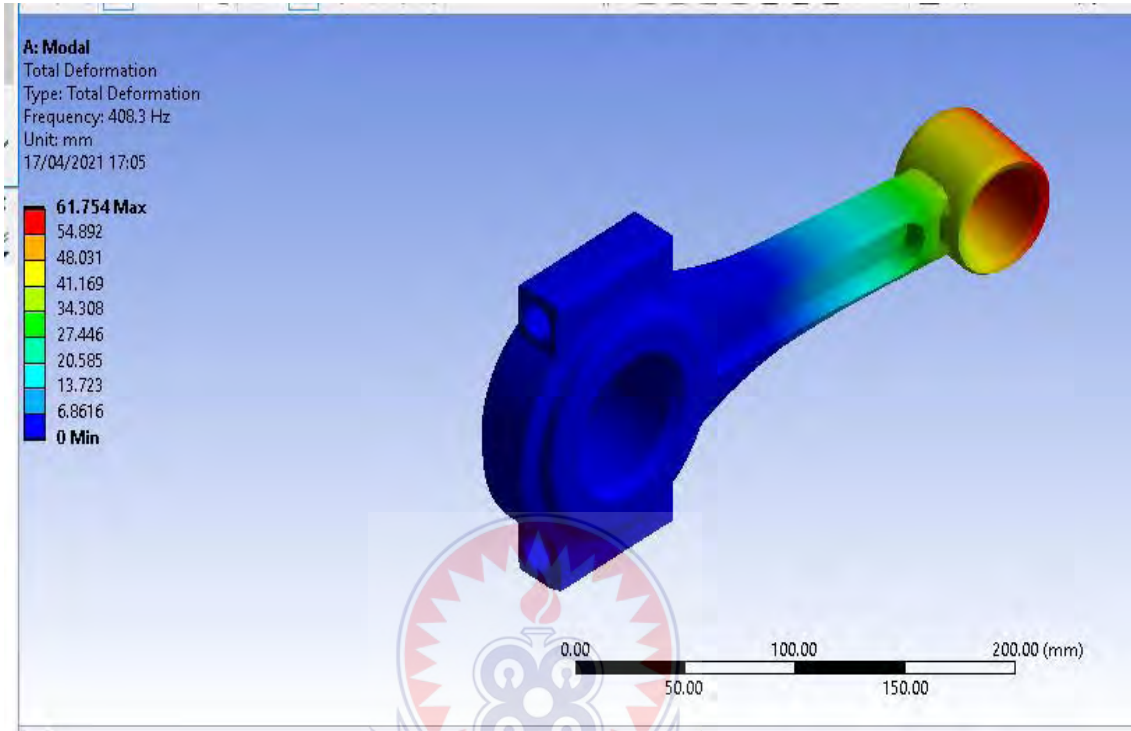


Figure 4.43 Vibration Mode Shape with Natural Frequency 408.3 Hz

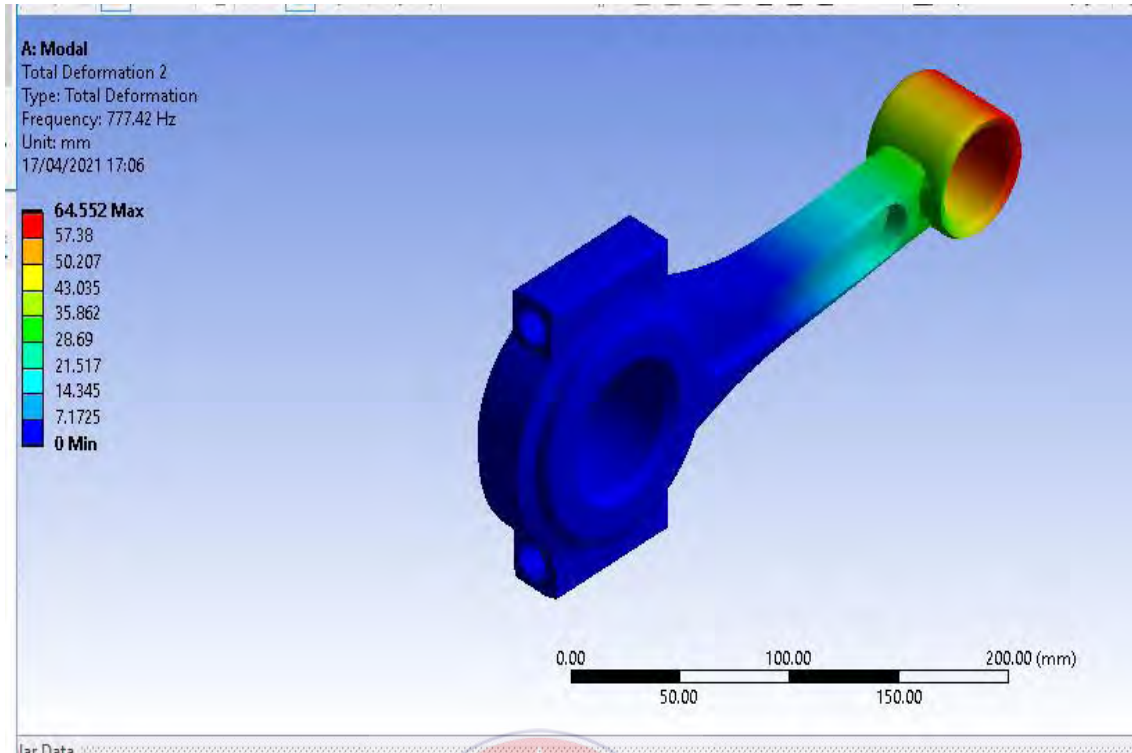
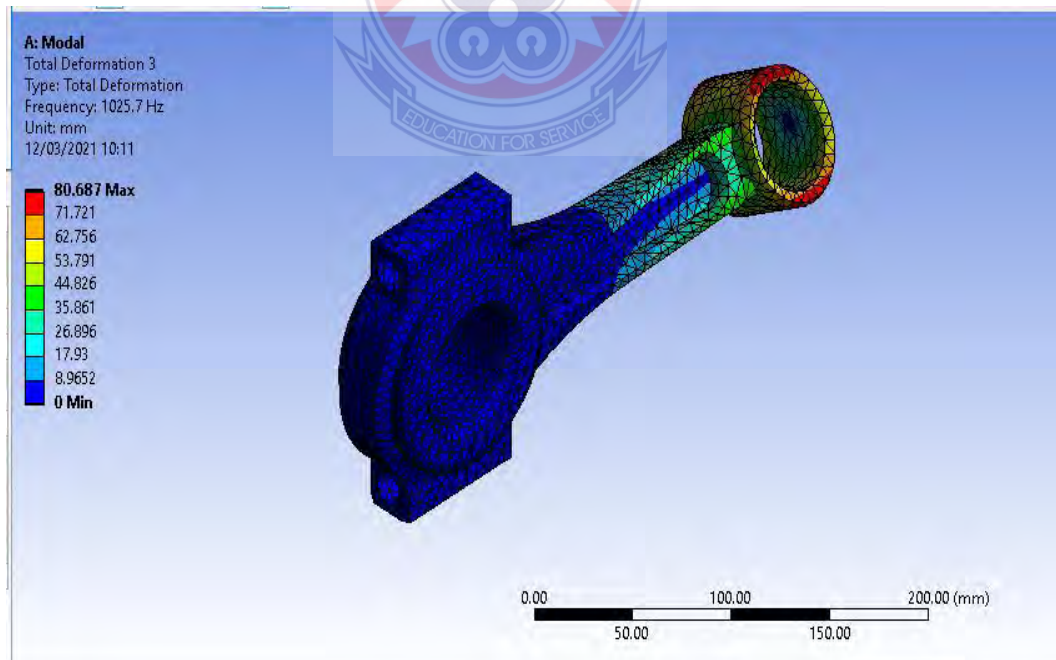


Figure 4.44 Vibration Mode Shape with Natural Frequency 777.42 Hz



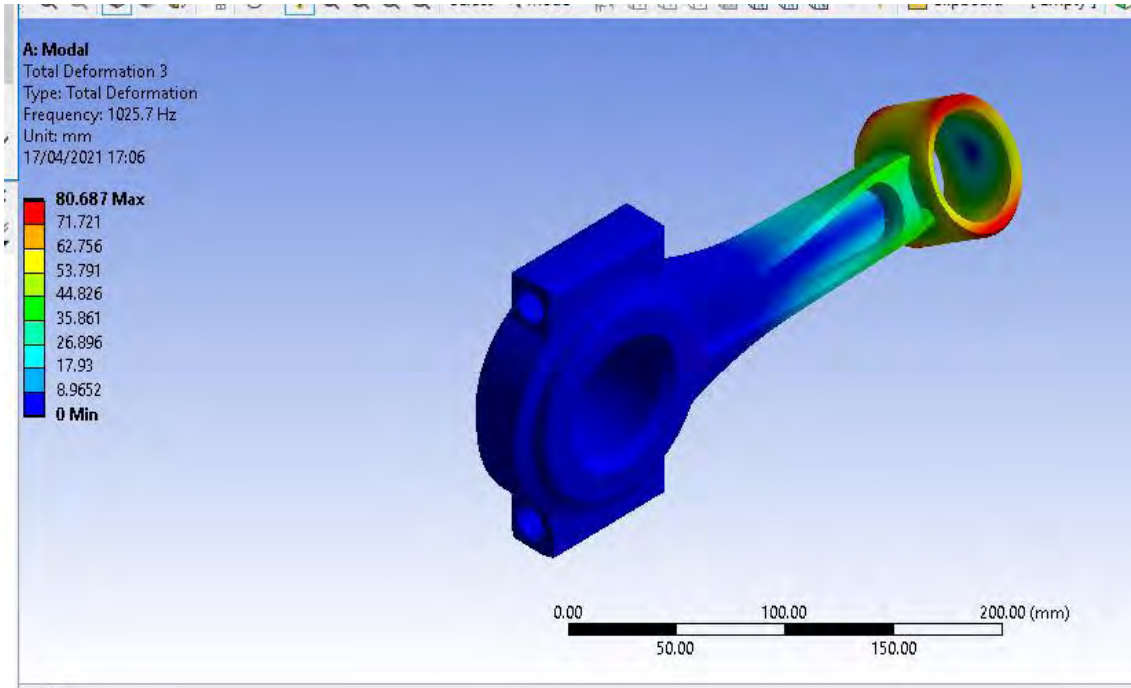


Figure 4.45 Vibration mode shape with natural frequency 1025.7 Hz

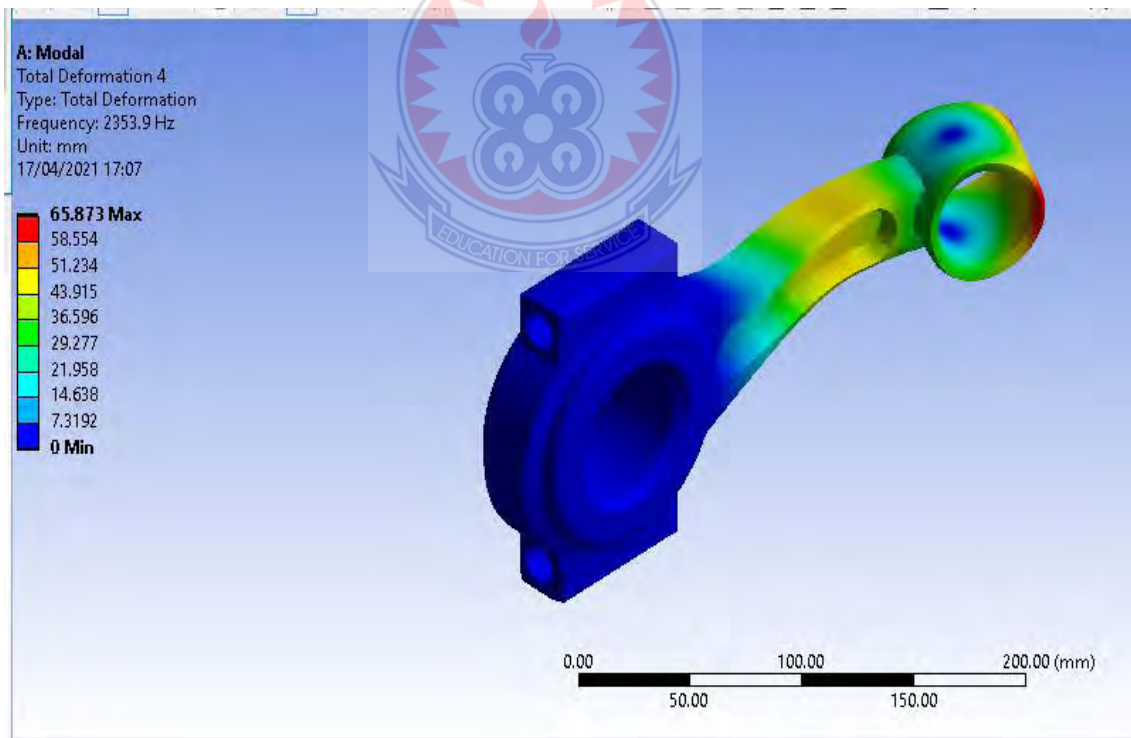


Figure 4.46 Vibration Mode Shape with Natural Frequency 2353.9 Hz

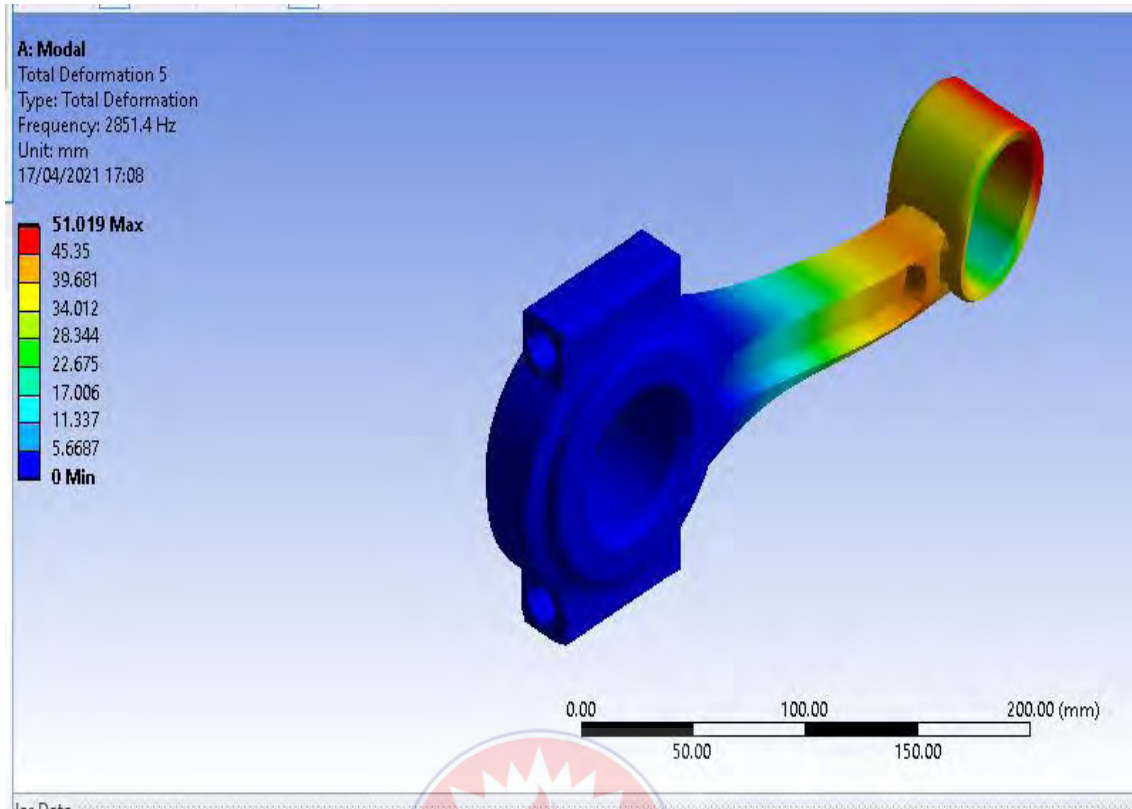


Figure 4.47 Vibration Mode Shape with Natural Frequency 2851.4 Hz

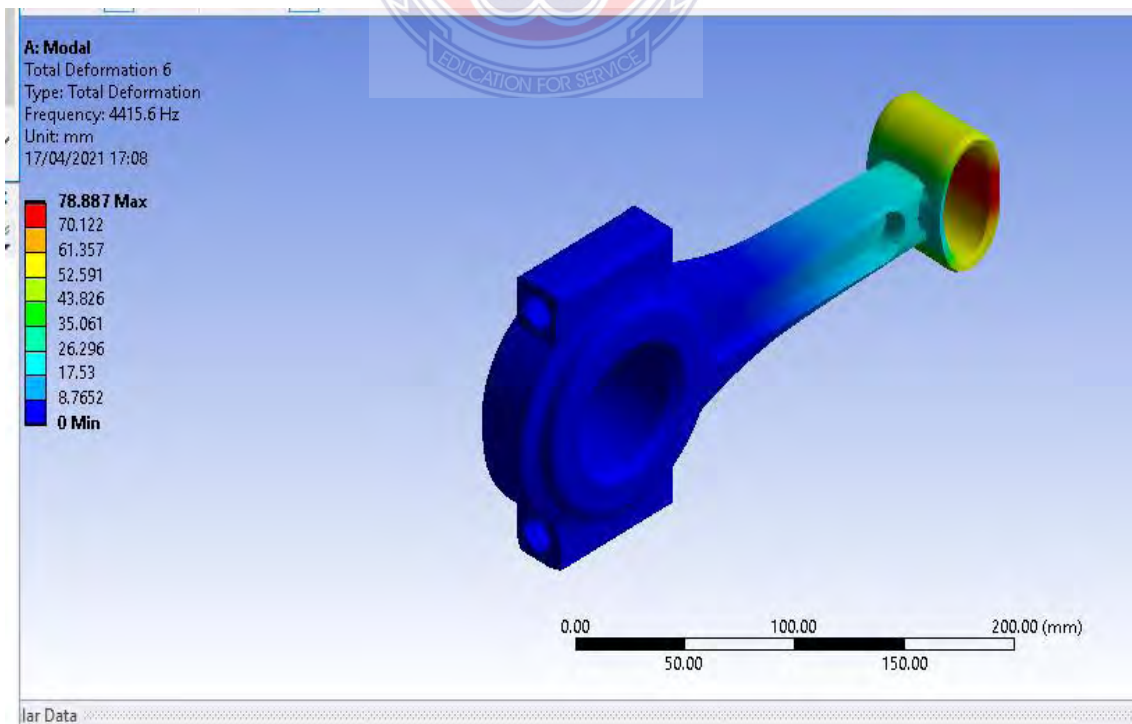


Figure 4.48 Vibration Mode Shape with Natural Frequency 4415.6 Hz

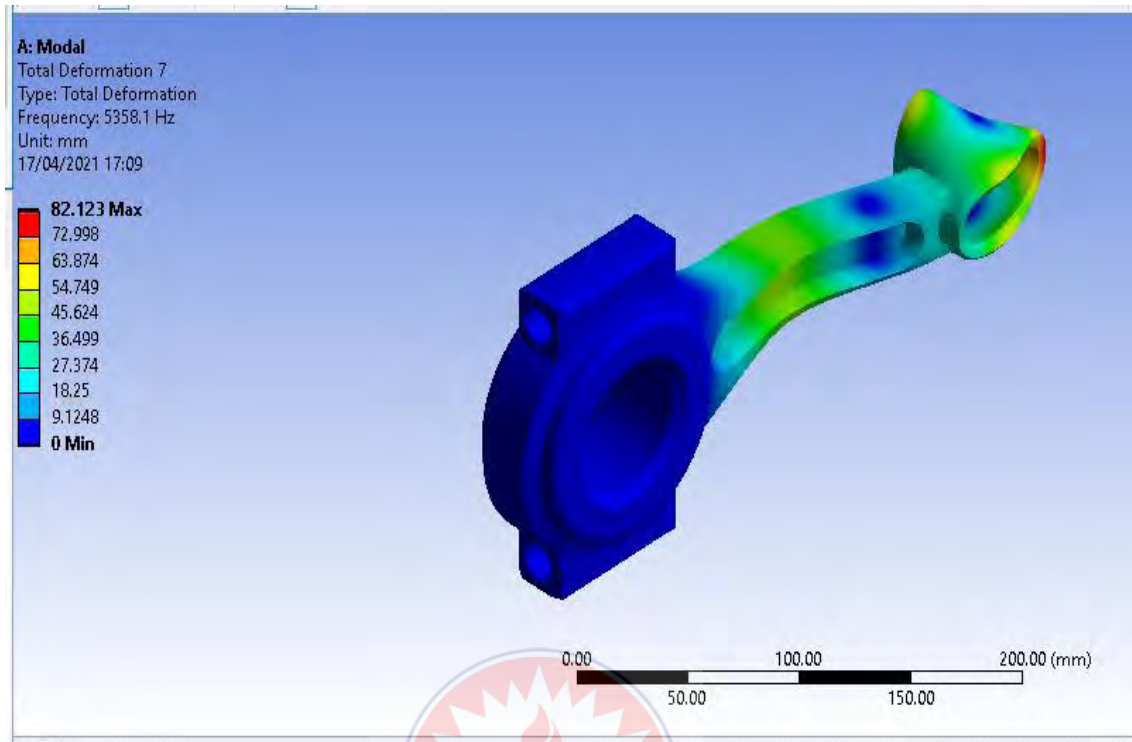


Figure 4.49 Vibration Mode Shape with Natural Frequency 5358.1 Hz

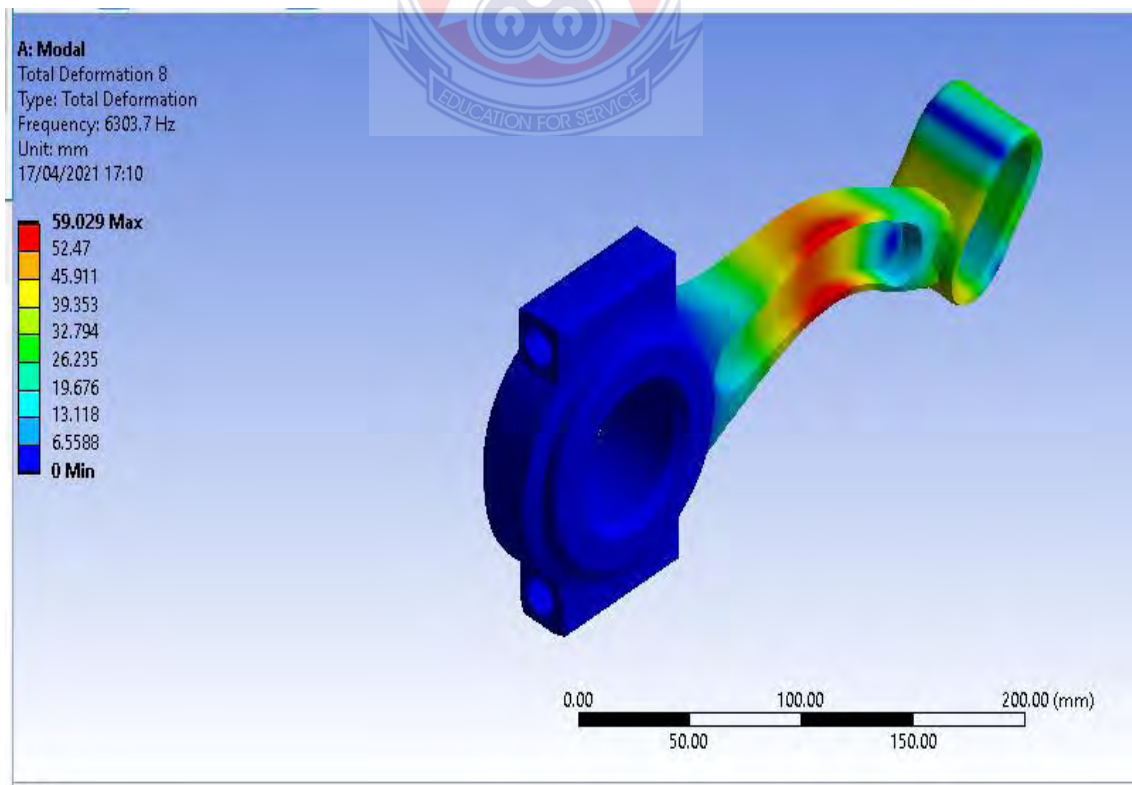


Figure 4.50 Vibration Mode Shape with Natural Frequency 6303.7 Hz

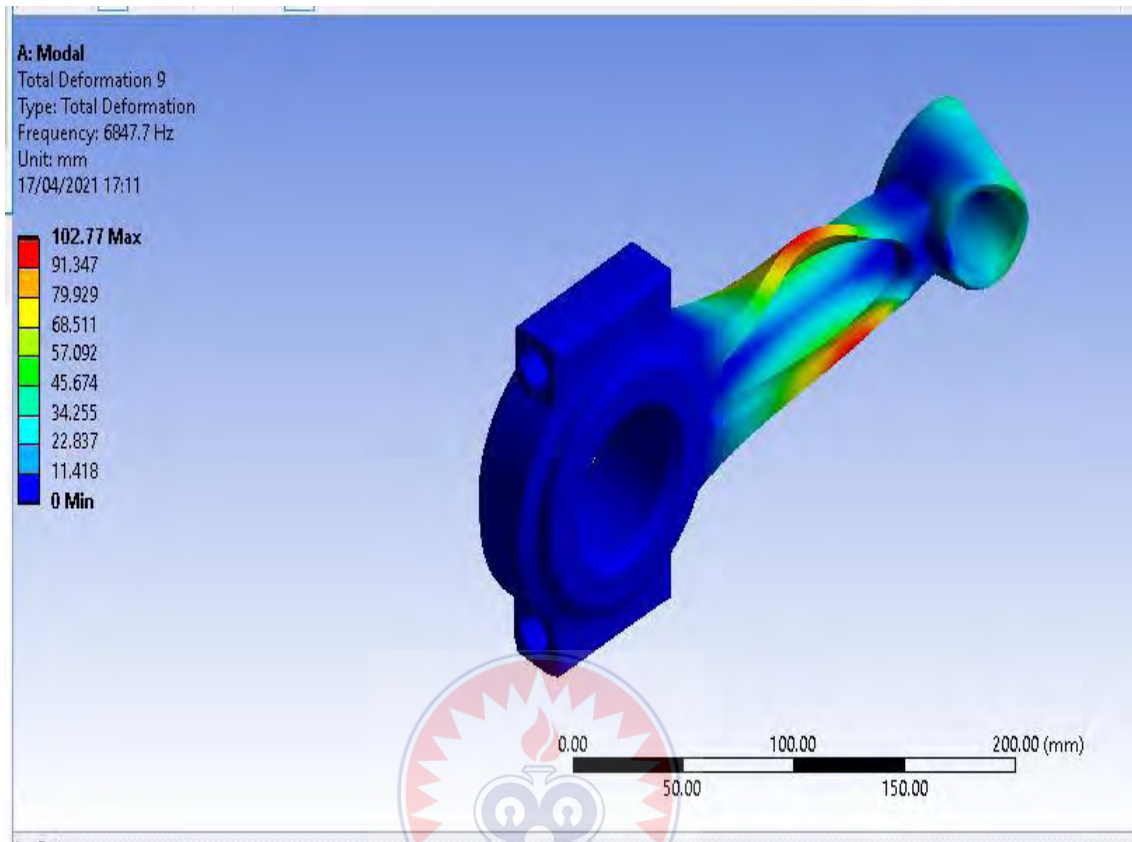


Figure 4.51 Vibration Mode Shape with Natural Frequency 6847.7 Hz

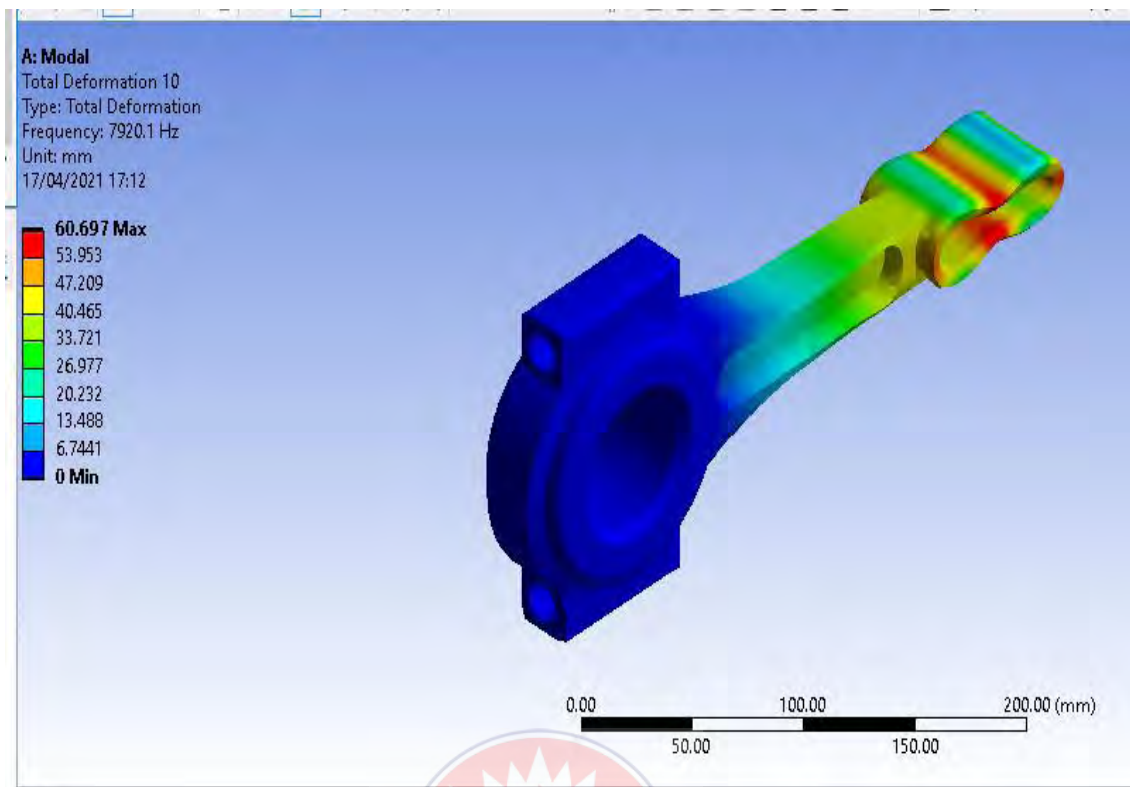


Figure 4.52 Vibration Mode Shape with Natural Frequency 7920.1 Hz

Table 4.7 Deformations and Natural Frequencies of Connecting Rod of Structural Steel

Mode number	Structural Steel Material	
	Deformation (mm)	Natural frequency (Hz)
1	61.754	408.3
2	64.552	777.4
3	80.687	1025.7
4	65.873	2353.9
5	51.019	2851.4
6	78.887	4415.6
7	82.123	5358.1
8	59.029	6303.7
9	102.77	6847.7
10	60.697	7920.1

Table 4.7 shows the deformations and the natural frequencies when modal analysis was performed on connecting rod of structural steel material. It was observed from Table 4.7 that the modal number with the highest deformation of 102.77 mm is mode 9 corresponding to a natural frequency of 6847.7 Hz. It was also observed that mode 5 has the least deformation of 51.019 mm corresponding to a natural frequency of 2851.4 Hz. From Table 4.7, it is clear that, the highest vibrational frequency of 7920.1 Hz corresponding to mode 10 has a low deformation of 60.697 mm compared to some of the modes with low frequencies. It was again observed that the deformation of the connecting rod of structural steel is not proportional to the magnitudes of the natural frequency.



c. Gray Cast Iron Material

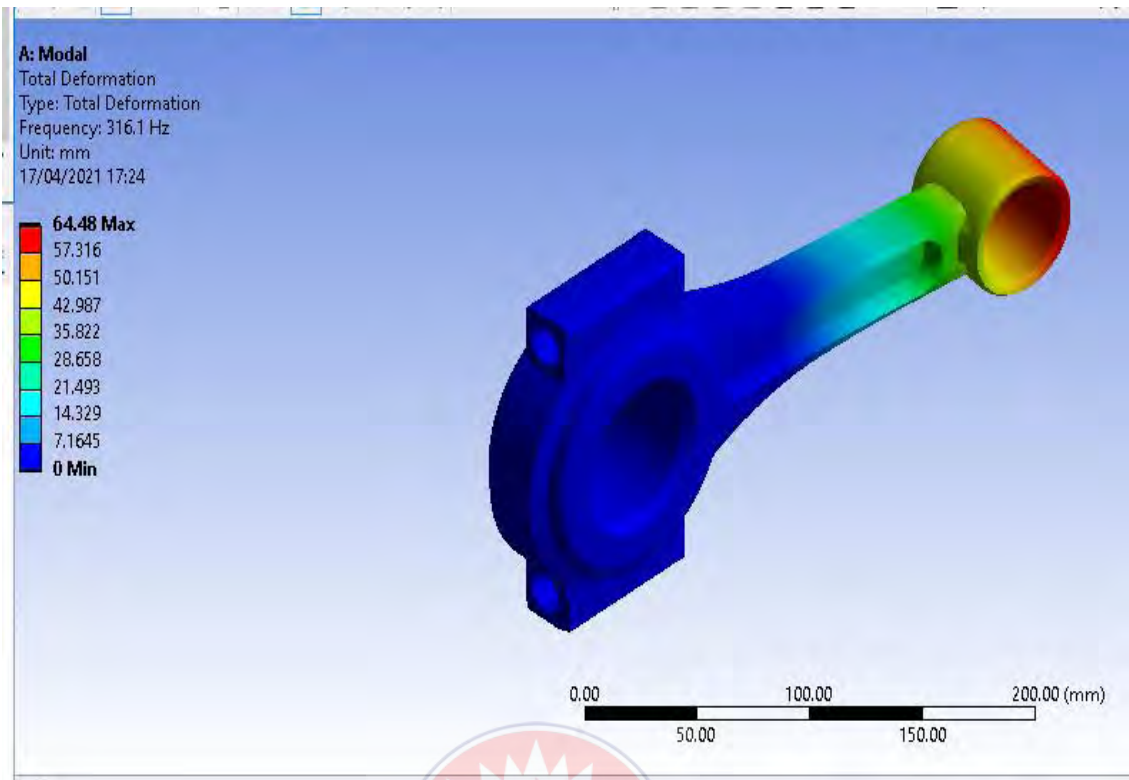


Figure 4.53 Vibration Mode Shape with Natural Frequency 316.10 Hz

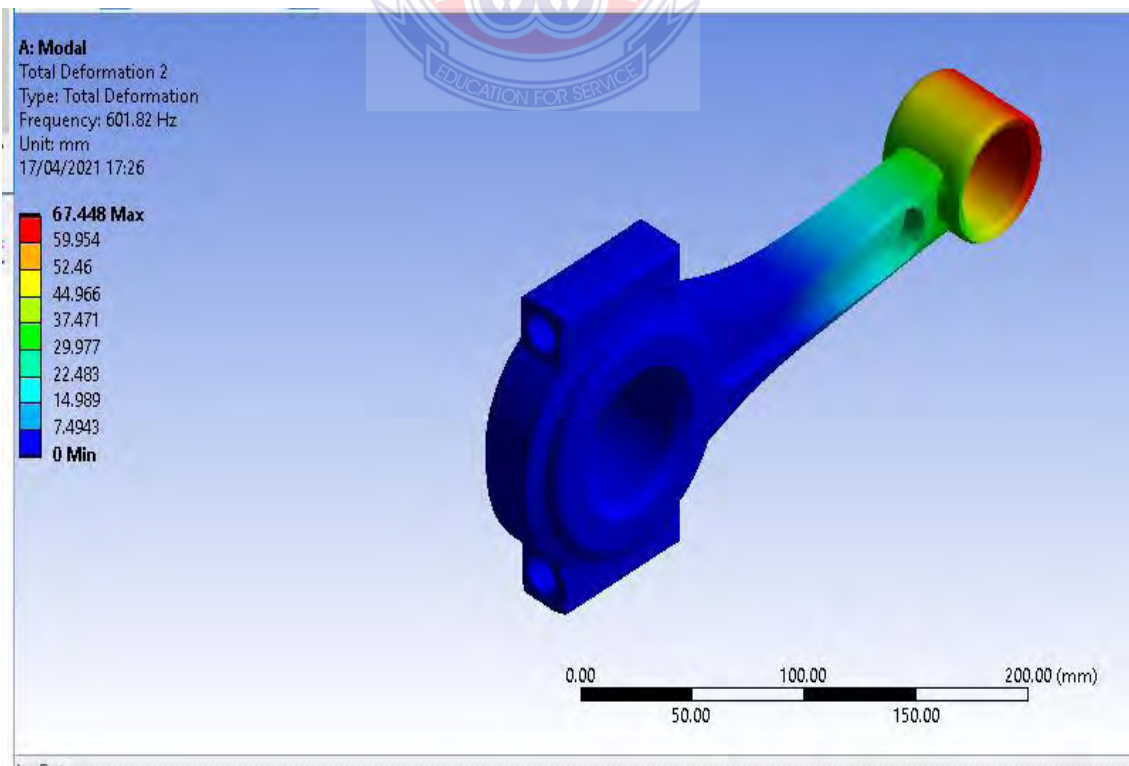


Figure 4.54 Vibration Mode Shape with Natural Frequency 601.82 Hz

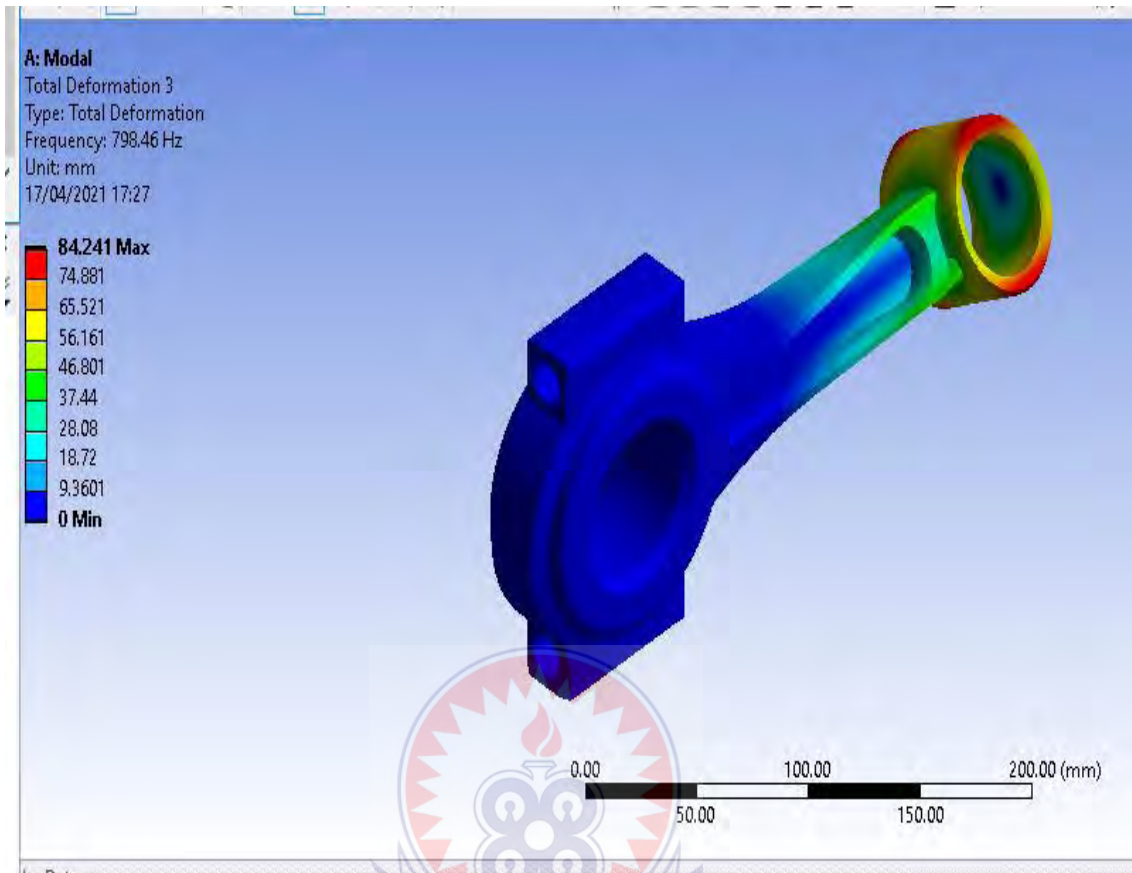


Figure 4.55 Vibration Mode Shape with Natural Frequency 798.46 Hz

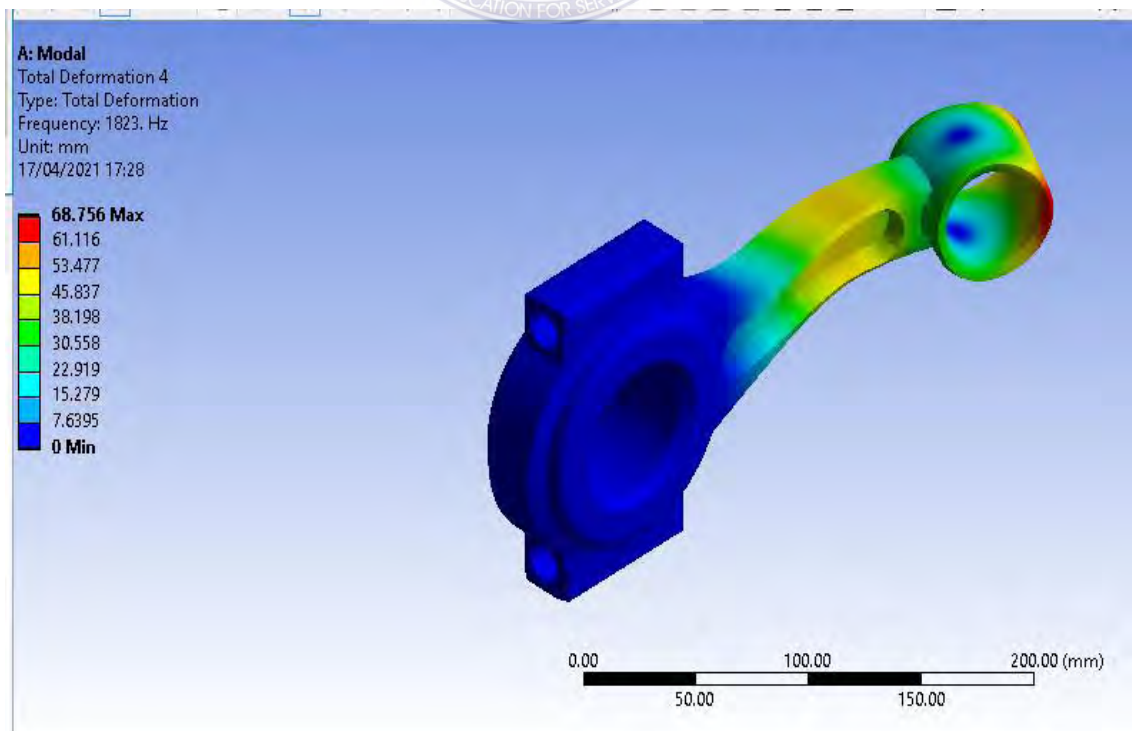


Figure 4.56 Vibration Mode Shape with Natural Frequency 1823.0 Hz

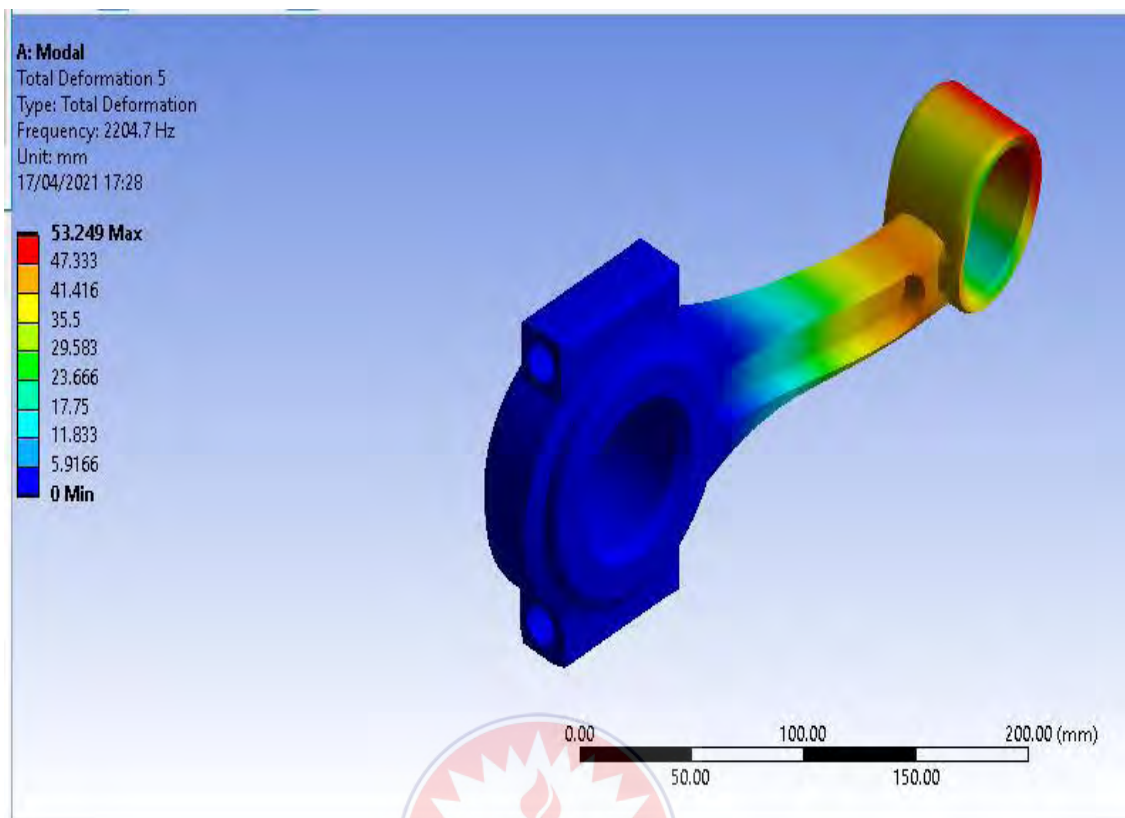


Figure 4.57 Vibration Mode Shape with Natural Frequency 2204.70 Hz

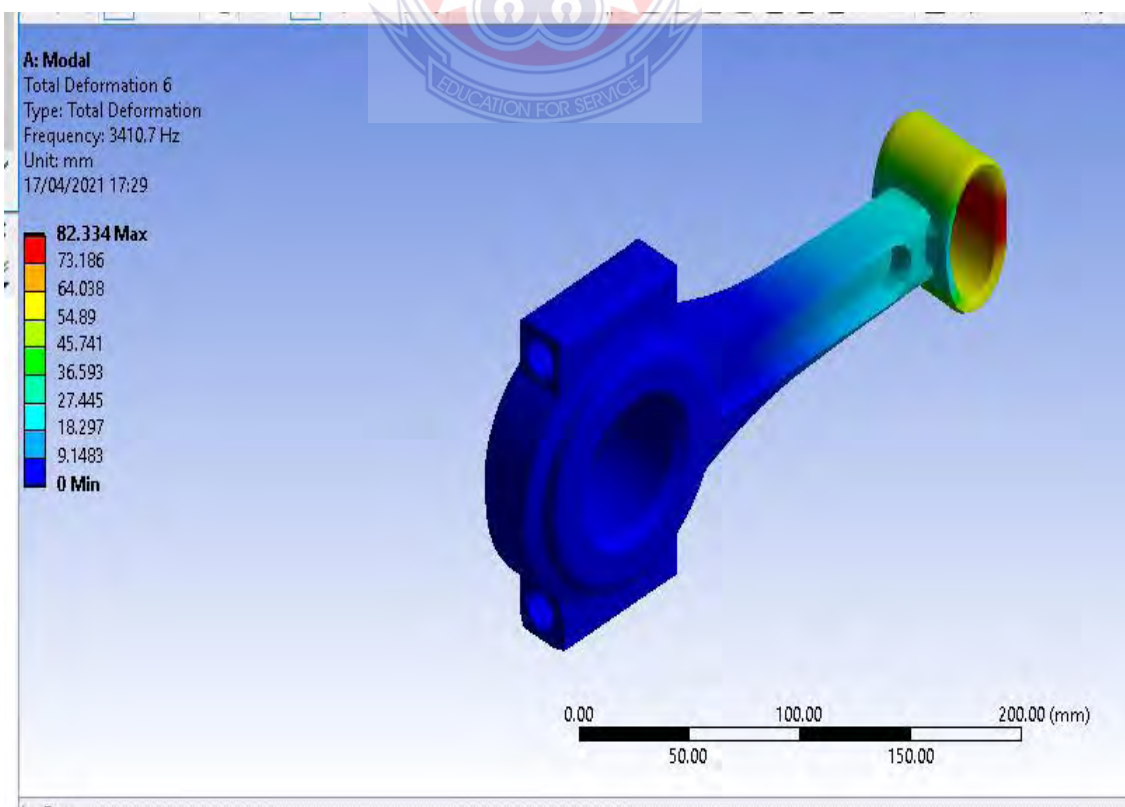


Figure 4.58 Vibration Mode Shape with Natural Frequency 3410.70 Hz

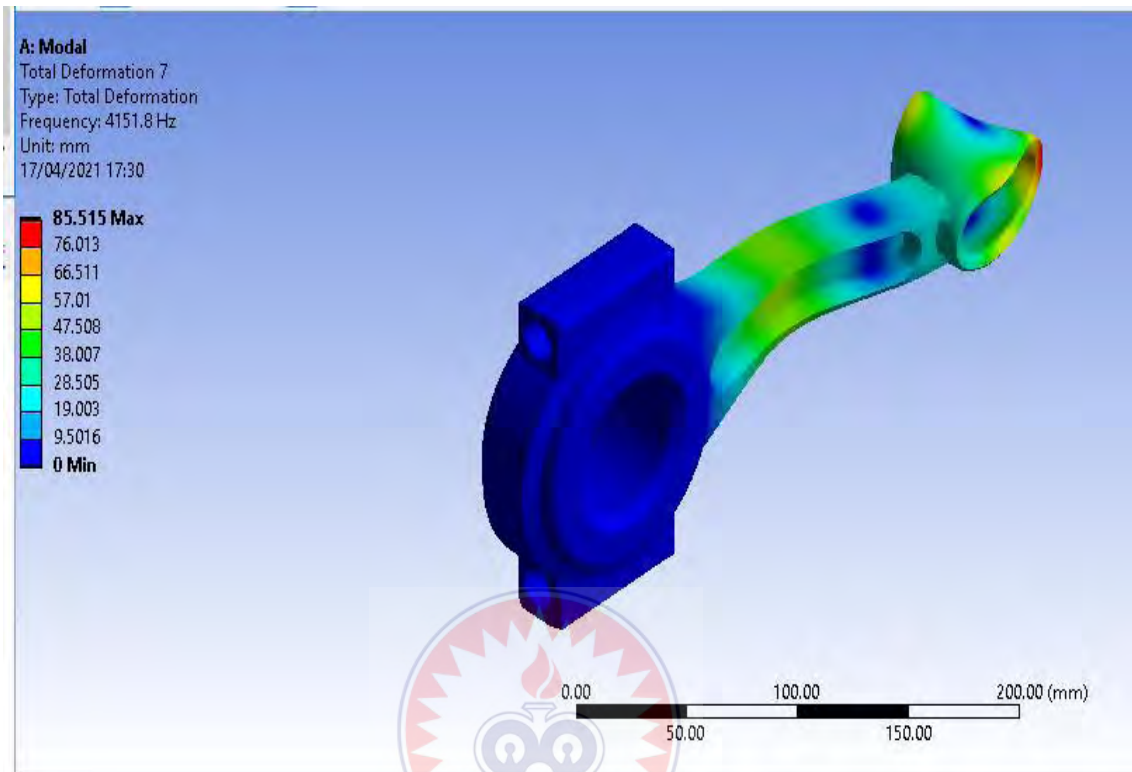


Figure 4.59 Vibration mode shape with natural frequency 4151.80 Hz

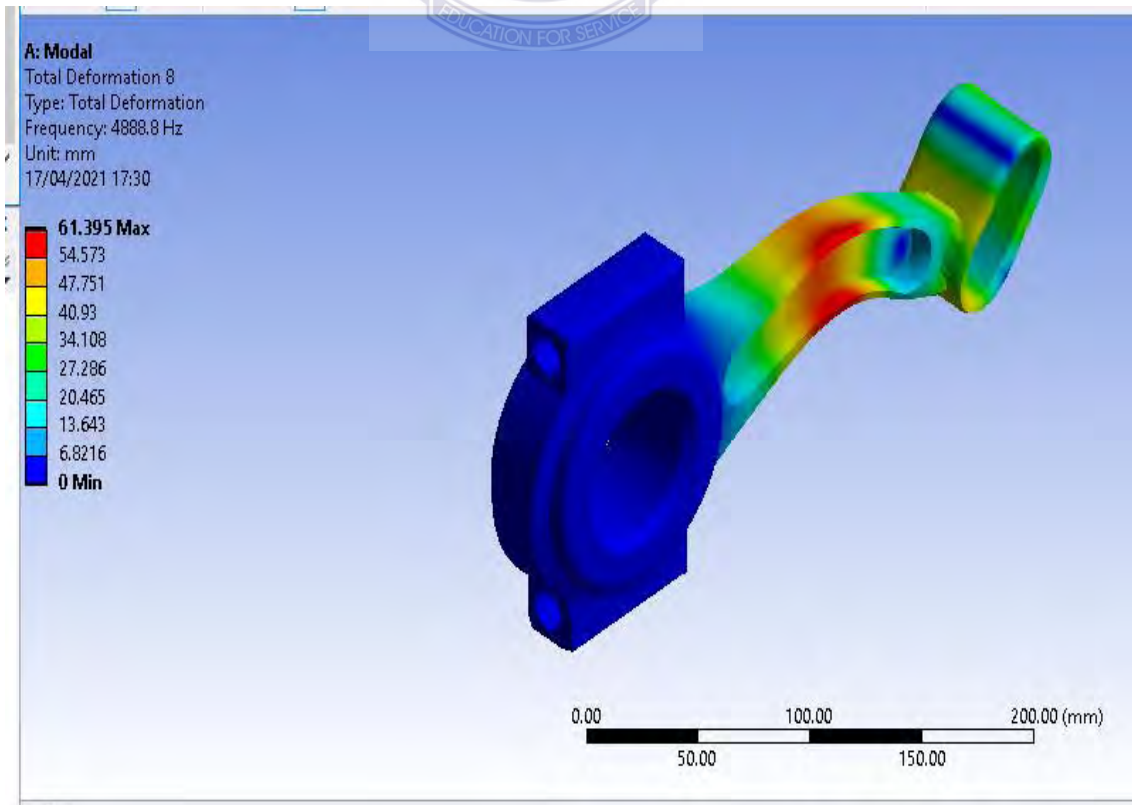


Figure 4.60 Vibration Mode Shape with Natural Frequency 4888.80 Hz

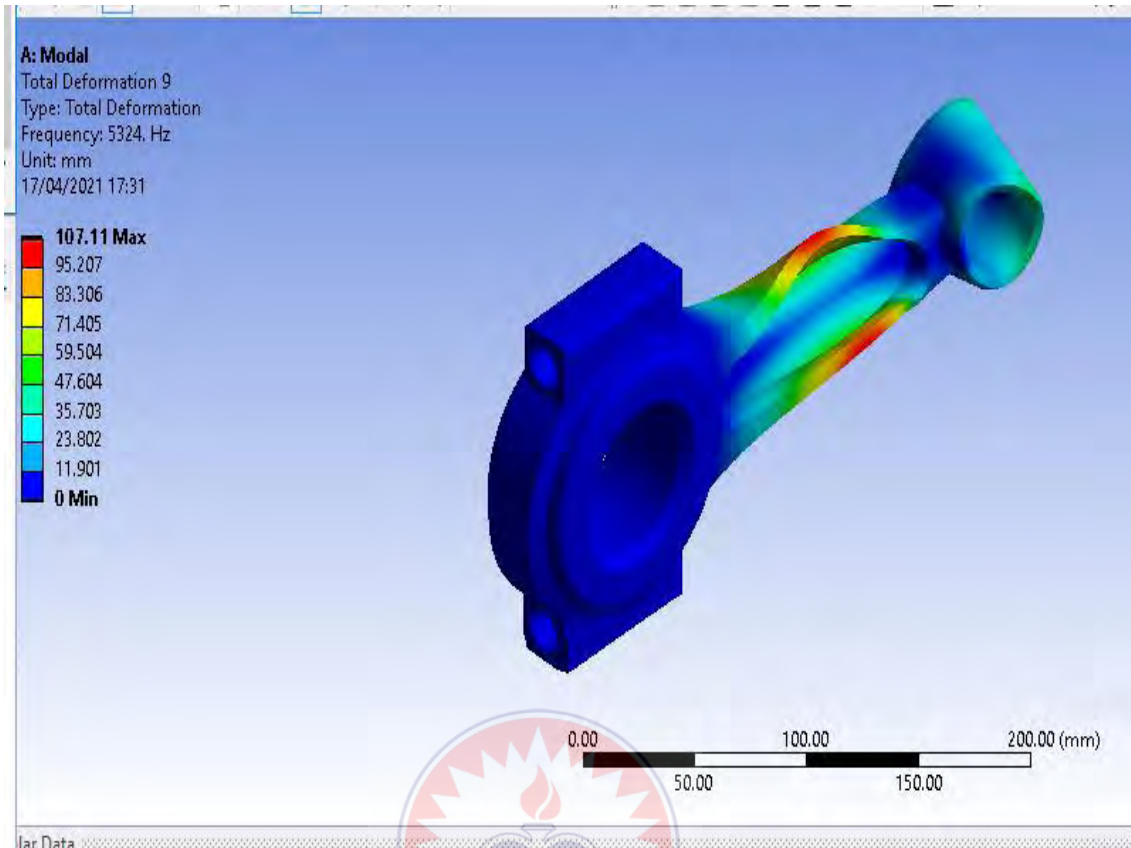


Figure 4.61 Vibration Mode Shape with Natural Frequency 5324.00 Hz

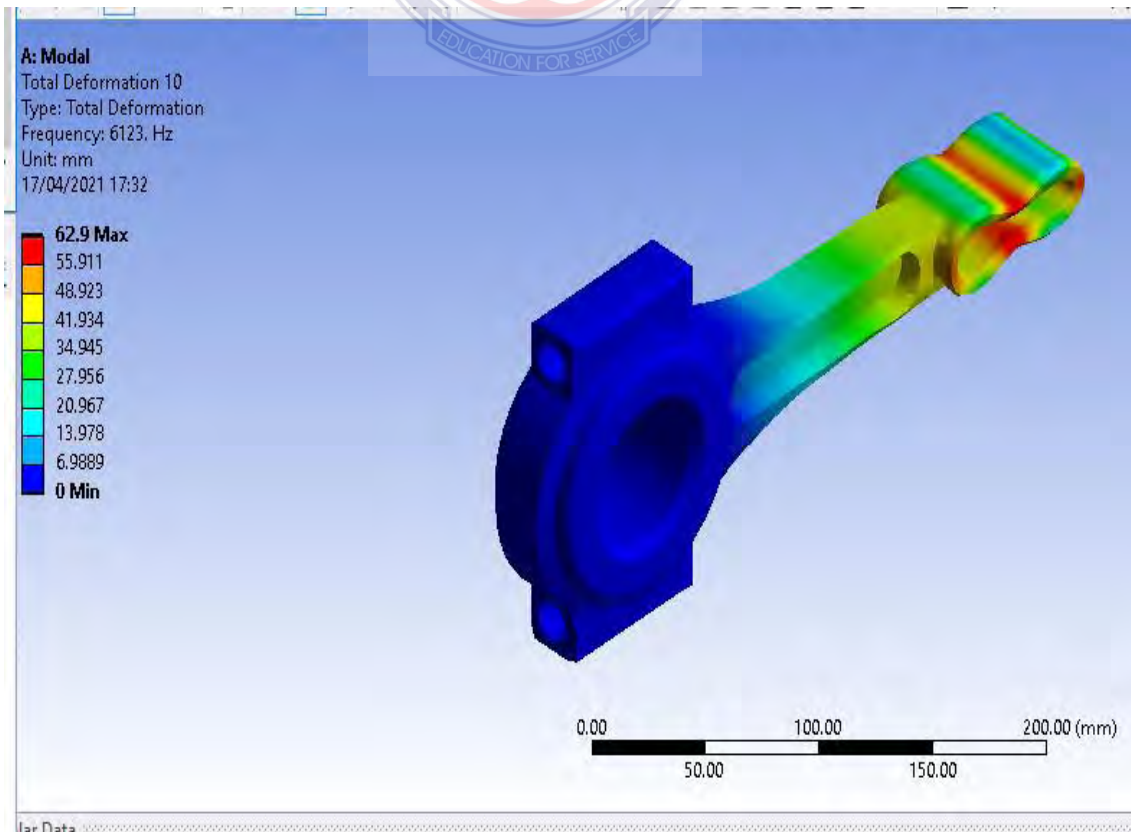


Figure 4.62 Vibration Mode Shape with Natural Frequency 6123.00 Hz**Table 4.8 Deformations and Natural Frequencies of Connecting Rod of Gray Cast Iron**

Mode number	Gray Cast Iron Material	
	Deformation (mm)	Natural frequency (Hz)
1	64.480	316.10
2	67.448	601.82
3	84.241	798.46
4	68.756	1823.00
5	53.249	2204.70
6	82.334	3410.70
7	85.515	4151.80
8	61.395	4888.80
9	107.11	5324.00
10	62.90	6123.00

Table 4.8 shows the deformations and the natural frequencies when modal analysis was performed on connecting rod of gray cast iron material. It was observed from Table 4.8 that the mode number with the highest deformation of 107.11 mm occurred in mode 9 corresponding to a natural frequency of 5324.00 Hz. It was also observed that mode 5 has the least deformation of 53.249 mm corresponding to a natural frequency of 2204.70 Hz. From Table 4.8, it was clear that, the highest vibrational frequency of 6123.00 Hz corresponding to mode 10 has a low deformation compared to some of the modes with low frequencies. It was again observed that the deformation of the connecting rod of gray cast iron material is not proportional to the magnitudes of the natural frequencies.

d. Aluminium 7075 T6 Alloy Material

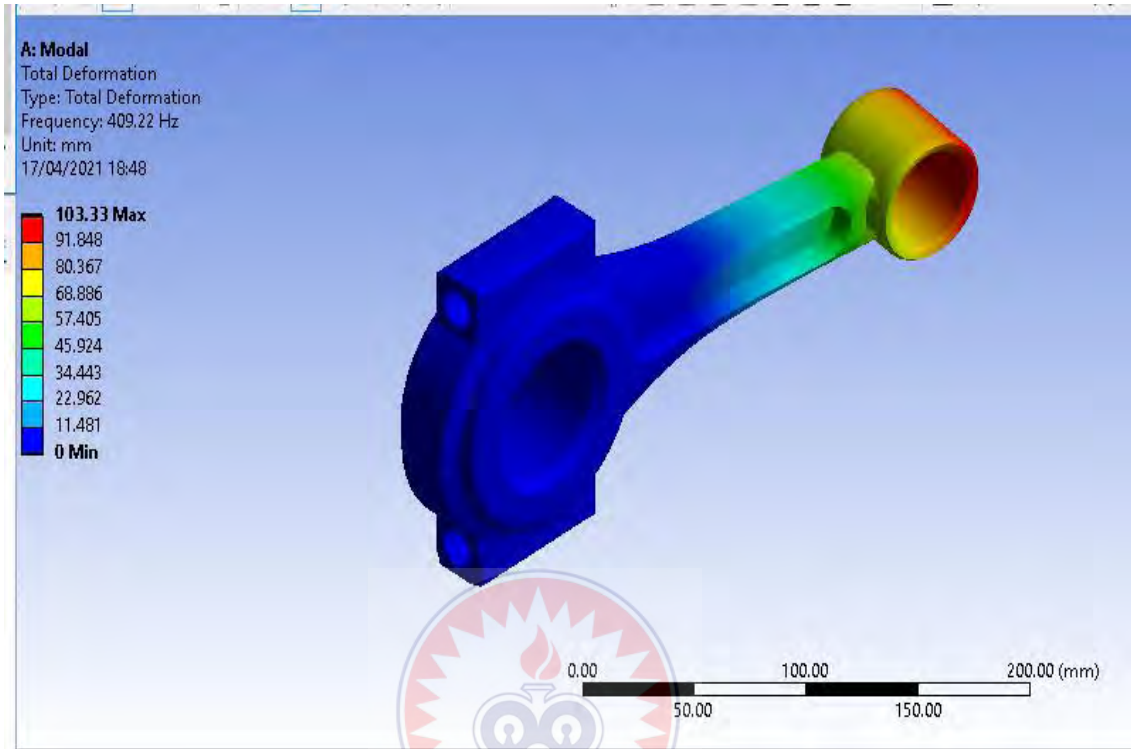


Figure 4.63 Vibration Mode Shape with Natural Frequency 409.22 Hz

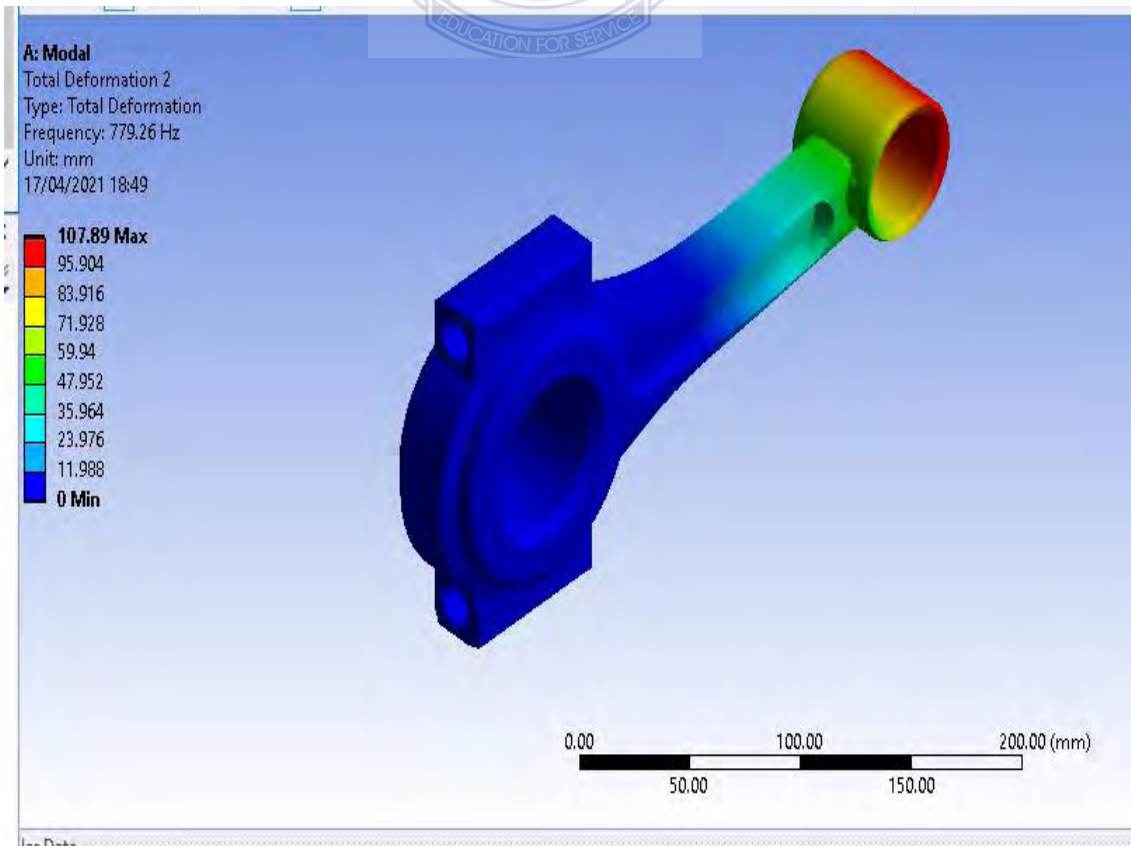


Figure 4.64 Vibration Mode Shape with Natural Frequency 779.26 Hz

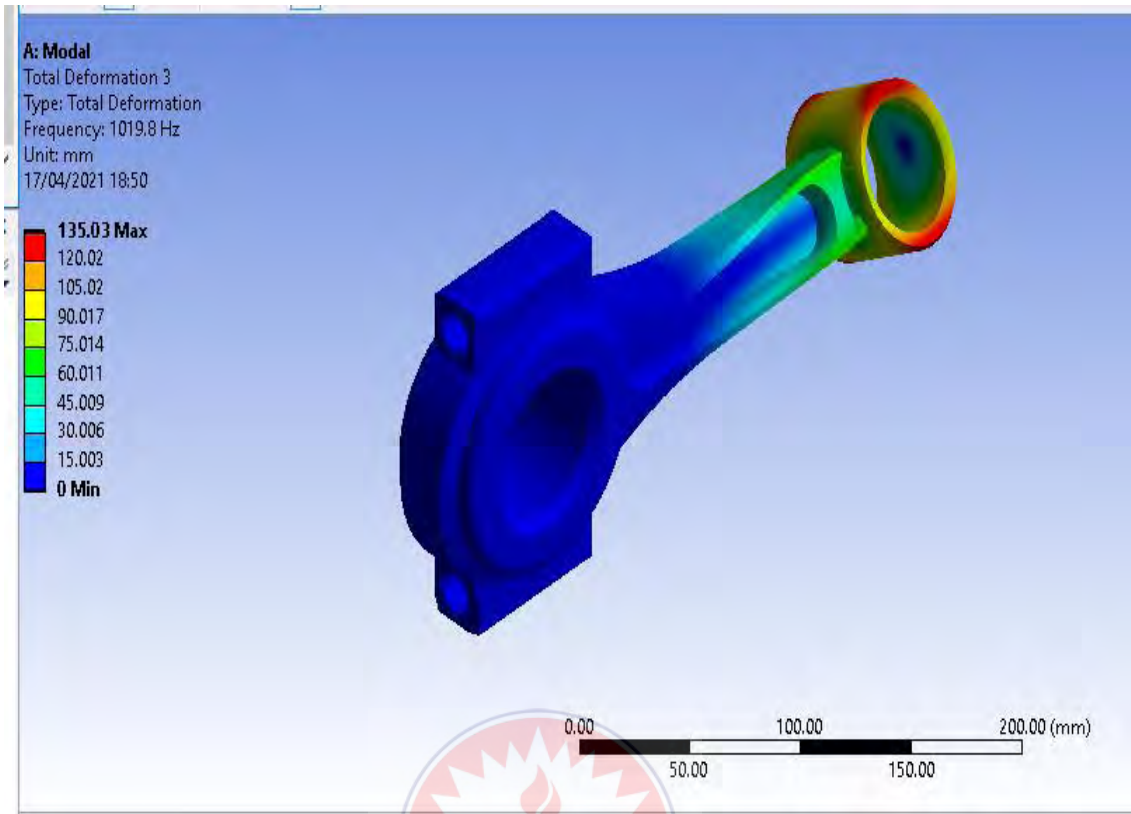
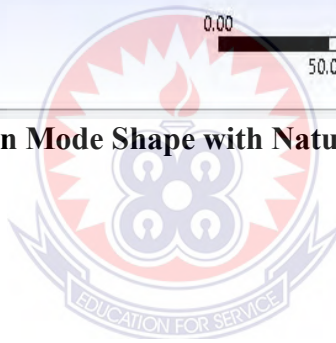


Figure 4.65 Vibration Mode Shape with Natural Frequency 1019.80 Hz



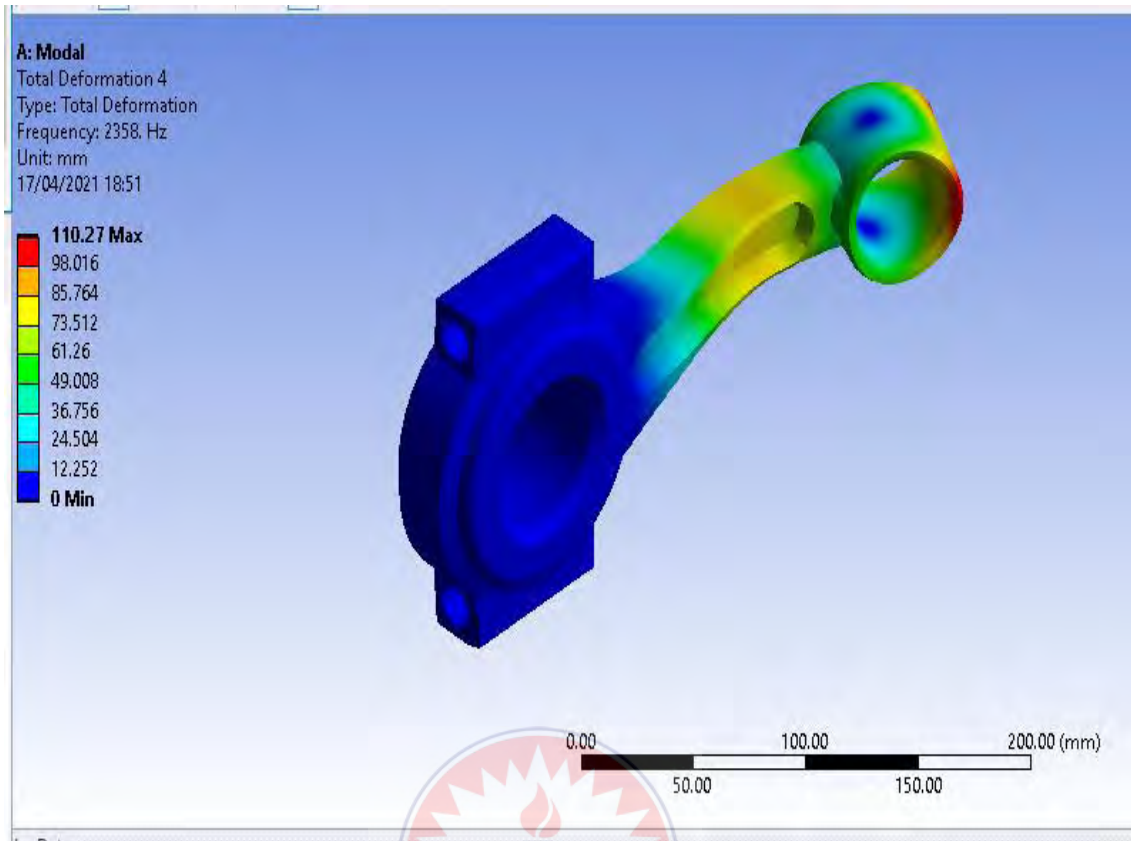


Figure 4.66 Vibration Mode Shape with Natural Frequency 2358.00 Hz



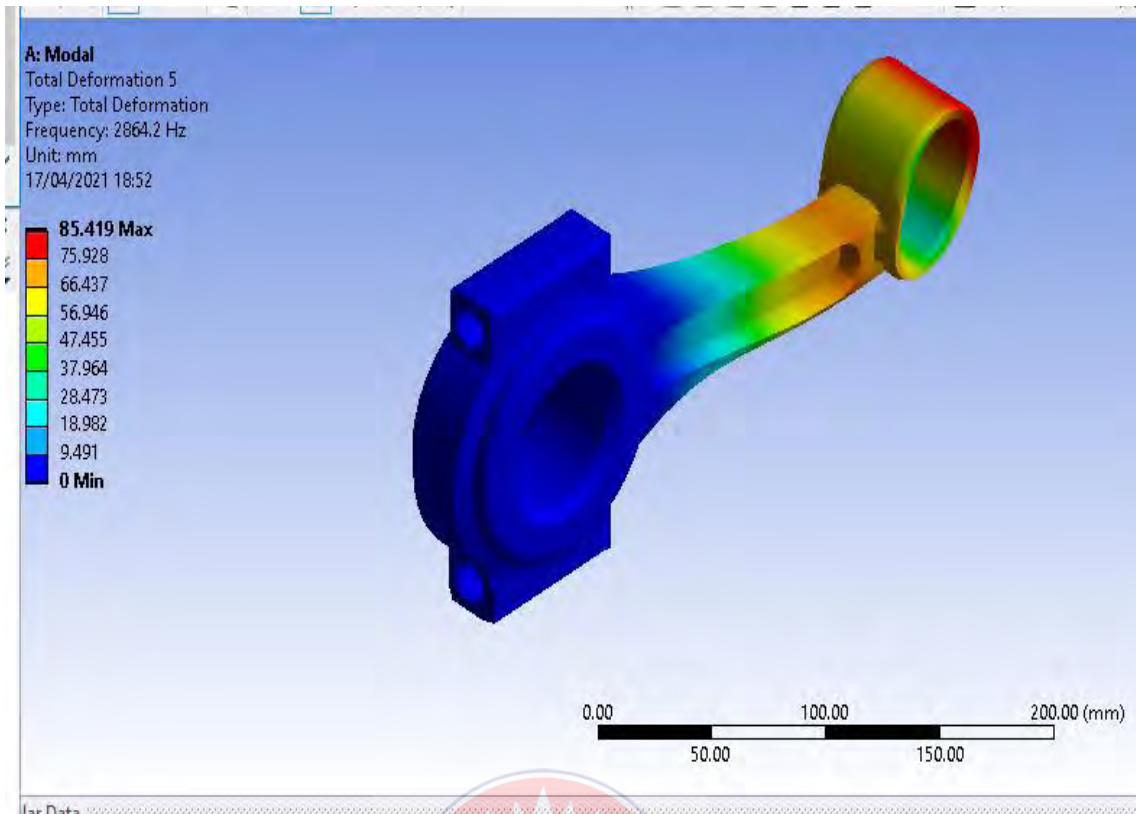


Figure 4.67 Vibration Mode Shape with Natural Frequency 2864.20 Hz

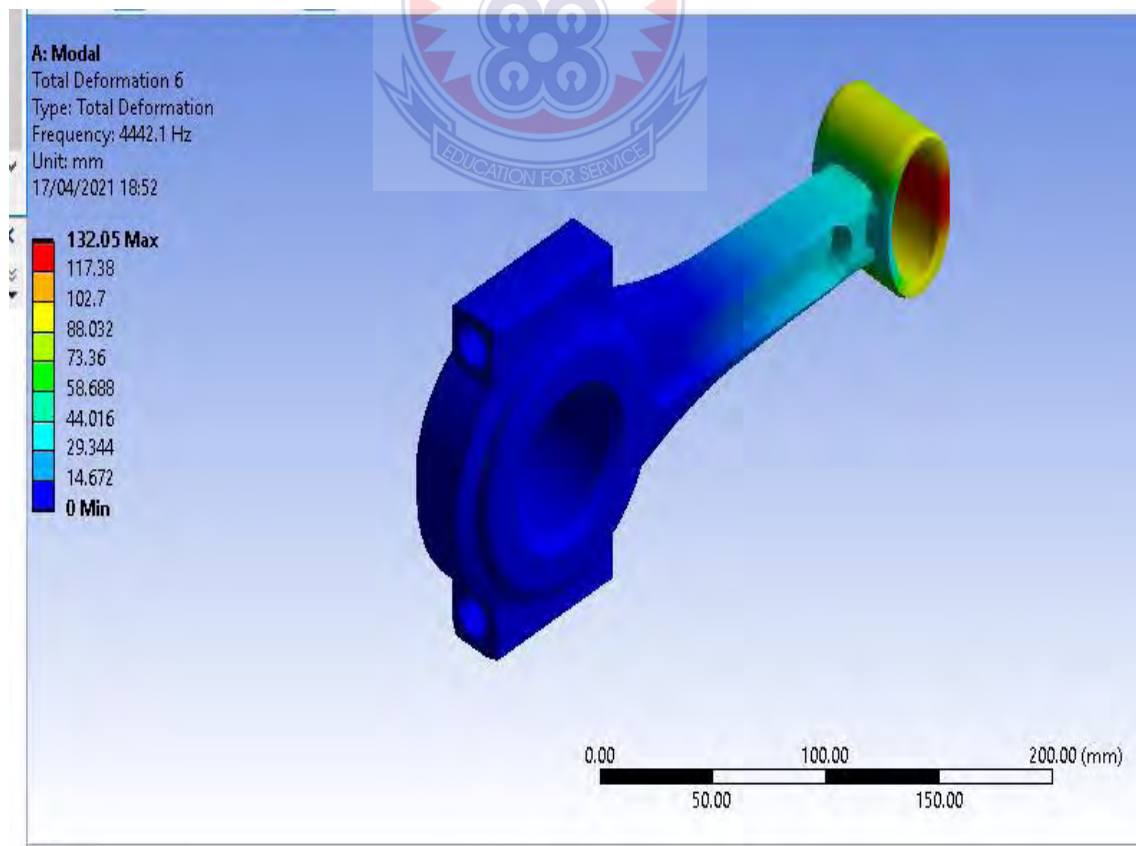


Figure 4.68 Vibration Mode Shape with Natural Frequency 4442.10 Hz

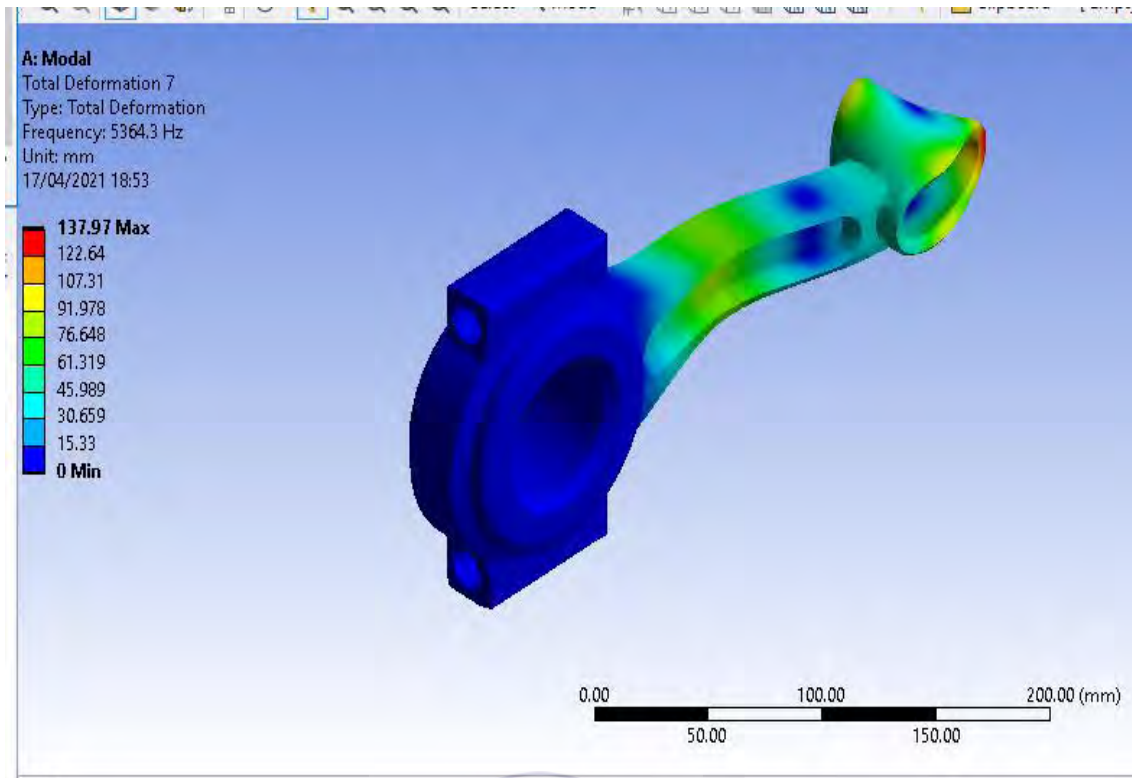


Figure 4.69 Vibration Mode Shape with Natural Frequency 5364.30 Hz

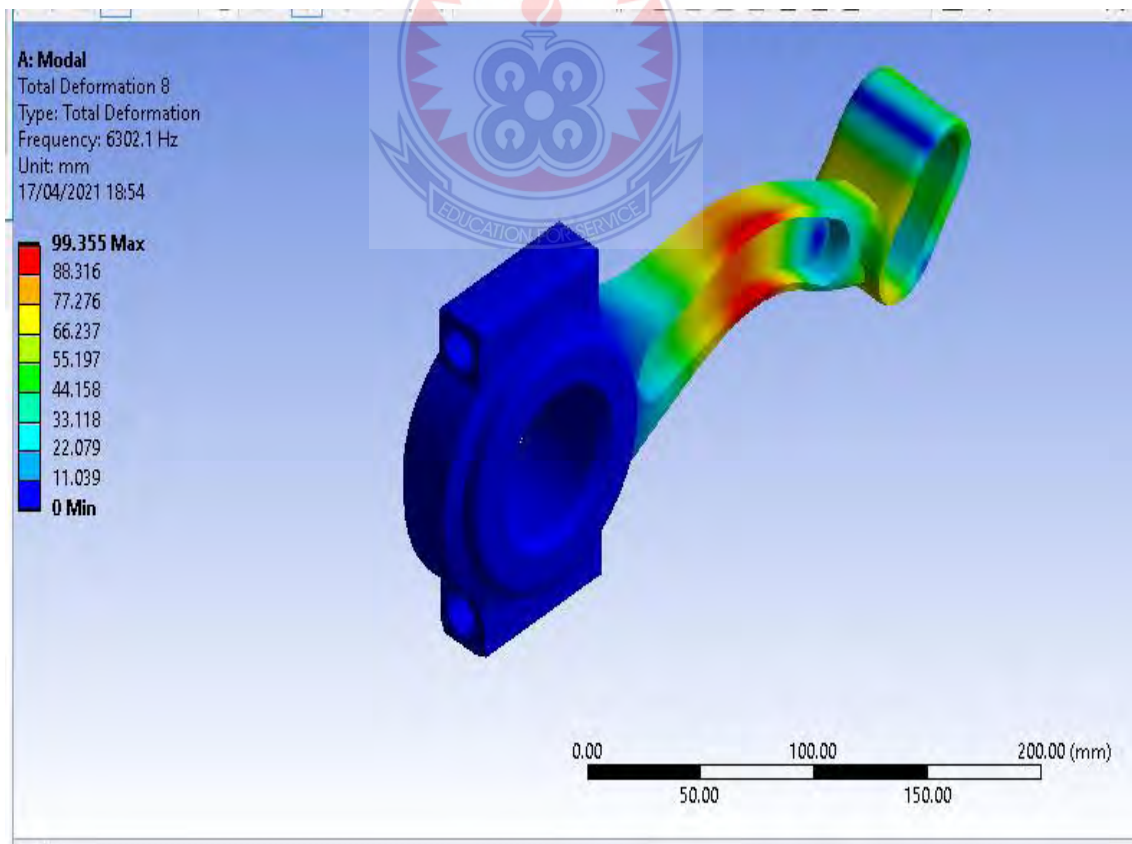


Figure 4.70 Vibration Mode Shape with Natural Frequency 6302.10 Hz

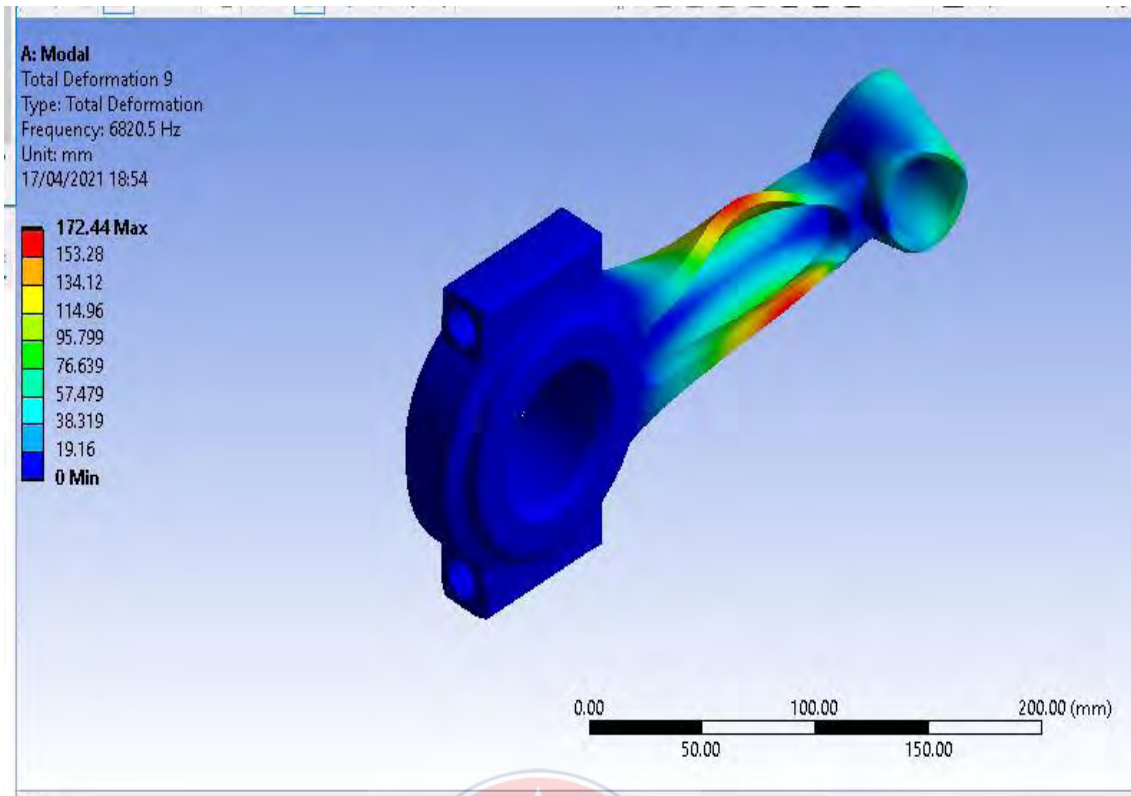


Figure 4.71 Vibration Mode Shape with Natural Frequency 6820.50 Hz

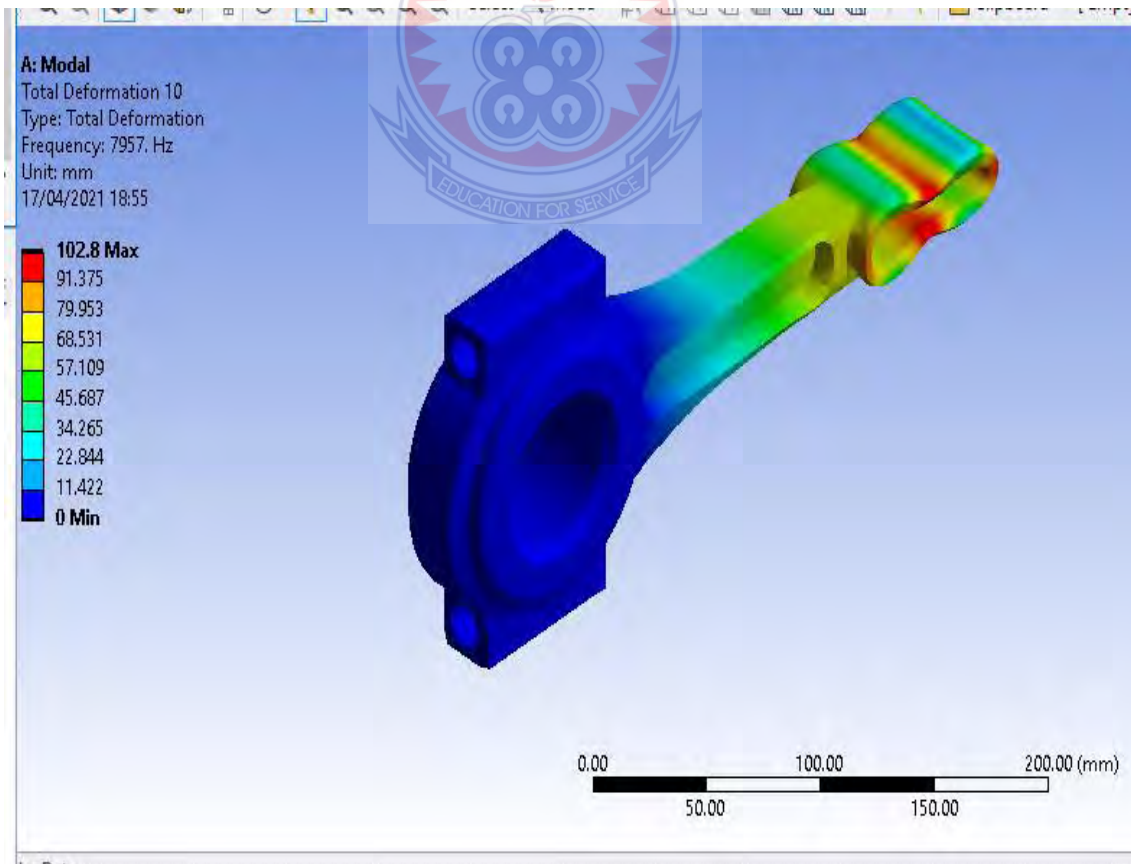


Figure 4.72 Vibration Mode Shape with Natural Frequency 7957.00 Hz

Table 4.9 Deformations and Natural Frequencies of Connecting Rod of Al7075

Mode number	Aluminium 7075 T6 Material	
	Deformation (mm)	Natural frequency (Hz)
1	103.33	409.22
2	107.89	779.26
3	135.03	1019.80
4	110.27	2358.00
5	85.419	2864.20
6	132.05	4442.10
7	137.97	5364.30
8	99.36	6302.10
9	172.44	6820.50
10	102.80	7957.00

Table 4.9 shows the deformations and the natural frequencies when modal analysis was performed on connecting rod of Aluminium 7075 T6 alloy material. It was observed from Table 4.9 that the mode number with the highest deformation of 172.44 mm occurred in mode 9 corresponding to a natural frequency of 6820.50 Hz. It was also observed that mode number 5 has the least deformation of 85.419 mm corresponding to a natural frequency of 2864.20 Hz. From Table 4.9, it was clearly observed that, the highest vibrational frequency of 7957.00 Hz corresponding to mode 10 has a low deformation of 102.80 mm compared to some of the modes with low frequencies. It was again observed that the deformation of the connecting rod of aluminium 7075 T6 alloy material is not proportional to the magnitudes of the natural frequencies.

4.4 Discussion of the Modal Analysis Results

The deformations and natural frequencies of the connecting rods made with the four different materials were compared using graphs as follows:

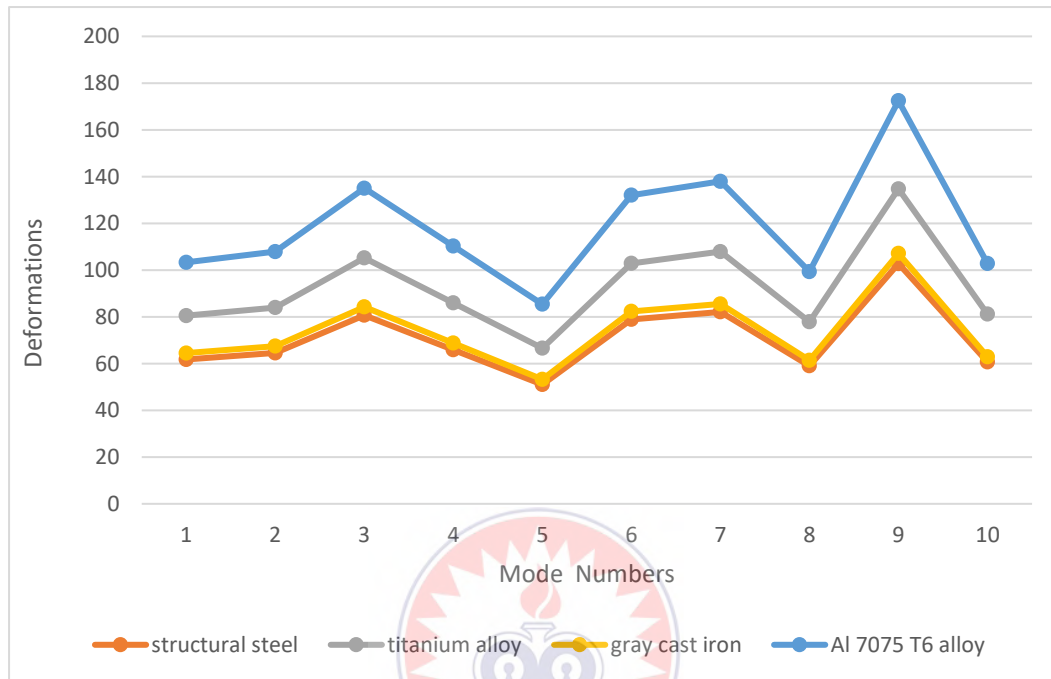


Figure 4.73 Comparison of Deformations of Different Materials of Connecting Rod

From Figure 4.73, when the deformations of the connecting rods made with the four different materials were compared, it was observed that the connecting rod made with aluminium 7075 T6 alloy yielded the highest deformations across all mode levels. It was also observed that mode number 5 yielded the least deformation of 85.416 mm while mode number 9 yielded the highest deformation of 172.44 mm within the ten (10) mode levels of the aluminium 7075 T6 alloy material. The Figure shows that titanium alloy connecting rod also significantly deformed but not as compared to aluminium 7075 T6 alloy connecting rod. It was also revealed that mode number 5 has the least deformation of 66.588 mm while mode number 9 yielded the highest deformation of 134.74 mm within the ten (10) mode levels of titanium alloy material. The graph in Figure 4.73 shows almost the same levels of deformation for structural

steel and gray cast iron connecting rods but with a careful observation, structural steel appeared to have the least deformations across all mode levels. The deformations of the connecting rods of the four materials appeared to follow the same trend as in all cases, mode numbers 5 having the lowest deformations while mode numbers 9 having the highest deformations. The deformations were observed to be trending downward at mode number 10. The comparison revealed that, structural steel and gray cast iron materials have superior properties to resist deformation than aluminium 7075 T6 and titanium alloy materials. If a connecting rod were to be selected on the bases of deformation, the ranking would have been first structural steel, gray cast iron, titanium alloy and aluminium 7075 T6 alloy respectively.

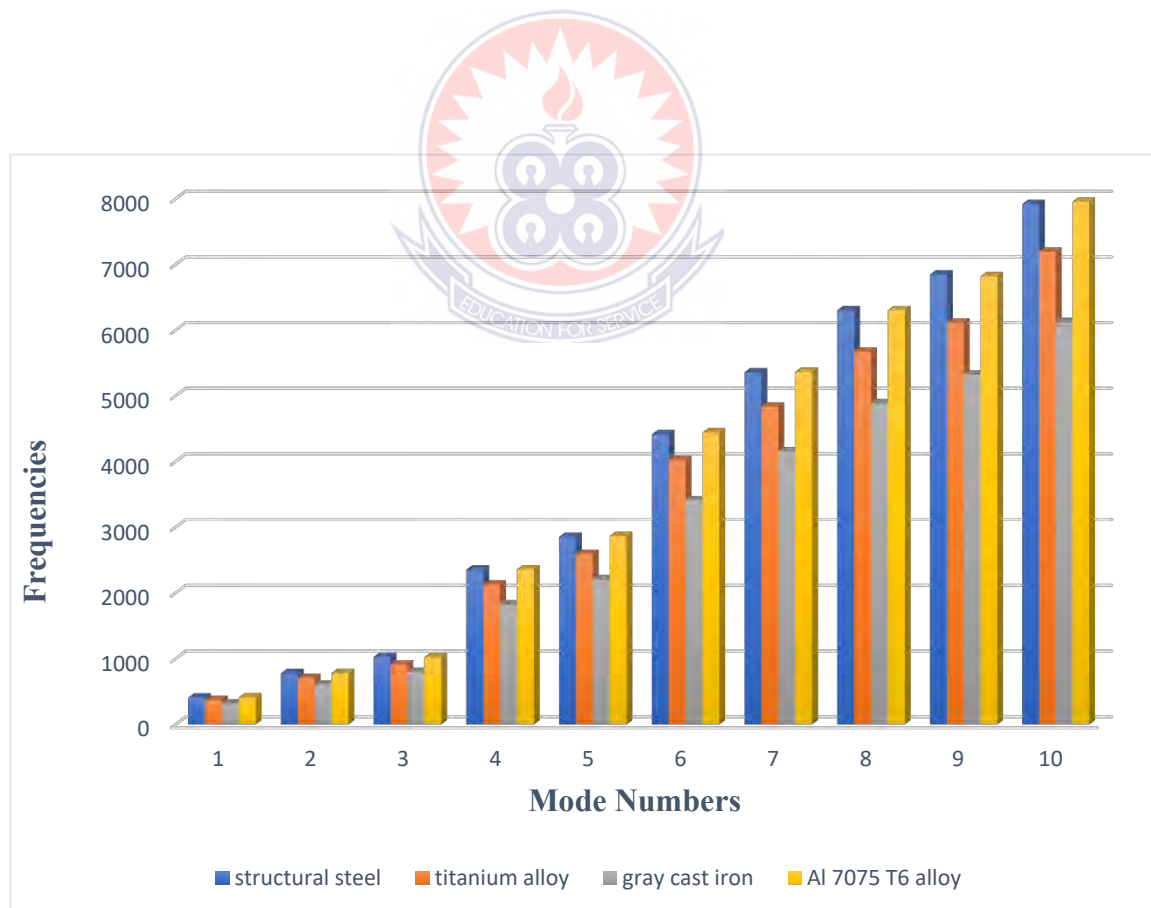
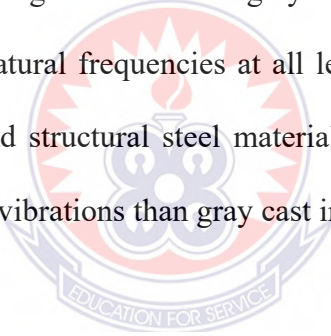


Figure 4.74 Comparism of Natural Frequencies of Connecting Rod Materials

Figure 4. 74 is a graph showing the comparison of the natural frequencies of the free vibrations of the connecting rods of the four different connecting rod materials at no load conditions. The trend as shown in the graph indicates that the natural frequencies increases along with an increasing mode number. Figure 4.74 shows that aluminium 7075 T6 alloy connecting rod has the highest natural frequencies at all levels of mode numbers ranging from mode 1 to 10. When the highest vibrational frequencies corresponding to mode 10, of all the connecting rod materials were compared the frequencies obtained were: aluminium 7075 T6 alloy connecting rod produced 7957 Hz, structural steel material connecting rod produced 7920.1 Hz, titanium alloy material connecting rod produced 7196.4 and gray cast iron material connecting rod produced 6123 Hz respectively. The figure show that gray cast iron material connecting rod produced low vibrational natural frequencies at all levels of modes. Aluminium 7075 T6 alloy connecting rod and structural steel material connecting rods appear to have superior properties in terms vibrations than gray cast iron material connecting rod.



4.5 Test Results for Validation

In this work, the aluminium 7075 T6 alloy material was used to fabricate the connecting rod of an internal combustion engine. The fabricated connecting rod was tested by using compressive testing machine and the results compared with the structural steel connecting rod. The compressive strengths of the two materials connecting rods were compared. It was observed that although the structural steel connecting rod was much stronger but the aluminium 7075 T6 alloy material connecting rod was equally strong but not as much as the structural steel connecting rod. The hardness of the aluminium 7075 T6 alloy connecting rod was compared to structural steel connecting rod and it

was found that both connecting rods have almost the same hardness. When the fabricated connecting rod made with aluminium 7075 T6 alloy material was weighed and compared to the weight of an existing structural steel connecting rod, it was observed that the aluminium 7075 T6 alloy material connecting rod has less weight when compared to the structural steel material connecting rod. The comparison of the final results are as shown in Table 4.10.

Table 4.10 Comparison of the Final Results

S/N	Parameters	Structural Steel Connecting Rod	Aluminium 7075 T6 Connecting Rod
1	Tensile Strength	845 MPa	780.34 MPa
2	Tensile Yield Strength	540 MPa	549.6 MPa
3	Compressive Yield Strength	720 MPa	607.9 MPa
4	Young's Modulus	210 GPa	71.7 GPa
5	Poisons Ratio	0.3	0.33
6	Weight	0.795 kg	0.286 kg

4.6 Weight of the Connecting Rod Calculations

a. Weight of the connecting rod for structural steel.

The volume of the connecting rod used is $523613 \text{ mm}^3 = 0.000523613 \text{ m}^3$.

Therefore the mass of the structural steel connecting rod is;

$$\text{mass} = \text{volume of the component} \times \text{density of the material}$$

The density of structural steel is $7.900 \text{ g/cm}^3 = 7.9 \times 10^6 \text{ g/m}^3$

Therefore;

$$\text{mass} = 0.000523613 \text{ m}^3 \times 7.9 \times 10^6 \frac{\text{g}}{\text{m}^3} = 4136.54 \text{ g} = \mathbf{4.13654 \text{ kg}}$$

weight of the connecting rod

$$= \text{mass of the connecting rod} \times \text{acceleration due to gravity}$$

$$w = mg = 4.13654 \times 9.81 = 40.58 \text{ kgm/s}^2 = \mathbf{40.58 \text{ N}}$$

Therefore;

The weight of structural steel connecting rod is **40.58 N**

b. Weight of the connecting rod for gray cast iron.

The volume of the connecting rod used is $523613 \text{ mm}^3 = 0.000523613 \text{ m}^3$.

Therefore the mass of the gray cast iron connecting rod is;

$$\text{mass} = \text{volume} \times \text{density of the material}$$

The density of gray cast iron is $7.196 \text{ g/cm}^3 = 7.196 \times 10^6 \text{ g/m}^3$

Therefore;

$$\text{mass of gray cast iron connecting rod} = 0.000523613 \text{ m}^3 \times 7.196 \times 10^6 \text{ g/m}^3$$

$$= 3767.919 \text{ g} = \mathbf{3.767919 \text{ kg}}$$

Weight of the gray cast iron connecting rod

$$= \text{mass of the gray cast iron connecting rod}$$

$$\times \text{acceleration due to gravity}$$

$$w = mg = 3.767919 \times 9.81 = 36.963 \text{ kgm/s}^2 = \mathbf{36.963 \text{ N}}$$

Therefore;

The weight of gray cast iron connecting rod is **36.963 N**

c. Weight of the connecting rod for Titanium alloy.

The volume of the connecting rod used is $523613 \text{ mm}^3 = 0.000523613 \text{ m}^3$.

Therefore the mass of the Titanium alloy connecting rod is;

$$\text{mass} = \text{volume} \times \text{density of the material}$$

The density of Titanium alloy is $4.84 \text{ g/cm}^3 = 4.84 \times 10^6 \text{ g/m}^3$

Therefore;

$$\text{mass of the Titanium alloy connecting rod}$$

$$= 0.000523613 \text{ m}^3 \times 4.84 \times 10^6 \text{ g/m}^3$$

$$= 2534.287 \text{ g} = \mathbf{2.534287 \text{ kg}}$$

$$\text{Weight of the Titanium alloy connecting rod}$$

$$= \text{mass of the Titanium alloy connecting rod}$$

$$\times \text{acceleration due to gravity}$$

$$w = mg = 2.534287 \times 9.81 = 24.861 \text{ kgm/s}^2 = \mathbf{24.861 \text{ N}}$$

Therefore;

The weight of the Titanium alloy connecting rod is **24.861 N**

d. Weight of the connecting rod for Aluminium 7075 T6 alloy.

The volume of the connecting rod used is $523613 \text{ mm}^3 = 0.000523613 \text{ m}^3$.

Therefore the mass of the Aluminium 7075 T6 alloy connecting rod is;

$$\text{mass} = \text{volume} \times \text{density of the material}$$

The density of Aluminium 7075 T6 material is $2.81 \text{ g/cm}^3 = 2.81 \times 10^6 \text{ g/m}^3$

Therefore;

$$\begin{aligned} \text{mass of the Al 7075 T6} &= 0.000523613 \text{ m}^3 \times 2.81 \times 10^6 \text{ g/m}^3 \\ &= 1471.353 \text{ g} = 1.471353 \text{ kg} \end{aligned}$$

Weight of the Aluminium 7075 T6 alloy connecting rod

$$\begin{aligned} &= \text{mass of the aluminium 7075 T6 alloy connecting rod} \\ &\times \text{acceleration due to gravity} \end{aligned}$$

$$w = mg = 1.471353 \times 9.81 = 14.434 \text{ kgm/s}^2 = \mathbf{14.434 \text{ N}}$$

Therefore;

The weight of the Aluminium 7075 T6 alloy connecting rod is **14.434 N**



Table 4.11 Mass and weight of S. steel, G. C. Iron, Ti. Alloy and Al 7075 T6

	Structural Steel	Gray Cast Iron	Titanium Alloy	Aluminium 7075 T6 Alloy
<i>Mass (kg)</i>	4.14	3.77	2.53	1.47
<i>Weight (N)</i>	40.58	36.96	24.86	14.43

Table 4.11 shows the weights of the model connecting rods of the four different materials. When the weights were compared, it was observed that aluminium 7075 T6 alloy has the least weight followed by titanium alloy, gray cast iron and structural steel respectively. The implementing material which is aluminium 7075 T6 alloy is the best

material for weight and cost optimisation, since it is the lightest connecting rod with the weight of 14.43 N compared to the connecting rod made with the other three materials. Aluminium 7075 T6 alloy connecting rod is 73.77% lighter than the connecting rod made with structural steel which is the most common connecting rod material. The implementing material (Aluminium 7075 T6 alloy) connecting rod is 71.92% lighter than the connecting rod made with gray cast iron and 63.19 % lighter than Titanium alloy connecting rod.



CHAPTER FIVE

SUMMARY OF FINDINGS, CONCLUSIONS AND RECOMMENDATIONS

5.0 Introduction

This chapter presents the summary of findings of the study and conclusions drawn based on the findings discovered by the study. Recommendations were made to guide policy makers, Automotive component manufacturers and vehicle assembly companies in Ghana to revolutionised the Automotive industry in Ghana and Africa as a whole to create jobs.

5.1 Summary of Findings

The following findings were made from the study into modelling and simulation of a connecting rod of an internal combustion engine using local aluminium alloy.

5.1.1 Findings from finite element analysis

1. The study found that, the strongest aluminium alloy so far on the market is aluminium 7075 alloy which has a composition of 90.0% Al, 5.6% Zn, 2.5% Mg, 0.23% Fe, and 1.6% Cu. This metal is used for designing components that requires high strength materials such as connecting rods. It was discovered that when the compressive gas load of 49637.2 N was applied to the aluminium 7075 T6 connecting rod using Ansys 2020R3 software, the stresses induced were

found to be far lower compared to the compressive yield strength of 607.9 MPa of aluminium 7075 T6 alloy material. The model aluminium 7075 T6 alloy connecting rod is therefore considered to be safe since it can withstand the given compressive gas load imposed. Hence, the suitability of local aluminium alloy such as Al 7075 T6 to design and manufacture connecting rod of an internal combustion engine has been established.

2. It was again revealed from the study that when the load of 49637.2 N was imposed on the connecting rods of the four different materials and their deformations compared, the maximum and minimum total deformations of structural steel connecting rod was 0.22733 mm and 0.025258 mm respectively, the maximum and minimum total deformation of titanium alloy connecting rod was 0.46668 mm and 0.051854 mm respectively, the maximum and minimum total deformation of gray cast iron connecting rod was 0.41499 mm and 0.046109 mm respectively, and the maximum and minimum total deformation of aluminium 7075 T6 connecting rod was 0.62979 mm and 0.069976 mm respectively. The comparison showed that structural steel connecting rod deformed less while the implementing material (Al 7075 T6) deformed more but it was also observed that the deformations of the connecting rods of the four different materials were within the percentage reductions of the materials hence all the connecting rods were found to be satisfactory.
3. Moreover, when the equivalent elastic strains of the connecting rods were compared, it was revealed that, the maximum and minimum elastic strain of structural steel connecting rod was 0.001955 and 2.4452×10^{-7} respectively, the maximum and minimum elastic strain of titanium alloy connecting rod was 0.0039991 and 5.7791×10^{-7} respectively, the maximum and minimum elastic

strain of gray cast iron connecting rod was 0.003579 and 4.2117×10^{-7} respectively and the maximum and minimum elastic strain of aluminium 7075 T6 connecting rod was 0.0054028 and 7.3223×10^{-7} respectively. It was further observed from the results that, structural steel connecting rod suffered the least elastic strain while the implementing material (Al 7075 T6) connecting rod suffered the worst elastic strain.

4. Furthermore, the equivalent Von Mises stresses induced in the connecting rods of the four different materials were also compared and it was found that, the maximum and minimum Von Mises stress induced in structural steel connecting rod was 378.75 MPa and 0.024154 MPa respectively, the maximum and minimum Von Mises stress induced in titanium alloy connecting rod was 372.51 MPa and 0.030258 MPa respectively, the maximum and minimum Von Mises stress induced in gray cast iron connecting rod was 381.04 MPa and 0.024559 MPa respectively and the maximum and minimum Von Mises stress induced in aluminium 7075 T6 alloy connecting rod was 375.52 MPa and 0.025789 MPa respectively. The observation from the data showed that, titanium alloy has the least induced Von Mises stress which was closely followed by the implementing material (Al 7075 T6) whiles gray cast iron connecting rod has the highest induced Von Mises stress. It was found that, the Von Mises stresses induced in all the connecting rods of the four different materials were below the compressive yield strengths of the individual materials, hence the connecting rods can withstand the load imposed.
5. When the modal analysis results were compared with the static structural results, it was observed that, the trend of deformation between the two analyses were consistent or the same. When the no load vibration deformation was compared,

it was found that the lowest deformation of all the connecting rods of the four different materials occurred in mode 5 with structural steel connecting rod having a deformation of 51.019 mm, titanium alloy connecting rod having a deformation of 66.588 mm, gray cast iron connecting rod having a deformation of 53.249 mm and aluminium 7075 T6 alloy connecting rod having a deformation 85.419 mm.

6. When the factor of safeties of the connecting rods were compared, it was found that gray cast iron connecting rod has no factor of safety whiles the connecting rods of the remaining three materials has very good factor of safety values.
7. Finally, when the highest natural frequencies of all the connecting rods of the four different materials which occurred in mode 10 were compared, it was observed that, structural steel connecting rod has the highest natural frequency of 7920.1 Hz, titanium alloy connecting rod has the highest natural frequency of 7196.4 Hz, gray cast iron connecting rod has the highest natural frequency of 6123 Hz and aluminium 7075 T6 alloy connecting rod having the highest natural frequency of 7957 Hz. It was further observed that aluminium 7075 T6 alloy connecting rod has the highest natural frequency when the highest natural frequencies of all the connecting rods were compared which was closely followed by structural steel connecting rod whiles the connecting rod with the least natural frequency was gray cast iron connecting rod.

5.1.2 Findings from test results

In a way to validate the results obtained from the finite element analysis, the implementing material (Al 7075 T6) was used to manufacture a prototype connecting rod. A compressive test was performed on the connecting rod of the

implementing material (Al 7075 T6) and an existing connecting rod made from steel. The results obtained from the two tests were compared and the following were the findings:

1. The two connecting rods which were connecting rod made from steel and the connecting rod made from the implementing material were found to have tensile strengths of 845 MPa and 780.34 MPa respectively. Both connecting rods were considered to have satisfactory tensile strengths, hence they are both strong.
2. The compressive yield strengths of the two connecting rods were compared and it was found that, the steel connecting rod has a compressive yield strength of 720 MPa while the compressive yield strength of aluminium 7075 T6 alloy connecting rod was 607.9 MPa. It was found that both connecting rods have compressive yield strength high enough to withstand the gas load.
3. Finally, when the weights of the two connecting rods were compared, the connecting rod made from steel weighed 0.795 kg representing 74% while the connecting rod made with aluminium 7075 T6 alloy weighed 0.286 kg representing 26%. It was found that, the weight of connecting rod made with aluminium 7075 T6 alloy was 48 percent lower than the connecting rod made with steel. The total cost of manufacturing the connecting rod made with aluminium 7075 T6 material was GH¢ 65 which is lower compared to steel connecting rod which cost GH¢120 on the market. Hence, the main objective of using local aluminium alloy to design and manufacture connecting rod of an internal combustion engine for weight and cost reduction has been achieved.

5.2 Conclusions

This study considered two methods of analysis which were static structural and modal analyses. The parameters that were considered under the static structural analysis were: total deformation, directional deformation, equivalent elastic strain, equivalent Von Mises stress, maximum principal stress, minimum principal stress and the factor of safety of the four connecting rods made with titanium alloy, gray cast iron, structural steel and aluminium 7075 T6 alloy respectively. Both compressive and tensile loads act on the connecting rod but the compressive loads are much greater than the tensile loads, therefore the connecting rod was designed for the compressive load. Since, the connecting rod is hinged at both ends by piston pin and crank pin and experiences compressive load, therefore it can be said that it behaves like a strut.

The main objective of this project was to determine the possibility of using local aluminium alloy material to design and manufacture a connecting rod for weight optimisation without losing the strength of the connecting rod. The connecting rod was modelled using Autodesk inventor 2017 software using the calculated dimensions. The dimensioning of the connecting rod was obtained through systematic and rigorous calculations based on theoretically empirical formulae for connecting rod design. The drawing interface of the Autodesk inventor was launched and the connecting rod was modelled based on the dimensions generated in a 2D format and later converted through extrusion into a 3D format. The 3D connecting rod was saved in an imported stp (step) format for easy importation into Ansys. The analysis of the connecting rod was done using Ansys 2020R2 student's software. The connecting rod in the Ansys was subjected to a compressive calculated load of 49637.2 N.

Then Finite Element Analysis technique was used to determine the total deformation, directional deformation, equivalent elastic strain, equivalent Von Mises stress, maximum and minimum principal stress and factor of safety of the connecting rod of the four different materials and compared. The results of the analysis showed that, the stresses induced in the four connecting rods which were made of different materials were far below the yield strengths of the materials. Hence, it can be concluded that all the connecting rods of the four different materials can withstand the compressive gas loads that was imposed on them. It was also found that, Al 7075 T6 connecting rod has the highest deformation of 0.62979 mm representing 36 % which was more than all the other connecting rods. Structural steel connecting rod was found to have the lowest deformation of 0.22733 mm representing 13%. The results were validated by using the implementing material (Al 7075 T6 alloy) to fabricate a connecting rod and was tested using tensile test machine to determine the strength of the connecting rod. The test result was then compared to an existing connecting rod made with steel and it showed that both connecting rods are strong. The weights of the connecting rods were also compared and the result showed that the weight of aluminium 7075 T6 alloy connecting rod is 48% lower than the connecting rod made with steel. The total cost of manufacturing the connecting rod made with aluminium 7075 T6 material was GH¢ 65 which is lower compared to steel connecting rod which cost GH¢120 on the market. There is a cost savings of GH¢55 when the connecting rod of aluminium 7075 T6 material is considered.

5.3 Recommendations

The following recommendations have been arrived at based on the summary of findings revealed by the study:

1. Aluminium 7075 T6 alloy should be considered as one of the aluminium alloy materials for connecting rod manufacture since it is strong, less in weight and cost GHC55 equivalent to \$1.0 less than steel connecting rod. If a material of this nature is considered for manufacturing automotive components, it will not only make the vehicle lighter for improved speed and fuel consumption, it will also make the vehicle cost less.
2. Engines that require strong and robust connecting rod to transmit high power should consider steel connecting rod since it deforms less and it is able to take more compressive loads comparable to the connecting rod made with aluminium alloy and titanium alloy materials.
3. It is again recommended that, if a connecting rod which can endure more stresses is required then, titanium alloy and aluminium alloy such as Al 7075 T6 alloy materials connecting rod should be considered. But because titanium alloy materials are very expensive, the study therefore recommends aluminium alloy 7075 T6 material for connecting rod which can take more stresses and also light weight and cost less.
4. Ghanaian entrepreneurs should be encouraged to set up automotive components manufacturing companies for skilful graduates from our skill training institutions to help nurture their talent for the automotive industry.

5.4 Future Studies

Future studies into connecting rod design and simulation should concentrate on the following areas:

1. Future study into using aluminium alloy to design and manufacture connecting rod of an internal combustion engine should consider finding out the best method of manufacturing that is suitable for aluminium alloy connecting rods production.
2. Further study should also consider conducting further test by fixing the prototype connecting rod in a real engine to identify any issues with the design.
3. Further study into connecting rod design and manufacture should also consider conducting fatigue and thermal tests to identify if there are any issues with the design.



REFERENCES

Aluworks Ghana (2019). Chairman's Statement of Address. *Aluworks@Auworks.com*.

Biradar A., Vinayakrad and Swami M. C. (2017). Analysis and Optimisation of Connecting Rod used in Heavy Commercial Vehicles. *International Journal of Engineering Development and Research (IJEDR)*. ISSN 2321-9939.

- Davis J. R. (2019). Alloying: Understanding the Basics. Retrieve from *www.Asminternational.Org*.
- Khurmi R. S. & Gupta J. K. (2005). Theory of Machine, First Edition. *Eurasia Publishing House (PVT) Ltd*. Ram Nagar, New Delhi.
- Khurmi R. S. & Gupta J. K. (2015). Textbook of Machine Design, First Multi-Colour Edition. *Eurasia Publishing House (PVT) Ltd*. Ram Nagar, New Delhi.
- Leela Krishna V. & Venu G. V. (2013). Design and Analysis of Connecting Rod using Forged Steel. *International Journal of Scientific and Engineering Research*. ISSN 2229-5518.
- Malleshwara N. R. (2013). Design optimisation and analysis of a Connecting Rod using ANSYS. *International Journal of Science and Research (IJSR), India*. ISSN 2319- 7064.
- Ministry of Trade and Industry (2019). The Ghana Automotive Development Policy. *www.Moti.gov.gh*.
- Ministry of Trade and Industry (2019). Ghana Beyond Aid. *7beyond-aid-agenda*.
- Mohankumar D. & Rakesh L. (2017). Design and Analysis of Connecting Rod. *International Journal of Pure and Applied Mathematics*. P-105-109.
- Mohamed A. H. et al (2014). Design and Analysis of Connecting rod using Aluminium Alloy 7068 T6, T6 511. *International Journal of Mechanical Engineering and Technology (IJMET)*. PP-57-69.

- Nachimuthu A. K. et al (2014). Analysis and Optimising Connecting Rod for Weight and Cost Reduction. *International Journal of Research and innovation in Engineering Technology*. P-1-7.
- Nitturkar H. D., Kalshetti S. M. and Nadaf A. R. (2020). Design and Analysis Connecting Rod Using Different Materials. *International Research Journal of Engineering and Technology (IRJET)*, P-ISSN 2395-0075.
- Nilam P. et al (2017). Design and Analysis of Connecting Rod for Weight Reduction in Case of CI Engine. *International journal of Engineering Sciences and Research Technology*. ISSN 2277-9655.
- Noor M. M. et al (2008). Analysis of Connecting Rod Based on Finite Element Approach. *Malaysia Technical Universities Conference on Engineering and Technology*. Putra Palace.
- OmPrakash S., Natrayan M. and Dineshkumar S. (2018). Optimisation of Connecting Rod for Weight Reduction by Finite Element Analysis. *International Research Journal of Automotive Technology (IRJAT)*. P-80-87.
- Palamisamy S. et al (2015). Improvement of Various Parameters in Different Application of Connecting Rod. *Journal of Applied Sciences Research*. P-30-33.
- Pravardhan S. & Ali Fatemi (2015). Connecting Rod Optimisation for Weight and Cost Reduction. *SAE International, the University of Toledo*. P-01-0987.
- Prof. Doshi N. P. & Prof. Ingole N. K. (2013). Analysis of Connecting Rod using Analytical and Finite Element Method. *International Journal of Modern Engineering Research (IJMER)* P- 65-68.

- Raviraj Y. T. & Abhay A. U. (2015). Analysis of connecting Rod used in Two-Wheeler Under Static Loading by FEA. *International Journal of Engineering Trends and Technology (IJETT)*.
- Sumit D. & Ankit C. (2019). Weight Optimisation of Connecting Rod of Internal Combustion Engine Using Finite Element Analysis. *International Journal for Research Trends and Innovation (IJRTI)*.
- Srihersha B. & Sudhakar Rao P. (2020). Design Consideration for Connecting Rod. *International Journal of Engineering and Advance Technology (IJEAT)*. ISSN 2249- 8958.
- Tanya Buddi et al (2021). Fabrication and finite element analysis of two-wheeler connecting rod using reinforced aluminium matrix composites Al7068 and Si3N4, *Materials Today: Proceedings*, Volume 44, Part 1, 2021.
- The aluminium Association, Inc. (1998). *Aluminium Selection and Applications*. Washington D. C. 20006, 900 19th Street, N. W. Suite 300.
- Venkatesh S. et al (2014). Design and Analysis of Connecting Rod with Modified Materials and FEA Analysis. *International Journal of Engineering Research and Technology (IJERT)*.